8-19-2020 1:45 PM

Computational Modeling of the Human Brain for mTBI Prediction and Diagnosis

Yanir Levy, *The University of Western Ontario*

Supervisor: Mao, Haojie, *The University of Western Ontario*

A thesis submitted in partial fulfillment of the requirements for the Master of Engineering Science degree in Biomedical Engineering

Abstract

Sports related concussions and mild traumatic brain injuries have seen an increase in frequency over the past decade. The creation of highly biofidelic computational head models is an important step in understanding the mechanisms of these mild brain injuries and preventing them. Hence, the purpose of this research is to combine state-of-the-art computational models, brain imaging modalities and traditional head injury assessment protocols to simulate and predict the brains responses during traumatic head impacts. A novel, atlas-based, parcellated axon fiber embedded head model was developed which allows for in-depth analysis of the brain's structural connectome tracts for injury diagnosis and analysis. New axon strain metrics were developed along with traditional head kinematic methodologies to create one of the most advanced finite element head models for concussion injury reconstruction which allows for comparison to patient symptoms through tract injury level prediction.

Keywords

Traumatic brain injury, concussion, mathematical models, computational model, finite element analysis, axon fiber, cognition, sports concussion, DTI

Summary for Lay Audience

With the ever-growing evidence of the major health risks associated with traumatic brain injuries and concussions, development of new methods for researching and diagnosing injury mechanism is required. Our lab is attempting to tackle this problem by incorporating finite element methods to the complex geometries and material properties of the human brain. This thesis was completed over the course of 2 years and begins with an exploration into the mechanisms that produce what are considered ‘signs’ of traumatic brain injuries. The work then progresses to examine some of the leading predictive injury criteria’s and assess their viability and limitations. Finally, this project led to the development of a new modified finite element head model and goes through the generation of parcellated fiber axon models that will help to better understand the injury mechanism of the brain’s communication neural network. This model, which currently encompasses 41 distinct fiber bundles, is, as of now, the only embedded finite element parcellated fiber axon model using group averaged diffuse tensor imaging data in the world.

Along with the development of the embedded and parcellated fiber axon model, a new injury prediction metric has been developed. Using the strains produced in the axial direction of the fibers, like previous cadaveric experiments, it is possible to determine the overall injury present in a specific fiber bundle as a percentage over a predetermined ‘injury’ threshold. This will allow for the comparison of different fiber tract damage under different dynamic impact scenarios.

The possibilities for future studies that look explore damage to specific fiber orientations, fiber lengths and fiber functionalities will allow for in-depth analysis of the inner mechanisms of the brain. The overarching goal of this research is to couple engineering principals with medical imaging techniques and neuroscience to understand, diagnose and prevent some of the symptoms and impairments associated with concussions and mild traumatic brain injuries.

Co-Authorship Statement

Chapter 2 (‘Development of a computational concussion injury prediction pipeline for ice hockey helmet performance evaluation’) co-authored by Dr. Haojie Mao, Marco Gallone, Kierra McDougall and Dr. Ryan Ouckama and is accepted as a peer reviewed paper into IRCOBI conference. Chapter 3 (‘Investigating injury metrics in predicting brain damage and evaluating helmets in hockey’) was co-authored by Dr. Haojie Mao and Dr. Ryan Ouckama and will be submitted to a journal. Chapter 4 (‘Development of Multiple Parcellated Axon Fiber FE models for TBI symptom diagnosis’) coauthored by Kewei Bian and Dr. Haojie Mao will be sent to a journal. Chapter 5 (‘Using fiber model for injury outcome prediction’) was co-authored by Dr. Haojie Mao and will be sent to a journal. All papers were drafted by Yanir Levy and reviewed by Dr. Haojie Mao.

Acknowledgements

I would like to thank my supervisor Dr. Haojie Mao along with my advisory committee of Dr. Ravi Menon and Dr. Mark Daley. I would also like to thank my lab group, Kewei Bian for assisting in some model development in chapter 4 as well as Kierra McDougall and Marco Gallone for assisting in code development and research. Finally, I would like to thank Bauer Hockey Ltd., Dr. Ryan Ouckama, and NSERC Engage for their contribution to chapter 2 and 3.

Table of Contents

List of Tables

List of Figures

Chapter 1

1 Introduction

1.1 Research Rationale

Traumatic brain injury (TBI) is estimated to affect close to 70 million individuals every year [1], with 80-90% of those injuries considered to be mild, more commonly known as concussions. The victims of these injuries have remarkably little information into how to prevent or even understand the long term implications of these injuries [2]. This injury is a considerable burden on the health and well-being of society, and its repercussion leads to physical and mental health declines as well as significant negative economic effects. Mild TBI, more commonly referred to as the concussion, has made its way onto mainstream news due to its obvious and dramatic symptoms. Typical short term effects to brain functionality can induce chronic symptoms such as; memory loss, cognitive impairments and motor disturbances and has been shown to cause long term neurodegeneration that results in death [3]. Some of the greatest challenges that arise from this injury type are the knowledge gaps between understanding not only the mechanisms that cause mTBI, but the thresholds and post-injury outcomes that distinguish between the severity and diagnosis for this life altering injury. The need for improved diagnostic methods, and better understanding of the biomechanics that lead to functional changes, to assist in injury prevention and rehabilitation are crucial in improving patient outcomes and increasing post injury quality of life.

1.2 Head and Brain anatomy and functions

1.2.1 Skull and brain protection anatomy

The brain is protected from injury in several ways, one of those ways is a thick bone which encloses the brain, known as the skull. The skull is made up of three layers, an inner and outer layer made of dense cortical bones and a middle layer made of porous trabecular bone and consists of 8 cranium bones and 14 facial bones. The second inner layer of this protective incasing is the meninges which include the outer dura mater, the middle arachnoid membrane and the inner pia matter. These layers encase the brain and

are combined with the third method of the body's natural protection on the soft brain which is the cerebrospinal fluid (CSF). The CSF helps cushion the brain from shock and sudden pressure changes by circulating through the four ventricles and in the subarachnoid space and absorbing some of the energy that could occur in a traumatic impact. Finally, the blood-brain barrier, helps with the brain's protection through the limitation of movement of chemical, toxic substances and infection from other parts of the body. All four of these protective mechanisms protect the brain from everyday activities. However when a traumatic head impact occurs, one or more of these systems reaches its failure threshold producing injury [4].

1.2.2 Brain anatomy

The brain is one of the most complex and least understood organs, especially in the human body. The various anatomical components and different material and geometric properties that each of those different components showcases, not to mention the complex chemical composition of the brain, makes it extremely difficult to recreate. In the study of impact injury mechanisms, the brain can show injury patterns from much lower energy level injuries than that of any other soft – tissue component in the body, such as muscles and ligaments [5]. The brain, segmented regions and anatomical features shown in Figure 1, is made up of gray, white and reticular matter, with each showing unique mechanical and functional characteristics. The gray matter, named after its distinct gray-brown color, is made up of capillaries and neuronal cell bodies predominately and can be found primarily in the cortex. White matter, of which this research focuses on, consists mainly of axon fibers, which form connection between neurons [4]. The brain structure is broken down further into various different subcomponents, which include components like the brainstem made up of; (1) the hindbrain (cerebellum), (2) the midbrain, (3) the diencephalon (hypothalamus, thalamus) and the forebrain (basal ganglia, limbic system, and cerebral cortex). With each of these structures performing different functions and working together to allow for the body to regulate movement, cognitive processing and everyday activities.

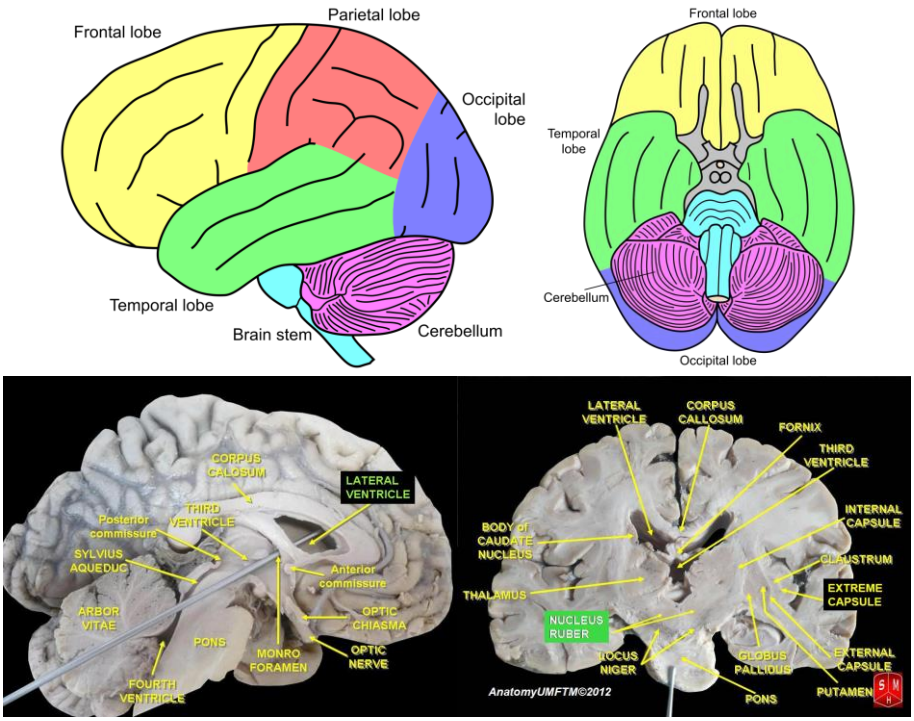

Figure 1, schematic of the different brain regions and anatomical cross section of sagittal and coronal planes with labelled landmarks.

1.2.3 Functions of the brain

The different subcomponents of the brain communicate with each other and the different parts of the body through the network known as the central nervous system (CNS) made up of neurons and myelinated axons. The human brain has approximately 85 billion neurons, each making as many as 15,000 synaptic connections with other cells to engage in information processing and neuronal function [6]. The brain itself is divided into different distinct regions that act differently and provide different functions to the brain.

1.2.3.1 Deep brain

This is made up of the; (1) the Midbrain which includes superior and inferior colliculi (vision and hearing, motor function), (2) the Diencephalon which includes 3 thalamic structures; the epithalamus (pineal glands for biorhythms), the thalamus (relays sensory information to cortex) and hypothalamus (contains nuclei for regulatory functions (internal temp, eating/drinking/sexual activity) and (3) the Hindbrain which contains

nuclei that give rise to cranial nerves [4]. All these regions are highlighted in the schematic provided in Figure 2 and exist in all vertebrate brains.

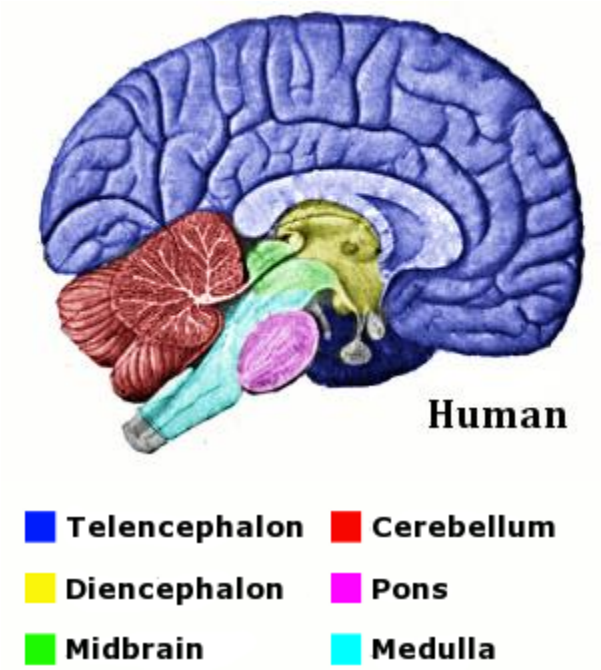

Figure 2, breakdown of main regions in brain, sliced along the midline, with different regions highlighted [7].

1.2.3.2 The Forebrain

The forebrain is made up of several components which include (1) the basal ganglia which is thought to dictate motor coordination, (2) the limbic system which is involved in one's emotion, motivation and memory, (3) the cortex (neocortex) which is involved in sensory, motor and cognitive function and is made up of four cortical regions each with a specific function; (vision - occipital), (audition - temporal), (somatosensations - parietal) and (movement-frontal). These lobes can then be broken down into primary secondary and tertiary regions which preform more complex sensory-motor and associative functions. An example of how these all work together; the cortical structures receives sensory information through thalamus and works through basal ganglia to produce movement and through limbic system to organize emotion and memory.

1.2.3.3 Fiber axons and the brains neural network

The myelinated axons in the brains white matter transport electric signals from neurons in different regions of the brain to form a communication highway of information, these pathways, made up of axon fibers, are referred to as tracts. Using different imaging technologies, specifically diffuse tensor imaging (DTI) and functional magnetic resonance imaging (F-MRI), different axon fiber tracts and their associated functionalities have been determined, a step into understanding how the human brain functions [8].

To understand how these imaging modalities work, along with their associated uses and connection to this study, it is important to understand the structures that they are attempting to locate and quantify. Methods of understanding these white matter connections arise from the field of connectomics, with graphical representations of these connections represented in graphs called connectograms, see Figure 3 as an example of these graphs. The different colors represent different parcellated regions in the brain, each with its own intrinsic function. This is one of the more recent methods of visualizing the CNS architecture and is used for efficiently analyzing the human connectome and investigating both subject specific and clinical population models [9]

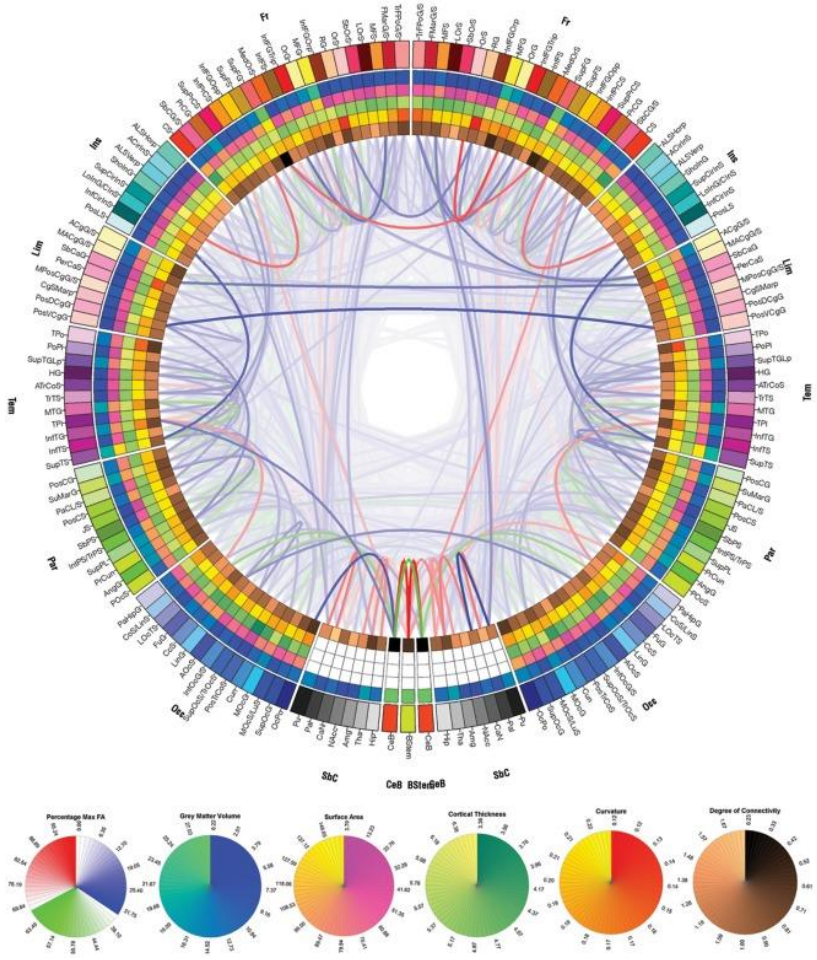

Figure 3, Connectogram representing the different white matter fiber tracts and their connections, this is the basis of brain parcellation a method of understanding brain function [10].

1.2.3.3.1 Imaging techniques

The use of DTI as a method for assessing and diagnosing changes in the brain which lead to brain injury are widely cited in literature [11-19]. This imaging modality is commonly used as a method of examining the integrity and determining the pathways of the brains white matter tracts [18]. DTI was introduced as modified DWI tool over conventional MRI to determine the structural changes of the brain as it is more sensitive in its ability to quantify changes to the microstructure of white matter. This is the reason for increased use as a diagnostic tool for mTBI. DTI also provides another useful function, its ability to

produce three-dimensional tractography, Figure 4, allows for the visualization of the brains myelinated long-fiber axon tracts, which relay the information produced by the neurons. The bases of DTI and how it can model these incredibly complex and intricate tracts is through the diffusivity of water molecules inside the brain. This non-invasive method allows for the visualization of the anisotropy that is present in the brain as the diffusion in the direction of the myelinated fibers is faster in parallel than in a perpendicular direction [20]. In terms of its relation to the biological mechanism in the brain, diffusion tensors work by transferring material from one spatial location to another at a point in time, i.e. water molecules inside the tube-like myelinated fibers. Diffusivity is typically modeled as ellipsoids where the direction of the greatest diffusivity is assumed as the direction which is parallel to the local direction of the white matter (i.e. axon fibers). Methods of measuring diffusivity include mean, axial and radial diffusivities along with fractional anisotropy.

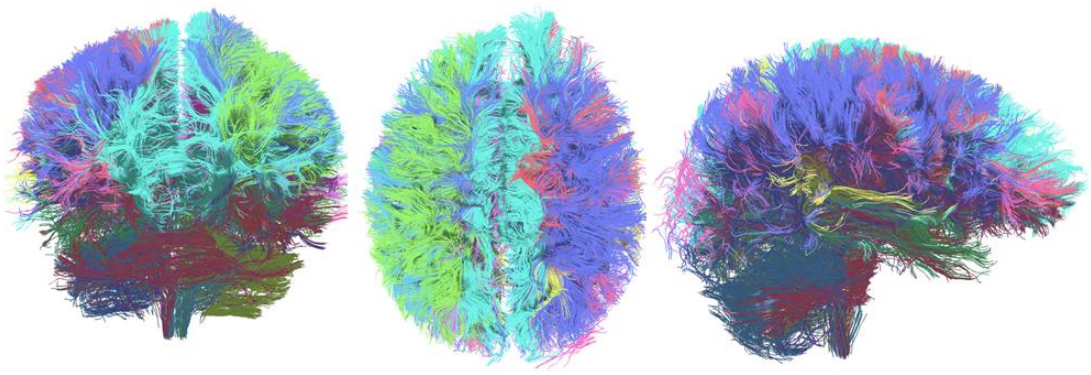

Figure 4, parcellated 3D human brain axon tractography derived from DTI, images extracted from a single subject using DSI studio software.

Imaging modalities such as functional MRI (fMRI) allow for a mapping of the metabolic function of the brain rather than the 3D anatomical mapping done by MRI. This metabolic mapping allows for analysis of the brain network connectivity changes over time [7]. In particular it is used to evaluate regional interactions that occur, with resting state MRI (rs-fMRI) occurring when the patient is resting or in a task-negative state [21]. These imaging techniques have paved the way for understanding the functions associated with the brain's different regions and how those regions are connected by the

axon fibers. Table 1 summarizes literature findings that highlight specific tract locations and anatomical orientations (association, commissural and projection) as well as the functions and impairments that are caused when damaged. These neuroscience concepts are the basis of functional and structural brain research.

Table 1, breakdown of 22 major axon fiber tracts and their functions based on literature.

Name of Tract	*Location*	*Function*
Arcuate Fasciculus (AF)	Association tract located in parietal, temporal, and frontal regions connecting Wernicke's area to Broca's area.	Damage associated with conduction aphasia, impairments in naming reading and apraxia [22, 23].
Cingulum Bundle (CB)	Association tract connection located in parietal, temporal, and frontal lobes of cortex, above CC and under cingulate cortex (made up of five regions).	Executive control, emotion, pain, episodic memory, and cognitive functions, damage associated with Alzheimer's disease, schizophrenia, depression, PTSD, OCD and autism spectrum disorder [24, 25].
Corpus Callosum (CC)	Commissural tract connecting cortical regions of both hemispheres through corpus callosum.	Interhemispheric interaction, damage leads to inhibited transfer of somatosensory information and learning processes between sides of cerebral cortex, decline cognitive function[26, 27].
Cortico-Ponto-Cerebellar pathways (CPC)	Projection tract from associative and limbic areas of cerebellar cortex to the contralateral half of the cerebellum.	Coordination and regulation of movement damage associated with progressive ataxia, atrophy, dysmetria, dysarthric speech, or tremor [28].
Corona-radiata-frontal and parietal (CR-F & CR-P)	Along brainstem projection tract.	Motor and sensory patterns, loss of motor function and muscle weakness, damage leads to sever motor and sensory deficits (faciobrachial or brachiocrural and hemihypethesia)[29].
Corticospinal Tract (CST)	Originates at primary motor cortex and passes through internal capsule and cerebral ending in the grey matter of spinal cord.	Pathway for voluntary motor function (fine motor activities in hand)[30, 31].
External Capsule (EC)	Association fibers connecting cerebral cortex to striatum, fibers from basal forebrain to cerebral cortex.	Damaged associated with anterograde and retrograde axonal damage[32].
Extreme Capsule (EmC)	Cortical Association bundle that interconnects the frontal, insular and temporal cortices, inferior frontal cortex through superior temporal gyrus to inferior parietal lobe.	Language processing and expression [33].
Internal Capsule (ICP)	Along brainstem, divided up into 5 subdivision	Damage shows deficits in storage and retrieval of verbal memory, visual and auditory processing.
Inferior Longitudinal Fasciculus (ILF)	Connects the temporal and occipital lobes	Right – involved in visual memory and facial identification Left – visual analysis and recognition of colors, works, shapes and objects Damage causes language processing deficient, and disruption of information between visual, limbic and memory regions [33].
Intracerebellar input and Purkinje tract (Intra-CBLM -IP)	In the Cerebellum GABAergic neurons that receive input from the cerebellar cortex and outputs to the cerebellar cortex	Important in motor learning and coordination as well as cognitive information processing. Damage leads to reduction in white matter volume, disorganized pathways, mossy fibers, and abnormal fibers running to/from the cerebellum[34]. [35]
Intracerebellar Parallel Tract (Intra-CBLM-PaT)		
Inferior Occipito-frontal Fasciculus (IOFF)	Connects ventrolateral and dorsolateral prefrontal cortex with posterior temporal cortex and occipital lobe	Facilitates higher visual processing, recognition of objects, places, colors, faces, and words; also associated with ventral language pathways, damage/lesions can cause deficits in visuospatial processing [33].

Middle Cerebellar Peduncle (MCP)	Composed of fibers that carry input from contralateral cerebral hemisphere relayed via the pontine nucleus, information from contralateral cerebellar hemisphere, main afferent pathway to the cerebellum.	Motor coordination, difficulty walking, speaking vertigo and facial weakness [36].
Middle Longitudinal Fasciculus (MdLF)	Connects superior temporal gyrus to the parietal lobe made up of two tracts (angular gyrus and superior parietal lobule)	Involved in attention and language and visuospatial and intergrative audiovisual functions. Associated with neurodegenerative disorders such as primary progressive aphasia, posterior cortical atrophy, frontotemporal dementia, and Alzheimer's disease [33]
Striato-frontal (SF)	Connections between the lateral prefrontal cortex and dorsal striatum via basal ganglia; front end of a larger cortical-basal ganglia-thalamo-cortical circuit	Damage associated with cognitive impairments regarding visuospatial processing, executive functioning, and motor speed. Disorders attributed to the frontal-striatal system include schizophrenia, impulsive disorders, drug addiction, Parkinson's disease, and Tourette's syndrome [37].
Superior Longitudinal Fasciculus (SLF)	Major association fiber pathway connecting the postrolandic regions to frontal lobe, made up of four components	Facilitates cognitive processes; attention, memory emotion and language as well as a connection for working memory, damage to left SLF is language disorders, right SLF spatial attention deficits [32]
Superficial-F/FP/O/OT/P/PO/PT/T Superficial-frontal, frontal-parietal, occipital, occipital-temporal, parietal, parietal-occipital, parietal-temporal, temporal	Superficial white matter, is located directly below cortex and is a mixture of short association fibers that include intra-cortical, subcortical and termination fibers.	
Thalamo-frontal (TF)	Diencephalon to prefrontal cortex	Region has been associated with executive functioning (skills necessary for purposeful, goal-directed activity). Damage associated with impairments in concept formation, abstract reasoning, mental flexibility, cognitive speed and planning. [38]
Thalamo-occipital (TO)	Important relay pathway that receives afferents from visual sensory organs and sends efferent to the primary sensory cortex. Lateral geniculate nucleus signals to the occipital cortex	Decreased connectivity between thalamo-occipital projections were present in congenitally blind patients. Patients with temporal lobe epilepsy (TLE) demonstrate abnormal thalamo-occipital functional connectivity [39, 40].
Thalamo-parietal (TP)	Connects the dorso-lateral nuclei to the posterior associative cortex relay peripheral sensory information to the somatosensory cortex in the parietal lobe	Involved in central pain and pain relief, working memory. Damage leads to symptoms that include central imbalance, spontaneous pain or nociception, and central disinhibition [41, 42]
Unicate Fasciculus (UF)	Connects anterior tip of temporal lobe with orbitofrontal cortex	semantic and episodic memory; Damage to the right UF results in impaired retrieval of episodic memory including autobiographical and event-related memories; disrupts emotional empathy – makes patients apathic and indifferent , damage to the left UF results in impaired semantic memory retrieval (recalling concepts and facts) [33]

1.3 Mild traumatic brain injury

1.3.1 Diffuse injury

1.3.1.1 Injury tolerance at tissue level

The use of brain strain to quantify the deformation associated with diffuse injuries is deemed as a reasonable metric for predicting mTBI or concussions because the strain (stretch) is the direct cause of neuronal damage [43]. Studies report that a strain of 0.19 – 0.21 in brain regions is considered a threshold for experiencing mTBI [44, 45]. Different structures of the brain experience different strain thresholds, while some structures have different levels of injury susceptibility, the corpus callosum, the component connecting the left and right hemispheres, is damaged at strains of between 0.28 to 0.31 [46, 47]. The thalamus was reported to have a strain tolerance between 0.26 and 0.38 [46, 48]. Rotational head motions are the overarching contributor to brain strains, and factors such as the shape of the impact curve or its magnitude and duration, as hypothesized by Zhao et al., Yoganandan et al., Post et al, and Bian et al can have a considerable effect [49-52]. Impact location as reported by Zhang et al. and Elkin et al. can also influence the brain strains location and magnitude [53, 54]. The key to understanding this tissue tolerance level is combining large amounts of data with highly detailed FE models, animal data and imaging studies.

1.3.1.2 Diffuse axonal injury (DAI)

One of the primary mechanisms of brain injury is thought to be well understood, a rotational motion applied to the head causes a shearing force to the soft brain tissue which leads to tensile strains on the brains axon fibers [55]. The strains derived from the impact to the head are found to cause different injury outcomes such as diffuse axonal injury (DAI) [56], these types of injuries, specifically the ones associated with the axon fibers of the brain are the focus of this study as it has been proven that there is a specific injury threshold at this axonal level [57]. The study completed by Bain et al. 2001, showed through the stretching of the optic nerve of a guinea pig that at functional injury was present at a strain of 0.34 (false positives) and 0.14 (false negatives) with the optimal strain threshold for sensitivity and specificity measuring 0.21 [43]. Strains at the axonal level are believed to be a predominant

driving force in the negative outcomes associated with TBIs and concussions in humans [58]. While other studies have looked in depth at the response of the brain to traumatic head impact [46, 58, 59], few studies have looked at the axon fibril networks dynamic response in real world impact scenarios. Studies such as those completed by Giordano et al. and Wright et al. focused on the validation of a computational models that treat white matter as an anisotropic, hyperplastic material based on DTI to determine a threshold or probability of DAI [55, 60]. Both studies determined that strain in the direction of the fibers is a better predictor of injury then a generalized max principal strain (MPS), anisotropic equivalent strain (AESM) and cumulative strain damage measure (CSDM).

TBI also affects the cognitive ability and brain connectivity, due to the trauma on the axon fiber networks of the brain. Fagerholm et al. has been able to show with a 93.4 % accuracy that axonal injury in patients resulted in significant impairments in cognitive performance such as information processing speed, executive function and associative memory. These results suggest that TBI results from disconnection of network hubs in axonal injuries [61]. These results were directly related to the disconnection of the network hubs in the brain which were predominantly associated with deep brain regions such as the corpus callosum.

1.3.2 The sports concussion

1.4 Biomechanical methods to study head injury in hockey

To study the effects of impacts to the head in physical contact sport, such as hockey, there are several different methods to produce effective traumatic impact mechanism predictions in concussion like instances. Both researchers and industry use a wide variety of techniques to assess the viability of protective equipment and the range of forces that result in such injury types. Accident reconstruction, physical experimental methods and computational simulations, have been shown to be efficient in providing consistent and repeatable data for use in research [62, 63]. Our work focuses on the computational methods of accident reconstruction as it provides real world-relevant scenarios and allows engineers with a background in biomechanics the necessary tools to generate novel insights into brain injury. Understanding brain injuries in hockey can also mean understanding the benefit and overall effectiveness of the helmet in reducing

impact kinematics that contribute to brain motion[64-66]. Kraus et al. demonstrated that in ice-hockey a properly designed helmet, including tested foams and solid construction could reduce head injuries from 8.3 per 100 games to 3.8 per 100 games [67]. This study compared helmeted and non-helmeted players and proved that the use of helmets in the sport of hockey for head injury reduction is warranted.

1.4.1 Experimental methods

1.4.1.1 Laboratory test

Historically, surrogate, physical dummy models were used to measure the linear and angular accelerations associated with head impacts and created injury criteria to assess the damage of head injuries quantitatively [68]. The use of drop tests, pendulum impacts and other forms of blunt force impacts to the head proved effective in recreating some of the typical loading conditions that are associated with head injuries[44]. Recently, new methods of recreating impacts that involve tangential forces that result in rotational motion to the head have been introduced, in the form of helmet safety testing. One of the most popular and widely referenced helmet testing protocol is that of STAR. This methodology, which is examined in more detail in several of our studies, looks to introduce typical loading conditions present in helmeted sports, such as hockey and football and provide a consumer centric rating system to determine a helmets relative safety rating [66]. The STAR methodology and other similar physical dummy tests typically use a NOCSAE head form and Hybrid III neck to reconstruct game like impacts, with embedded sensor like accelerometers providing typical center of gravity head responses in kinematic form, typically providing, linear and rotational acceleration [64].

1.4.1.2 Brain injury prediction based on head kinematics

Traditionally, commonly used concussion prediction methods are kinematics-based head injury metrics. These metrics are typically calculated based on the peak resultant kinematic response of the head during a traumatic impact. One of the original and most widely referenced metric is the Wayne State Tolerance Curve (WSTC) for head injury, which is defined based on the relationship of linear acceleration and impact

duration [69, 70]. The WSTC hypothesis is that the head can tolerate higher peak linear acceleration for a very short duration, while injury occurs when same magnitude of acceleration is applied at a longer duration [71]. The WSTC data is considered the basis for many widely used injury metrics such as Gadd Severity Index (GSI). The GSI is described by the integration of linear acceleration to the power of 2.5 which in theory gives idealistically peak values for the impact with longer pulse duration [72, 73]. GSI is capable of quantifying severe skull fractures and brain injuries, but is not typically recommended in its ability to predict the risk of concussions [74]. The mathematical GSI is represented as equation 1.

$$GSI = \int a(t)2.5dt \tag{1}$$

Where 'a' is the effective acceleration of the head in terms of g, acceleration due to gravity, and 't' is the time in milliseconds [75]. Building on the GSI the Head Injury Criterion (HIC) is focusing on the severity index on the part of the impact that can be expected to be pertinent for the risk of brain injury. This measure is calculated by averaging the integrated curve of resultant acceleration and time over the time interval of maximum HIC value. The mathematical expression for HIC shown in equation 2.

$$HIC = \max_{t_1, t_2} \left\{ (t_2 - t_1) \left[\frac{1}{t_2 - t_1} \int_{t_1}^{t_2} a(t)dt \right]^{2.5} \right\} \tag{2}$$

When first developed the t_1 and t_2 in the HIC equation referred to any two arbitrary times on the acceleration pulse [76]. In 1972, the National Highway Traffic Safety Administration (NHTSA) narrowed t2 and t1 to be no more than 36 milliseconds (HIC_{36}) and the maximum HIC36 not to be greater than 1000. In addition, NHTSA further reduced impact duration time in HIC_{15} where t2 and t1 could be no more than 15 milliseconds with maximum value not exceeding 700 [77]. HIC is still widely being used in multiple industrial and research fields for risk predictions. This metric is often used to quantify traumatic brain injuries while its accuracy in predicting mTBIs has been consistently challenged. In the automobile testing, HIC has been recognized as the premiere metrics for predicting the head injuries related to motor vehicle accidents for

over three decades [45]. However, in a real-world collision, head injury occurs due to the combination of linear and angular acceleration and HIC is an experiential criterion that only takes linear acceleration into account. Being limited to only linear acceleration led to the rise of The Generalized Acceleration Model for Brain Injury Threshold (GAMBIT). This metric was proposed to consider the combined effect of linear and rotational kinematics. It can be calculated from maximum linear and angular acceleration measured at the center of gravity (COG) of the head. Mathematically, it can be expressed as equation 3.

$$GAMBIT = \left[\left(\frac{a_{max}}{a_{cr}}\right)^2 + \left(\frac{\alpha_{max}}{\alpha_{cr}}\right)^2\right]^{\frac{1}{2}} \quad (3)$$

Where a_{max} is the peak linear acceleration of the head in g and α_{mac} is the maximum angular acceleration in radians per square seconds [78]. With the use of scaled animal models and along with NHTSA, a rotational brain injury criterion – Brain Injury Criteria (BrIC) was developed. BrIC looked to introduce peak angular velocity and critical values which are directionally dependent on the anatomical planes of the anthropomorphic test dummy [79]. BrIC has become very critical to understand the vehicle and dummy motion during the development of the restraints system test. Recently, the New Car Assessment Program has updated BrIC as a new head injury criteria in automobile oblique impact crash test [80].

$$BrIC = \sqrt{\left(\frac{\omega_x}{\omega_{xC}}\right)^2 + \left(\frac{\omega_y}{\omega_{yC}}\right)^2 + \left(\frac{\omega_z}{\omega_{zC}}\right)^2} \quad (4)$$

Where ω_x, ω_y, and ω_z are maximum angular velocities in X, Y, and Z-axes respectively, and ω_{xC}, ω_{yC}, and ω_{zC} are the critical angular velocities (66.25, 56.46 and 42.87 rad/s) in their respective directions [79].

Due to the development of finite element and computational methods, deformation of the skull and internal organs were made possible. This greatly encouraged the discovery of new injury criteria. More than ten different three-dimensional finite element head models (FEHM) have been developed in the last decade. Thus bridging the

gap between macro-level kinematics and micro-level injury assessments, FEHM played an important role in simulating brain response subjected to external impact [81]. While taking into account the varying sizes of a human head-on impact, using FEHM from Stockholm Royal Institute, introduced KTH which emphasis the head size dependence of intracranial stress associated with injury [82]. To assess the potential of TBI in car crashes, new criteria called Simulated Injury Monitor (SIMon) criteria was introduced which can predict three different forms of brain injury using three injury metrics as follows [83].

I. Cumulative Strain Damage Measure (CSDM) - A correlate for Diffuse Axonal Injury (DAI) which is associated with the tensile strains of the cumulative volume of brain tissue over a predefined critical level. CSDM predicts DAI by calculating the strain levels at a volume fraction of the brain tissue [83].

$$CSDM20 = \frac{\#\ of\ elements\ MPS\ over\ 0.20}{total\ \#\ of\ elements} \tag{5}$$

Subsequently, from the outcome of volunteer sled tests and professional football reconstruction, Injury criteria for FEHM – Global Human Body Model Consortium (GHBMC) which have detailed skull, face and brain structures was developed [59, 84]. The concept that a second-order mechanical system behaves in a similar function to the typical brain deformation response to angular head motion has led to the development of several new brain injury metrics.

I. Universal Brain Injury Criterion (UBrIC**)** was developed based on the relation between the rotational head kinematics and strain-based injury metrics such as Maximum Principal Strain (MPS). This combinational equation was developed in part by the brain response outputs of FEHM in dynamic loading scenarios. Mathematically, UBrIC is represented as equation 6.

$$UBrIC = \left\{ \sum_i \left[\omega_i^* + (\alpha_i^* - \omega_i^*) e^{\frac{\alpha_i^*}{\omega_i^*}} \right]^r \right\}^{\frac{1}{r}} \tag{6}$$

Where ω_i^* and α_i^* are the directionally dependent ($i = x, y, z$) maximum magnitudes of head angular velocity and angular acceleration each normalized by a critical value (cr); $\omega_i^* = \omega_i / \omega_{icr}$ and $\alpha_i* = \alpha_i / \alpha_{icr}$ [85, 86].

II. Diffuse Axonal Multi-Axis General Evaluation (DAMAGE) was developed which predicts maximum brain strain using directional dependent angular acceleration time histories from head impacts. It is represented in eq. 7.

$$DAMAGE = \beta max_t\{\vec{\delta}(t)\} \quad (7)$$

Where β is a scale factor that relates the maximum resultant displacement of the system to the MPS value from the FE brain model [87]. Besides depending on the tolerance level of brain injury to SDH (Subdural Hematoma), a threshold curve called critical strain curve was suggested, expressed in terms of the peak angular acceleration and change in angular velocity which demonstrates that there was no axonal injury between 5% and 10% critical strain. Injuries such as concussions can be expected above these values, where DAI may also be expected [19, 88].

Due to the extensive use of FEHM, various physical parameters such as coup, contrecoup pressure, von Mises, and shear stress could be utilized to better predict the risk of brain injuries [89]. In addition, to classify and describe the severity of specific injuries, it is common to use a widespread injury severity scale named The Abbreviated Injury Scale (AIS), which was introduced by Association for the Advancement of Automotive Medicine (AAAM) and ranges from 0 (no injury) to 6 (fatal injury). It was initially adopted as an epidemiologic tool to define MVC but later adopted in all types of trauma[90-93]. Most of the previously listed injury prediction metrics attempt to compare their concussion assessment results to the AIS scale, a clear description of the level of injury is described in Table 2.

Table 2, the Abbreviated Injury Scale (AIS) *[93]*.

AIS- Code	*Injury*
AIS 1	Minor
AIS 2	Moderate
AIS 3	Serious
AIS 4	Severe
AIS 5	Critical
AIS 6	Maximum

1.4.2 Computational head and brain models

1.4.2.1 Mathematical modelling (FEA)

This numerical method is described as the simplification of complex structures through the discretization and meshing of large systems into smaller, simpler geometries through the technique of meshing. This method provides a finite number of elements and points that can be more easily solved using linear algebra and partial differential equations to extract important engineering measures such as mechanical stresses and strains. This technique is ideal for the prediction of mechanics related head damage, simplifying the complex structure of the head and brain for quantifiable analysis [5]. The benefits of using FE for head models is its ability to model the brain-damage related responses, particularly brains strain and pressure and simulated impacts and accident reconstruction. Most FEHM are generated based on anthropometric head geometries, derived from CT and MRI scans [59], which consist of different components that represent the brains anatomical regions both in terms of geometrical and material properties.

1.4.2.2 Different head and brain models

One of the earliest finite element head models was the Wayne State University brain injury model (WSUBIM), developed in the early 1990s. The benefit of this model and others like is its ability to be modified and updated as new research emerges, the latest version of this model contains 281,800 node and 314,500 elements [94]. Other models

soon followed with Kang et al. developing a 13,208 element model which included key anatomical features such as, the falx, tentorium, cerebrum, cerebellum and brainstem, known as the Universitè Louis Pasteur (ULP) human head model [95]. This model had several improvements over others during that time period yet used some outdated modeling techniques such as elastic material properties for brain matter instead of more complex constitutive models [96]. The continuous improvement in models with advancements in FE techniques was shown in 2002 where Kleiven developed a model known as the Kungliga Teknisha Höskolan (KTH) [82]. The KTH model is made up of 18,400 elements, includes anatomical features such as the skull, brain meninges and CSF, and has major improvements over other FEHMs of the past with its inclusion of different material properties such as homogenous, isotropic and non-linear materials. This was then proceeded in the following year by the Simulated Injury Monitor (SIMon) model, which was modelled after a 50^{th} percentile male [83], this model defined the skull as a rigid material while other components showed similar material properties to that of the KTH model. While all those models continued to be updated with slightly improved geometries and material properties, one of the larger jumps in FEHM was in 2013 with the development of the Global Human Body Models Consortium (GHBMC) FEM which was developed by Mao et al., shown in Figure 5 [59]. This model was a detailed model based on CT and MRI scans that contained a plethora of key anatomical features such as the cerebrum, cerebellum, brainstem, corpus callosum, ventricles, and thalamus, with each location individually marked and viscoelastic material properties applied pertaining to white matter and grey matter. The GHBMC model was validated against intracranial pressure data, brain displacements, nasal impacts and frontal horizontal impacts [59]. All of these models were recently compared by Miller et al. to determine which model provided the most comprehensive and accurate representation of brain skull displacement as mentioned by Hardy et al. [97]. In this study, top performers where the KTH (M-R) [98] , the ABM and the GHBMC models which all performed consistently well in the CORA, a tool that evaluates the similarities of curves. While there is some debate over using the Hardy validation cadavers as a good validation tool for FEHM in terms of the strains experienced in the brain, this validation protocol has been used extensively and is considered a golden standard for FEHM performance validation. So far, computational

head models have been well developed and available to the users in the field, these include validated models such as the atlas-based brain model, ABM [99], the Total Human Model for Safety (THUMS) head model [100], the Dartmouth Head Injury Model (DHIM) [17], as well as the University College Dublin Brain Trauma Model (UCDBTM) [101] and Strasbourg University Finite Element Head Model (SUFEHM) [102], aside from the aforementioned [97].

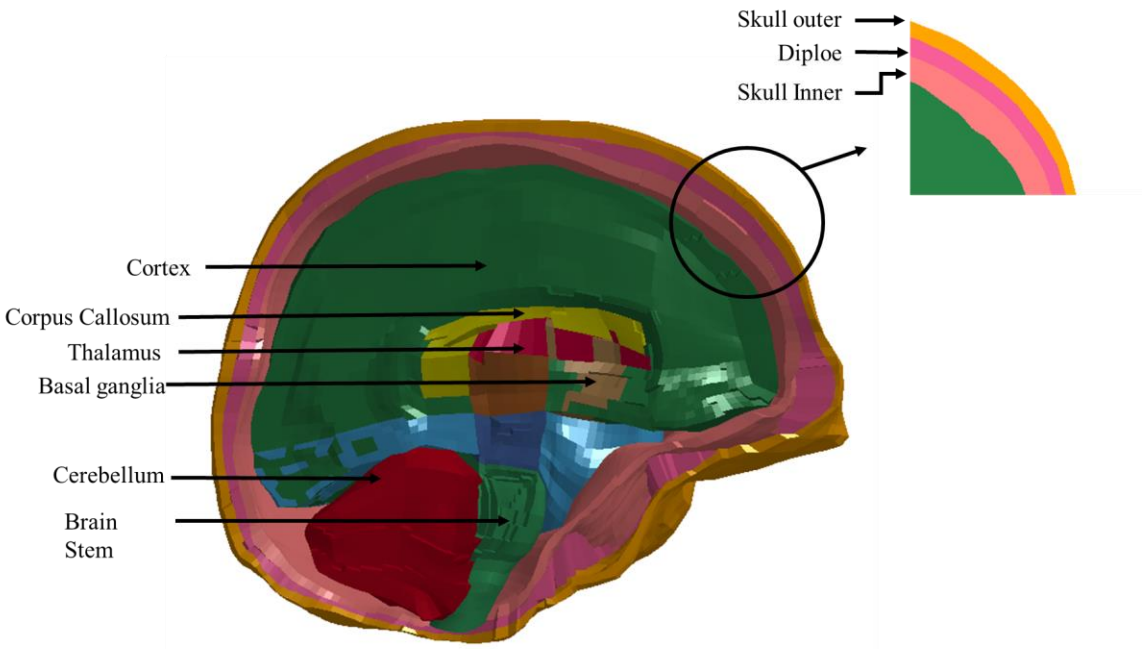

Figure 5, cross-sectional schematic of GHBMC head model, anatomical regions are represented in different colors for clarity

The improvement in the quality and accuracy of imaging modalities such as DTI brought on a new wave of these new detailed models. These finite element models have evolved the capability of numerical injury analysis by bridging the gap between the stress-strain thresholds obtained by FEHM and their relationship to the mechanical thresholds of cellular injury [103]. The new wave of FEHM, maximize the potential of DTI to provide mesoscopic (μm) insights into the brains structure and the potential effects that those structures have on the brain's anisotropic injury response. These models utilize different measures such as; fractional anisotropy (FA) or weighted average fiber orientation to introduce a combination in imaging measures and meshed finite elements to describe the

brains injury response in novel ways, a summary of the different models is presented in the table below.

These models however produced a variety of limitations, Chatelin et al. who projected strains from the bulk volume elements onto the fiber direction after post processing, lost important axonal strain information, compromising the accuracy of the material model, by averaging fiber direction, which may not direct anisotropy in the correct direction [103, 104]. Zhao et al. improved on this work by using DTI to incorporate fiber direction into the brain model to calculate axonal strain, comparing the different anisotropy implementations (voxel, tractography or multiscale sub-modeling) and determined that the implementation of discrete tractography in FEHM was the recommended method for accurate injury metric prediction [105]. This recent study advised that the combination of tractography and neuroimaging for region segmentation led to more accurate injury metrics based on brain strains and should be explored in future FEHM.

1.5 Research scope

This study will encompass four fields of medical and mechanical engineering research; computational modelling, neuroscience, soft tissue biomechanics and medical imaging to provide a new perspective on how traumatic head impacts affect deep brain responses. This will then, in turn, provide insight into how the connection networks of the brain are associated to cognitive function. Traumatic brain injury has been associated with high rates of mortality and disability and is usually associated with automotive accidents [106]. This research will focus primarily on a subset of the TBI know as a concussion which is commonly derived from sports related accidents and falls.

For this study, a high quality, extensively validated finite element human head model, known as a GHMBC model was used. This model was further improved by featuring axonal fiber tracts taken from real human subjects through a subset of the Magnetic Resonance Imaging modality called Diffuse Tensor Imaging. The overall objective of this research project is to create a geometrically accurate FE model of the neural connection network of the brain based on 3T and 7T DTI. This model was used to provide evidence

that certain impacts, based on impact location, duration and force have on deep brain responses, particularly axonal strain. This study looked to provide a novel approach at determining the strain to those axon fibrils and attempt to correlate that strain to cognitive functions that have been affected. The study utilized data accrued from surrogate, laboratory impact testing to determine the change in neural network composition post-concussion, while utilizing a computational model to predict injury location based on post injury rs-fMRI and literature resources.

1.6 Thesis outline

The breakdown of each subsection of this study are as follows. The computational modelling involved advanced finite element analysis using a currently validated GHBCM model. This provided a quantifiable mathematical approach to understanding the biomechanical responses of the deep brain and soft tissues and relating the output through a comprehensive state of the art review. This subsection has a direct relation to the soft tissue biomechanics that was also a focus of this paper. The brain is a very complicated organ and its structure and in vivo conditions result in complications when attempting to study real world responses and affects in human subject [5].The introduction of axon fiber tracts to the pre-existing model helped improve functional response of the white matter regions of the brain with the final goal to model and simulate real world traumatic head impacts. This further helped solve issues pertaining to the mechanical responses of tissue interaction in the deep brain to predict injury outcomes and aid in diagnosis [46]. Using diffuse tensor imaging which maps the pathways of which water flows through the brain it is possible to create three-dimensional computer tractography's that provide an accurate representation of the functional neural network of the brain [107]. The axonal fiber tract for this study focused primarily on the pathways of the brain and the neural connections that aid in cognitive function [108]. This thesis includes six chapters.

1. Introduction, background and literature review.

2. Development of tools for automated injury prediction and analysis.

3. Exploration of current injury criteria and future measures for brain injury, understanding the effect of a helmet.

4. Development and validation of a parcellated axon fiber FEHM for improved injury prediction.

5. Using new FEHM model to predict injury and pave way to the future, combining imaging, FEA, patient diagnosis and symptoms, with virtual brain injury prediction and symptom prediction.

6. Concluding remarks, future work within group, thoughts on where research should go, impact of study and novelty of research.

Chapter 2

2 Development of a computational concussion injury prediction pipeline for ice hockey helmet performance evaluation

This chapter was co-authored by Dr. Haojie Mao, Marco Gallone, Kierra McDougall and Dr. Ryan Ouckama and is accepted as a peer reviewed paper into IRCOBI conference. For this chapter and the following 4 chapters the introductions include information re-iterated in the introductory chapter, however, for the purpose of publication formats, information is repeated.

2.1 Abstract and Key Terms

Abstract *This study looks to develop and explore a computational approach, along with data gathered from conventional mechanical helmet testing procedures in ice hockey, to provide new insights into how the helmet could protect an individual from concussive type impacts. In this study, five samples of six different ice hockey helmet models were tested using the methodologies set forth by The Summation of Tests for the Analysis of Risk, the STAR helmet rating protocol. Head form kinematics collected during STAR testing were used as inputs to the Global Human Body Model Consortium head finite element model, and each impact (n=672) was simulated. A 15% cumulative strain damage measure threshold was chosen as the main response variable to predict brain injury probability. The results indicate that output kinematics of rotational velocity were most correlated ($r = 0.96$, $P < 0.05$) to cumulative strain damage measure and other strain measures. Impact direction also had significant effects on the strains in the brain, with impacts to the rear, front and side showing statistical significance to cumulative strain damage measure. It was also observed that specific helmets showed less deformation response in certain impact directions compared to others. This study developed a start-to-finish methodology to evaluate helmets for mild brain injury mitigation.*

Keywords *Concussion mitigation, cumulative strain damage measure, injury prediction pipeline, kinematic performance evaluation, mild traumatic brain injury*

2.2 Introduction

The traumatic brain injury (TBI) has become one of the most critical issues affecting global health systems with over 69 million individuals worldwide sustaining this injury every year [1]. An estimated 80% of these injuries are considered to be mild in nature, i.e. concussions, which poses a unique challenge to the researchers, physicians and medical trainers who are tasked with diagnosing, rehabilitating and mitigating their rate of occurrence [2].

In organized sports the issue of the mTBI is rampant, especially in adolescent aged participants [109]. The competitive environment which focuses on physical contact, especially in sports such as American Football and Ice Hockey, leads to increased instances of concussive and sub-concussive impacts that accumulate and could lead to negative short- and long-term neurodegenerative disorders [110, 111]. In both sports the use of a helmet is the primary method of head impact mitigation. The original purpose of a helmet was to provide its wearer protection from mechanical loading that lead to lacerations, abrasions, fractures and other forms of tissue disruptions by absorbing the energy acting on the head upon impact [66]. Helmets, however, need to be improved to cushion the brain and provide protective measures for the mitigation of concussive instances.

One common pathology of mild traumatic brain injury (mTBI) is the diffuse axonal injury (DAI), which is directly correlated to injury outcomes such as unconsciousness, cognitive impairments, and if the level of injury is severe enough, death [112]. The primary mechanical mechanism in DAI is inertial forces applied to the head following impact, that cause stretching of the deep and subcortical white matter. This *twisting* effect leads to extensive deformation of the brain structure and micro-tears to the underlying axon fiber bundles [56]. The issue with DAI, and moreover mTBI, is that it is extremely difficult to quantify the extent of the damage using traditional macroscopic pathology, typically used as assessment tools, post injury [112]. This along with the perceived

randomness associated with concussions, where no two impacts are alike and where the ability to see the difference in brain structure using traditional diagnosis tools, such as computed tomography (CT) and magnetic resonance imaging (MRI) scans, is difficult, spearheading the inability to properly diagnose the patients who suffer from them.

The use of physical dummy testing models has become common practice in both academia and industry to create injury criteria based on kinematics to assess injuries quantitatively. In the sport of hockey, the standards for the level of protection in helmets in Canada is governed by three different organizations; The Hockey Equipment Certification Council (HECC), The Canadian Standards Association (CSA), and the International Organization for Standardization (ISO). All three standards have very similar pass/fail criteria mainly targeted towards the reduction of the probability of sustaining catastrophic head injuries. These current testing protocols are geared towards high energy linear impacts to the head and dummy and have considerable disregard for more mild or concussive like impacts. The current issue with these organizations and the helmet standardization and testing, is that it currently does not take into consideration (1) the effects of rotational motion on the brain, and (2) the effects that more mild or sub-concussive impacts have on the brain structure and relationship to long-term neuro-degeneration. The obvious limitation of such methods is that (1) they do not allow researchers to recreate in vivo head impact scenarios and (2) they are not able to provide adequate representation of the complex, non-linear and anisotropic behavior of the soft-tissue in the brain [113].

Therefore, the need for the kinematic parameters of the helmeted head are required as they provide a direct correlation to the inertial response of the brain and hence could be an invaluable tool to predict the level of injury and provide instant insight into patient diagnosis. The introduction of the Summation of Tests for the Analysis of Risk (STAR) formula and safety testing methodology allows for a novel helmet testing procedures that looks to mitigate some of these inertial effects by examining the rotational forces applied to the helmeted head in low and medium energy level impacts [64, 66]. This STAR testing methodology utilizes the kinematic principles of linear acceleration, rotational acceleration and head impact exposure, a metric based on male and female collegiate

player's impact location and severity over several seasons [66], to provide a resource for consumers to make educated decisions on purchasing helmets which are perceived as most likely to mitigate concussive risk. The STAR Helmet rating system, in theory, should provide a conclusive rating to assess the safety of a specific helmet, acting to keep helmet manufactures truthful and innovative with their research and development into new and innovative concussion mitigation technology, benefiting consumers.

The introduction of computational head and brain models has allowed researchers and engineers to evaluate brain tissue loadings that directly link to damage. With the use of finite element (FE) head models we are now able to recreate the complicated geometries and material structure of the human head. These FE models have allowed for reliable prediction of mechanical response and an accurate description of the constitutive behavior of the nonlinear soft tissue response to loading, e.g., [59, 97, 114-117]][94]. With these computational head models available, developing a computational brain injury prediction pipeline for hockey helmets will help the field to better understand the effectiveness of protection and explore new designs that can better protect the brain.

This study looks to provide details of the development of an automated injury prediction pipeline for large kinematic datasets that will be used to provide new insights into how effective current methodologies such as that of the STAR are in assessing helmet performance and determining injury likelihood. One question that we look to solve is the validity of this methodology in assessing helmet protection and whether the use of linear and rotational acceleration are the best kinematic predictors for injury to the brain structure. This study looks to combine validated computational head models along with the use of validated physical surrogate models and assess the validity of the different testing methodologies and attempt to predict the level of injury mitigation that a hockey helmet helps provide when looking at common concussion-level impacts.

2.3 Methods

2.3.1 Experimental Procedure

To re-create an industry standard method for physical helmet evaluation, this study based its helmet testing procedure on that of Hockey STAR. This methodology of assessing the

biomechanical performance of hockey helmets differs from traditional methods provided by other standardization organizations as it primarily looks to recreate some of the rotational kinematics associated with head impacts. The Hockey STAR equation, Equation 1, includes several unique metrics that pertain specifically to the sport of Ice Hockey. The L represents the location of impact (rear, side, front or top), the θ represents different impact energy levels, these levels were determined in the original methodologies by the angle of the pendulum arm of the impactor. The E represents exposure, the number of times a player is expected to receive an impact in a season. Finally, R, is the risk of concussion as a function of linear (a) and angular (α) acceleration. One of the purposes of this study was to examine whether the variable 'R' is sufficient at assessing the correlation between the kinematic outputs of a traumatic impact and the true level of injury response of the brain.

$$Hockey\ STAR = \sum_{L=1}^{4} \sum_{\theta=1}^{3} E(L,\theta) * R(a,\alpha) \tag{8}$$

The impactor of this study differed slightly from that of the original methodology. Rather than a pendulum as the STAR methodologies originally call for, a pneumatic impactor was used as it allows for more consistent impacts transferred to the head-form and less of a safety risk in testing [62]. Figure 6 highlights the locations of impact, confirmed using slow motion video and pointed tip impactor heads, along with the placement of the accelerometer inside the NOCSAE head form. Like the original laboratory testing procedure; three impact energy levels (low, medium and high) with impact speeds of 2.6 m/s, 4.6 m/s and 6.0 m/s respectively, and four impact locations (front, rear, side and top), were recreated to assess the viability of each helmet sample, see Figure 6. While the front and rear impacts were directed at the center of gravity of the NOCSAE head form, the top and side impacts were not directed at the COG of the head form and hence added an element of tangential loading. It needs to be highlighted the top impact (Figure 6-D) was not a conventional impact delivered from the vertical side, but more an impact with an elevation. Each helmet was hit twice with the impactor (19.94 kg) per direction per impact speed per trial, with four to five helmet samples for each helmet model type. In this study six different helmet models were tested. In total each helmet went through an

average of 112 impacts for a total of 672 impacts with corresponding kinematics. Helmet tests were analyzed for repeatability by assessing the standard deviations of individual kinematic metrics of repeating trials.

The helmets were fitted onto a medium size National Operating Committee on Standards for Athletic Equipment (NOCSAE) head-form mounted on a Hybrid III 50th percentile neck with three Endevco 7264C-2KTZ-2-240 (Meggitt, Bournemouth airport, Dorset, United Kingdoms) accelerometers for linear acceleration, and three rotational velocity channels of the DTS6DX Pro (Diversified Technical Systems, Seal Beach, California, USA) mounted in the center of mass of the head form. Two Endevco Model 136 amplifiers provided excitation voltage and signal conditioning. The kinematic data of each helmet impact; linear acceleration, rotational acceleration and rotational velocity, were collected at 20 kHz with a filter chain of Hardware CFC1000 filter at amplifier for all channels, software CFC1000 filter on linear acceleration and software CFC155 filter on rotational velocity. A custom script was then developed to export the data into a spreadsheet including X, Y and Z axis data.

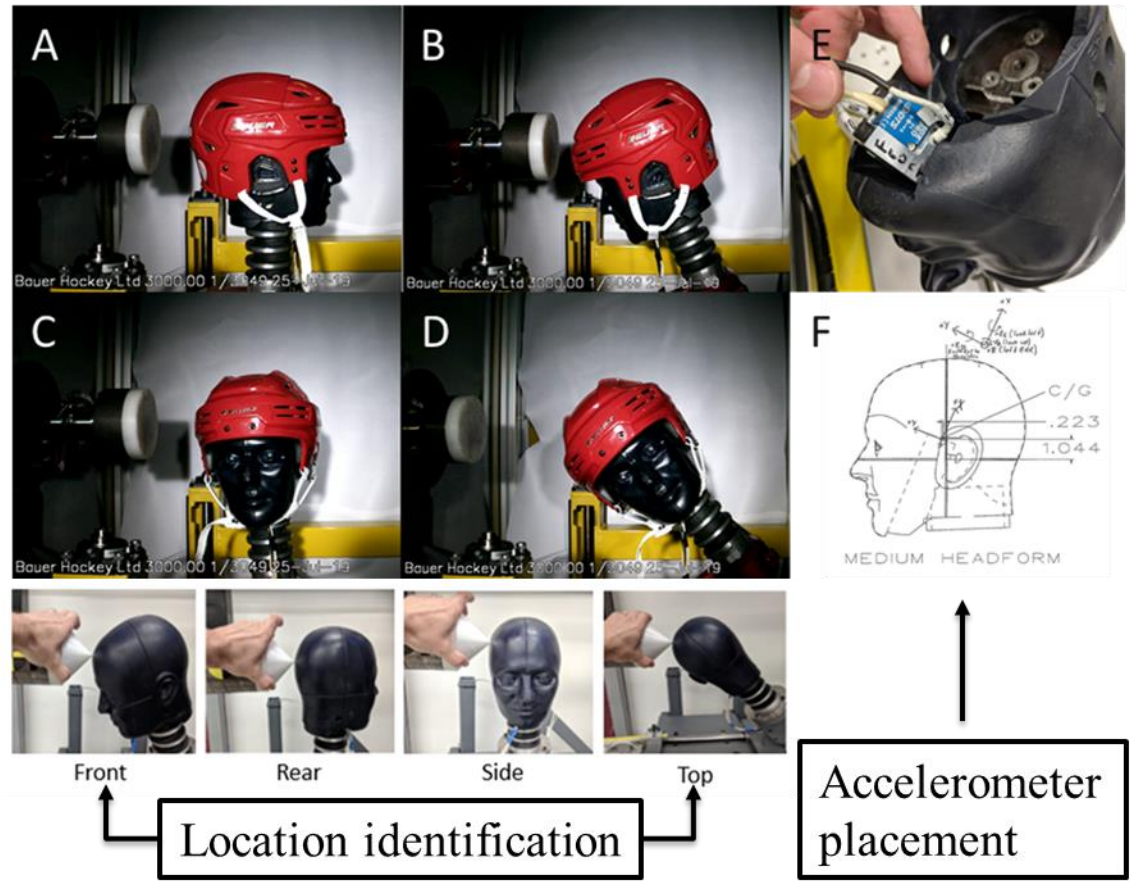

Figure 6, the experimental setup procedure and helmet impact locations modelling that of the Virginia Tech STAR Methodology (A) Rear Impact (B) Front Impact (C) Side Impact (D) Top Impact (E) placement of Endevco accelerometer in the center of gravity of the NOCSAE head form with Hybrid III neck and (F) the schematic of the placement of the accelerometer measured in inches for accurate recreation of kinematics in the computational model.

2.3.2 Computational Modelling

The finite element model used in this study to simulate the physical testing impacts was the Global Human Body Model Consortium (GHBMC) head model [59]. This validated model of the human brain and skull is based on (CT) and (MRI) scans of a healthy adult male brain of average height and weight. This model allows for a biofidelic computational model to simulate and interpret the mechanical stresses and strains associated with traumatic impact. The GHBMC model, as seen in Figure 7, allows for the

quantification and visualization of the mechanical soft-tissue material metrics in key anatomical regions such as; the corpus callosum, thalamus, cerebellum, brainstem and basal ganglia. In this model a linear visco-elastic material was used in both the grey and white matter with the skull modelled as a piecewise-linear-plastic material. In total the GHBMC head and brain model contains 62 components of bone and soft-tissue, 61 unique material properties and 270,552 total elements (beam, shell and solid), and is validated against intracranial pressure and brain displacement data [118, 119].

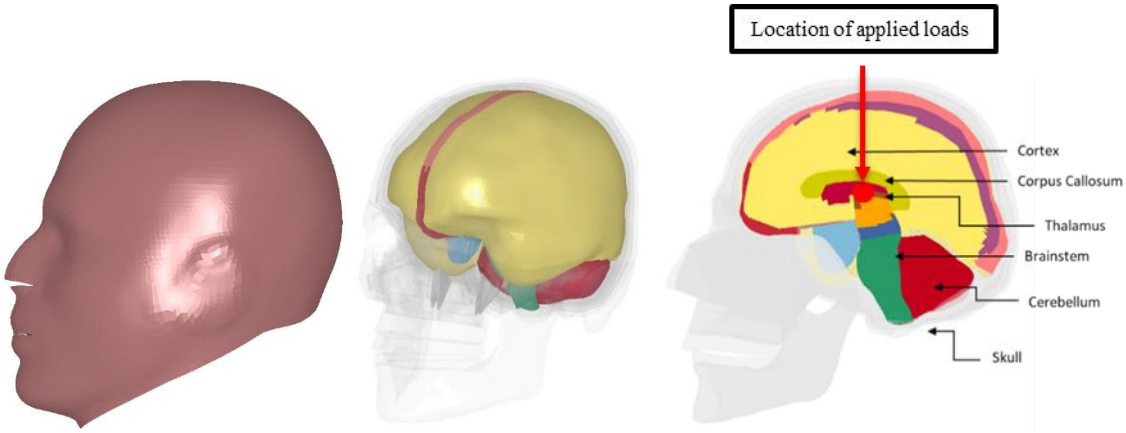

Figure 7, breakdown of GHBMC head and brain finite element model. From top to right, full GHBMC model with skin, isometric view of model with skull and skin transparent to view placement of brain and sagittal view of model showing the placement of different anatomical components of the brain along with the location of applied loading.

When setting up the model, the direction of the kinematics was reoriented to a 23-degree offset above the horizontal Y- axis to mimic the sensor setup in the original dummy head form. The orientation of the raw data provided by Bauer originally differed from the automotive standard orientation of the GHBMC model, hence the need for model orientation manipulation to align with the provided data for automated pre-processing. An initial dataset of an impact in three different impact energy levels in a single direction based on a single helmet sample was provided to determine an optimized time of impact to allow for both analysis of the moment of maximum principal strain as well as allowing for efficiencies regarding computational time and resources. The kinematic curves used

in this study were determined through an initial testing round, the overall time of simulation (80ms) (Figure 8, left) was used based on the peak strain responses of a test impact (t = 200ms) where peak max principal strain (MPS) (Figure 8, right) was included along with subsequent inertial response. The simulations were then completed on a Lenovo workstation (2 X Intel Xeon GOLD 5118 Processor (12 cores @ 2.3GHz), 128 GB DDR4 Memory) using LS-DYNA, finite element program, (Livermore Software Technology ANSYS LSTC, Livermore, CA, USA) with simulation time equivalent to ~2 hours per simulation at NCPU = 2, for a total computational time of ~1344 hours. Each simulation was then analyzed in LS-PrePost and checked over for any logical errors, such as accurate direction of motion and strain levels within an expect range.

2.3.3 Pipeline Logic

An in-house MATLAB script was created to orient the GHBMC head model, apply the kinematic data from the Excel file as a time history loading curve and save as the original file name into a new keyword file for the increased efficiency of setup for all 672 simulations automatically. This script also applied a rotation matrix to the original kinematics to orient peak kinematics to the GHBMC computational model's strain output and calculated the resultant linear accelerations, rotational accelerations and rotational velocities of each impact scenario. Each completed simulation was then passed through another in-house post-processing pipeline, which analyzed the maximum principal strains (MPS) of all elements throughout the time history plot and, using a customized script, determined the cumulative strain damage measure (CSDM) of each impact at a pre-set strain level. CSDM, which is suggested as a predictor of brain injury response, was used as a measure of brain responses induced by different impacts and provides the diffuse pattern of the total damage that could occur to the brain leading to a damage [79]. Based on the MPS of each element the algorithm can determine the percentage of the elements in the GHBMC model that are above a threshold specified by a user. This study examined five CSDM scenarios ranging from mild to severe in terms of predicted brain damage (CSDM5, CSDM10, CSDM15, CSDM20 and CSDM25). Where a value of CSDM20 = 0.50 would mean that 50% volume of the elements in the GHBMC head model would experience strains over 20%.

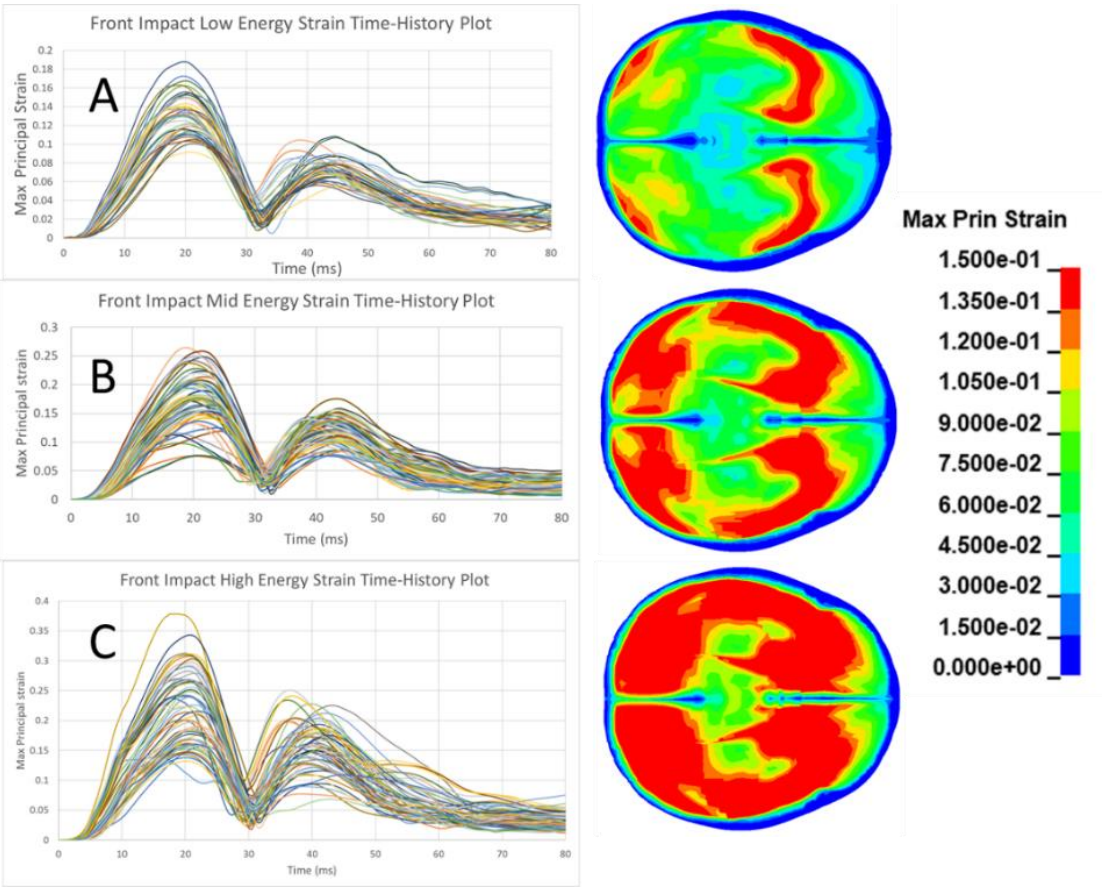

Figure 8, representation of the typical strain patterns in a frontal impact on helmet E at 15% max principal strain fringe level in the GHBMC model in the transverse cross-sectional view. Representation of typical time-history strain patterns of (A) low 2.6m/s, (B) Mid 4.6 m/s and (C) High 6.0m/s energy impact levels. Initially 200ms plots were used as justification for 80ms simulation time on all simulations to encompass the peak of the maximum strain to the brain elements while reducing computational time and cost.

2.3.4 Pre-processing Pipeline Explained

This script converted Excel kinematic data into the linear acceleration and rotational velocity time-history curves used as a boundary condition of a prescribed motion in LS-DYNA. Each kinematic impact scenario output manipulated a baseline GHBMC keyword file with new time history curves in the X, Y and Z directions for a total of six degrees of freedom, all of this being done automatically with the process pipeline which

is described with associated functions below. The kinematic curves were applied to a point at the COG of the GHBMC model. This point acted as a rigid connection to the skull and hence any applied kinematics are transferred directly to the skull motion. The brain motion is derived from the reaction to the skull motion where different brain-skull connectors act as the boundary conditions that facilitate the relative brain-skull displacements. This pipeline allows for a computational approach to convert easily reproducible XYZ data into a keyword file which is fully ready for input into the LS-DYNA solver.

2.3.5 Post-processing Pipeline Explained

The post processing pipeline looks to take the simulated GHBMC model and extracts the element data output (ELOUT) file. This process acts as a batch script to utilize a custom in-house script [120] and extract the MPS of each element and the total volume of the brain and calculate the CSDM of the brain at varying levels to provide a glimpse into the perceived level of sub-concussive and concussive injury likelihood. All files in a folder can be examined with a single click, and hence 672 individual CSDMS were examined in this experiment. A simplified schematic is provided in Figure 9. With a breakdown of the pipelines coding logic explained in Appendix A.

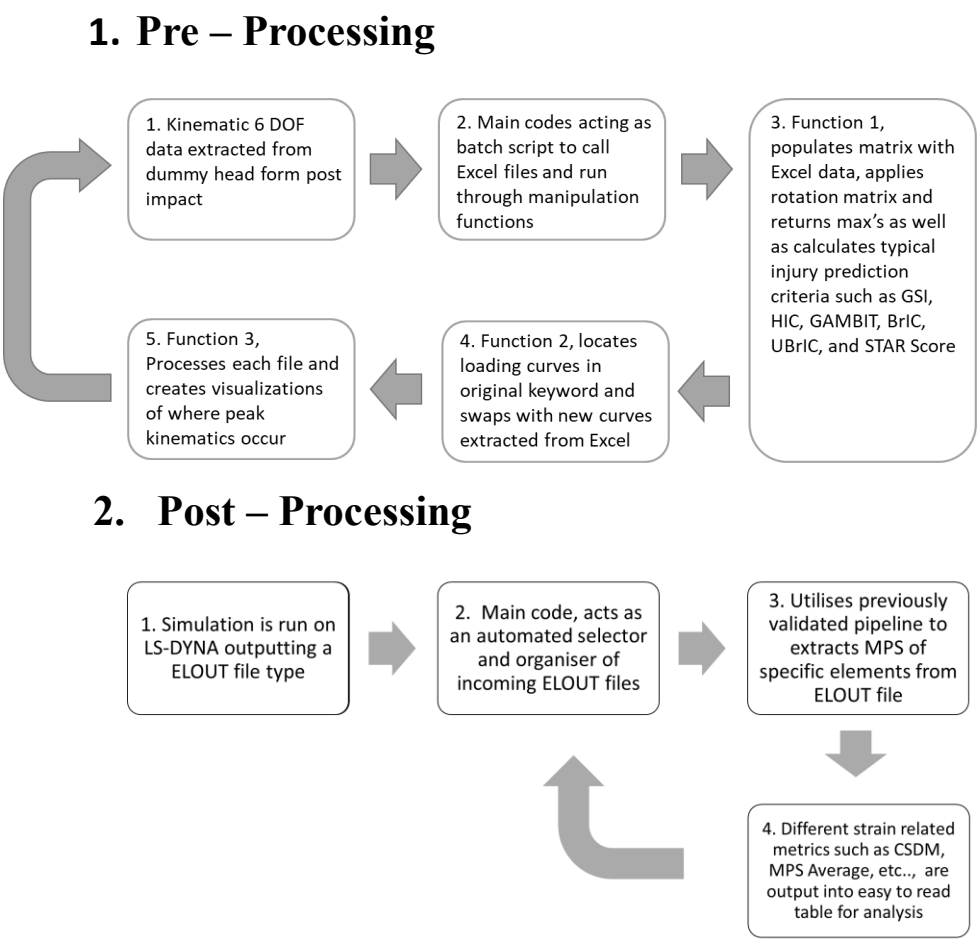

Figure 9, schematic of the pre- and post- processing pipeline in simplified terms. A full breakdown of the logic behind the kinematic injury prediction pipeline is available in the supplementary material.

2.3.6 Analysis

Statistical analysis tools were used to analyze the correlation between the CSDM values and the peak kinematics, along with comparing the relative safety of each helmet in terms of mitigating brain injury and reducing corresponding inertial factors. All values were analyzed using IBM SPSS Statistics 26 (IBM, Armonk, New York). Statistical tests performed included determining the R^2 values in a linear regression, Pearson correlations, and completing One and Two-way Analysis of variance (ANOVA) to compare resultant data.

2.4 Results

Repeatability tests show that overall differences for the same impact setting were small (Table 3). For example, for the helmet 'A', samples were broken down into its first and second trials, showing similarities in the resultant peak linear acceleration (RPLA), resultant peak rotational velocity (RPRV) and resultant peak rotational acceleration (RPRA) of each direction and at each energy level.

Table 3, example impact showing test repeatability under same experimental condition, in this example, helmet A is shown with average percent difference of all trail 1 vs trail 2 shown.

			Trail 1			*Trial 2*			*Avg Diff.*
Helmet	Impact Energy	Direction	**RPLA**	**RPRV**	**RPRA**	RPLA	RPRV	RPRA	
A	Low	Front	**54.15**	**22.04**	**2084.66**	50.26	22.37	2140.46	3.86%
	Mid	Front	**86.41**	**32.00**	**3604.53**	85.26	32.18	3526.64	1.36%
	High	Front	**166.64**	**43.91**	**4407.81**	181.08	43.95	4968.79	6.79%
	Low	Rear	**57.84**	**21.55**	**2556.78**	52.99	22.07	2331.47	6.78%
	Mid	Rear	**77.92**	**29.28**	**3527.65**	76.56	29.60	3433.27	1.85%
	High	Rear	**117.59**	**37.62**	**5257.20**	124.24	39.12	5148.83	3.83%
	Low	Side	**54.71**	**18.59**	**3502.87**	53.29	18.53	3612.59	2.01%
	Mid	Side	**107.26**	**26.22**	**6550.22**	110.20	26.23	6648.86	1.41%
	High	Side	**206.54**	**34.99**	**11522.78**	232.42	36.25	12756.8	8.50%
	Low	Top	**41.48**	**15.32**	**2886.14**	41.99	16.51	3142.34	5.73%
	Mid	Top	**72.44**	**18.46**	**4827.23**	79.37	22.78	5067.64	11.65%
	High	Top	**166.12**	**30.99**	**9589.87**	197.37	33.29	11748.32	14.86%

The range of linear accelerations, rotational velocities, and rotational accelerations is described in Table 4 for all 672 impact scenarios. On average, RPLA reaches 121 g's and RPRV reaches 28 rad/s.

Table 4, breakdown of the linear accelerations, rotational velocities, and rotational accelerations

Kinematic	*Minimum*	*Maximum*	*Mean*	*Std. Deviation*
Linear Acc. X (g)	6.81	228.65	41.01	43.23
Linear Acc. Y (g)	2.83	326.69	63.87	62.31
Linear Acc. Z (g)	1.29	355.17	62.38	79.98
RPLA (g)	31.85	417.05	121.01	80.56
Rotational Vel. X (rad/s)	0.37	19.56	4.29	3.77
Rotational Vel. Y (rad/s)	0.27	44.43	12.58	12.62
Rotational Vel. Z (rad/s)	1.51	47.28	18.31	14.43
RPRV (rad/s)	11.75	47.31	28.29	8.57
Rotational Acc. X (rad/s/s)	301.03	8492.54	1556.25	1647.92
Rotational Acc. X (rad/s/s)	273.90	18813.32	3778.66	4323.23
Rotational Acc. X (rad/s/s)	516.16	10940.55	2944.12	2005.51
RPRA (rad/s/s)	1635.78	19321.35	5814.78	3822.74

2.4.1 The Pipeline to Connect Head Kinematics and Brain Strains

A completed pipeline was developed and tested for all 672 impact scenarios. This pipeline reduced overall pre-processing time from approximately 20 minutes of manual keyword manipulation to approximately two minutes per scenario of automated computational manipulation. This pre-processing pipeline allowed for all 672 impacts XYZ kinematic output data to be converted into keyword files for simulation by LS-DYNA solver in approximately 22 hours of computational time compared to over 220 hours, or 10X less total time. Following the simulation of all 672 impacts, the post processing pipeline was engaged. This pipeline determined the CSDM of each simulation and organized all simulations into an Excel spreadsheet, in approximately five minutes per simulation or a total time of approximately 56 hours. The original manual extraction and manipulation of the post processed data into CSDM data was approximately 10 minutes per scenario or a total time of 112 hours. This represents a 100 percent increase in total computational time and the need for user intervention. The results were organized into an easy to read spreadsheet that allows for data analysis.

2.4.2 The Correlation between Head Kinematics and Brain Strains

Assessing all 672 scenarios the peak kinematics with averages were compiled from the initial dataset and the CSDM values were all computed and related to each impact test scenario. As seen in Figure 10 all peak impact kinematics were compared with CSDM15, which was determined as a valid assessment of DAI as a threshold for the maximum strain an axon could withstand before exhibiting signs of tearing or deformation [43]. The RPLA ($R = 0.61$ $P < 0.01$) and RPRA ($R = 0.51$ $P < 0.01$) were less correlated to CSDM15 than RPRV ($R = 0.96$ $P < 0.01$). This analysis was done using SPSS, and the bivariate correlation coefficient was Pearson with the test of significance being two-tailed (Figure 10). Of note, CSDM metrics correlated heavily with other similar strain-based metrics such as average MPS and MPS top 1 percent and 5 percent thresholds ($R=0.99$ $P < 0.01$, $R=0.98$ $P< 0.01$ and $R=0.99$ $P<0.01$). Other widely used kinematics based injury criteria, primarily the head injury criteria (HIC_{15}) and the Brain Injury Criteria (BrIC) were also included in the analysis to better understand their correlation to the different strain metrics, with BrIC showing strong correlation to average strain ($R=0.897$ $P<0.01$) (Figure 10). Interestingly while HIC_{15} produced a middling linear regression of $R^2 = 0.57$ when compared to average strain its cubic regression was $R^2 = 0.812$, meaning that the HIC scores while not linearly correlated to Strain did provide some correlation relationships.

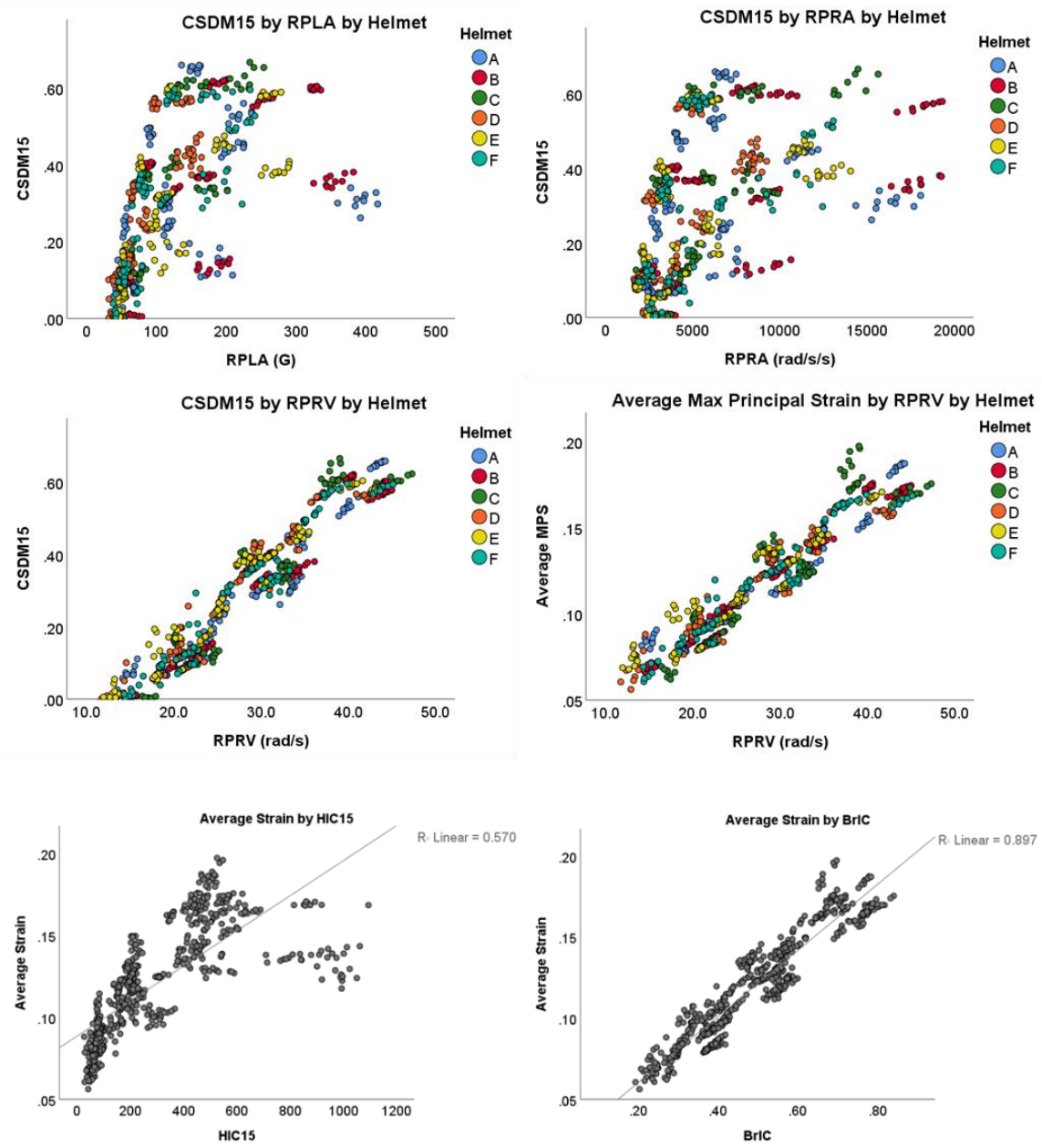

Figure 10, these graphs represent the peak resultant kinematic of each impact scenario (n=672); Top left, resultant peak linear acceleration (g) compared to CSDM15, top right, resultant peak rotational acceleration (rad/s/s) resultant compared to CSDM15, bottom left peak rotational velocity(rad/s) compared to CSDM15 and bottom right is RPRV compared to average max principal strain. The bottom two grayscale scatterplots show the relationship of common injury prediction criteria HIC15 and BrIC.

2.4.3 Impact Direction and Helmet Strain Effect on Brain Response

Impact direction and the effects of the helmets on reducing brain strains by way of CSDM was also analyzed. Results show that impact direction has effect on relating to relative CSDM value, with rear impacts showing the largest mean CSDM values across all CSDM levels and all impact energy levels. Rear impacts were followed by Front then Side and finally by Top impacts. It is also noted that helmets exhibited varying levels of success in different directions with some helmets mitigating brain strain response in one direction more effectively than other helmets and in other directions less effectively than other helmets. A representation of these results is shown in Figure 11 below. For impact direction relationship to CSDM15 there was a statistically significant difference between groups as determined by One-way ANOVA ($F(3, 668) = 39.846$ $p < 0.01$). A Tukey post hoc test revealed that CSDM15 was statistically significantly higher in impacts to the Front (0.337 ± 0.198 $p < 0.01$), Rear (0.382 ± 0.189 $p < 0.01$) and Side (0.295 ± 0.178 $p < 0.01$) compared to Top impacts (0.179 ± 0.195). There was no statistically significant difference between Side and Front impacts ($p = 0.139$). with the assumptions that the population was close to normal distribution, the samples independent population variance is equal and that the groups are of equal sample size ($n = 168$ each). The Two- Way ANOVA was also completed in SPSS, looking at impact direction and helmet type at the different energy levels. The results show that helmet type was not a statistically significant factor $p = 0.082$, with impact direction being the main signifier of strain $p < 0.01$. The combination of the two did provide a statistically significant factor $p = 0.045$, however the R^2 value of 0.162 was low. Therefore, helmet type has no significant effect on strain levels, however impact direction based on all three energy levels appears to have a significant effect. However, the combination of helmet type and impact direction appears to have some statistically significant effect on MPS average, and hence more analysis is needed.

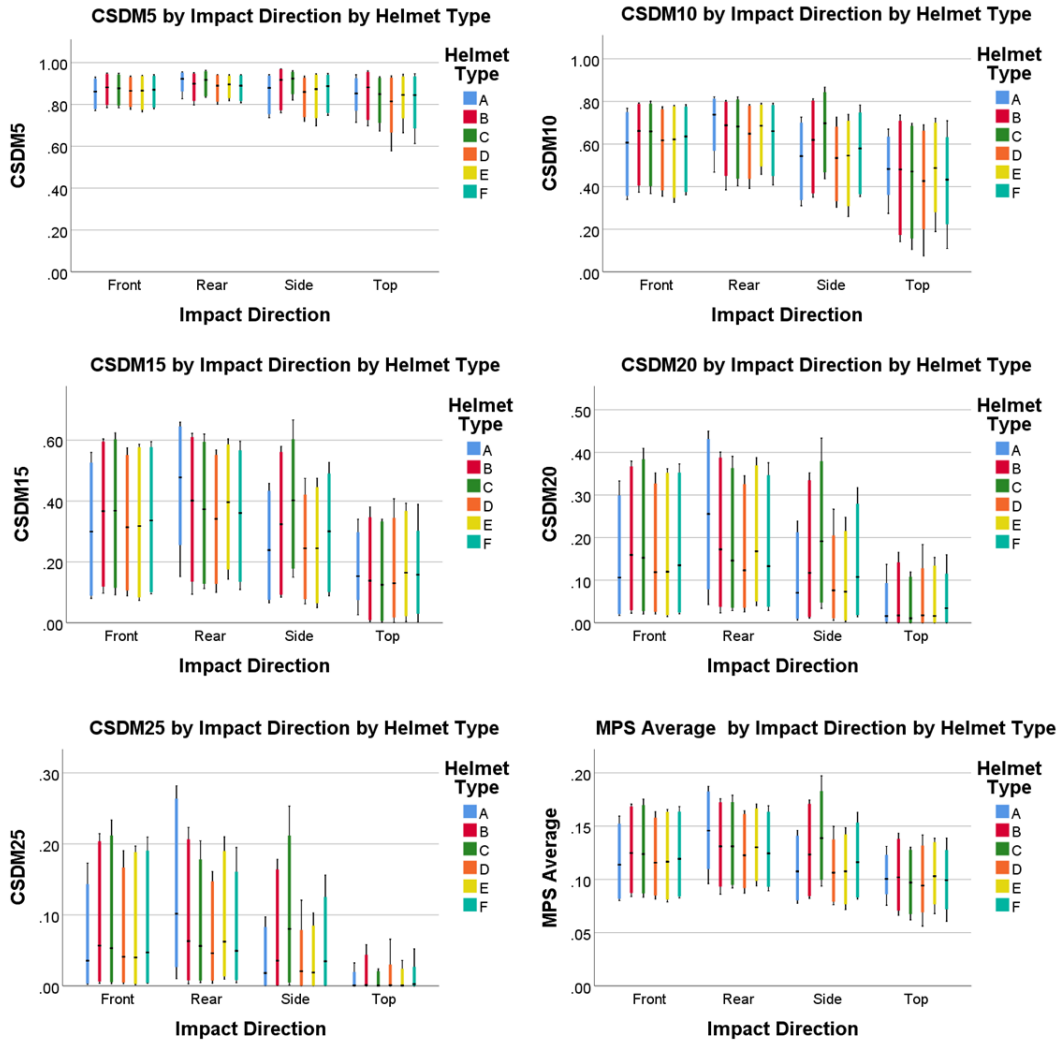

Figure 11, graphs examining the differences between impact direction and relative CSDM effect for all five CSDM levels analyzed (CSDM5 to CSDM25), each direction has then been further broken down into the relative effect each helmet has in mitigating the CSDM value and for comparison average MPS.

2.5 Discussion

2.5.1 Adopting a Computational Brain Injury Prediction Pipeline besides Experimental Testing

This study was established behind the theory that mechanical strain is an effective tool to evaluate the brain injury response using computational head models. The use of CSDM

has been an effective tool to correlate the overall strains experienced by the GHBMC model and the probability of brain injury that is to be expected following a similar impact in a real world traumatic head impact scenario [79]. Such a pipeline is justified as timely as both large quantity of experiment tests and high-quality FE human head models have been made available in the field. Such a pipeline will help to overcome the hurdle of time and difficulty of handling hundreds to thousands of head impact simulations, while allowing for quick comparisons of current injury prediction metrics and future metrics and brain strains. More datasets to be generated in the field, together with our study, will allow users to better understand the protective effects of helmets by understanding how helmets help to reduce brain strain. Where the real innovations will occur is with the compilation of such large datasets, with multiple parameters, to allow for in-depth analysis and the application of new technologies and research tools to provide a computational solution to this complex problem.

2.5.2 Using Peak Rotational Velocity rather than Peak Rotational Acceleration

This study was an effective indicator of the relationship between rotational velocity and the brain strain response of the brain based on 672 experimental impacts and 672 FE simulations. The correlation between rotational velocity and brain strain in the form of CSDM supports the usage of peak rotational velocity rather than peak rotational acceleration and peak linear acceleration, at least for the specific testing scenarios that we investigated. Linear acceleration as a good indicator of intracranial pressures [114], is substantially less effective in providing insight into the brains deformation incurred through maximum principal strains, maximum shear strains and other stress-strain related metrics [44]. In previous practice, the use of helmet-mounted head impact telemetry (HIT) system [65, 121] documented valuable peak head acceleration, but ignored the entire time histories of accelerations and hence missed the opportunity of calculating rotational velocity. Hence, newly developed sensors such as mouth guard sensors [122, 123] that not only rigidly attached to the skull to minimize helmet-to-head sliding effect, but also provided time histories of rotational kinematics, will help to collect rotational velocities from human participants. Hence, the correlation between rotational velocity

and observed concussion risks can be analyzed to further improve helmet evaluation approach.

Studies that involve the use of several FE head models, head kinematics, brain responses and brain injury risks have been conducted. A study which was also focused on ice hockey and used a specific guided drop tower to collect head kinematics, reported that resultant change in angular velocity best predicted MPS and CSDM15 [124]. Beyond ice hockey, Takhounts et al. also reported strong correlation between max resultant rotational velocity and CSDM with an R^2 of 0.92 [79]. Our in-house study using various theoretical loading curves supported rotational velocity best correlated with CSDM and average MPS [52]. It was also demonstrated that the peak change in angular velocity was shown to have a better correlation with strain levels for purely rotational impulses than angular acceleration, or HIC, both of which were demonstrated in this study [98, 125]. Given agreements made across research groups, injury metrics like BrIC that considers rotational velocity are recommended to predict strain-related brain damage. Together these studies highlighted that while linear acceleration is a good indicator of the intracranial pressure it lacks the ability to indicate the deformations in the brain. While rotational acceleration, which previously was believed to correlate to brain strain, is insufficient. Future helmet methodologies, particularly ones that attempt to quantify the potential risk of mTBI, are recommended to be focused on a combination of linear acceleration that correlates to brain pressure and rotational velocity that correlates to brain strain. This study reasons that injury assessment metrics, like that of Hockey STAR, can be further developed and improved by considering the inclusion of rotational velocity in combination with rotational acceleration to improve strain-based prediction accuracy.

2.5.3 Recommended use of Brain Strains Pipeline and Limitations

This study helps to highlight the potential applications of a fully automated testing to injury prediction pipeline for the categorization of consumer-focused helmets. While this paper focused its direction on that of hockey helmets, the possibilities of this helmet process are numerous. The STAR helmet rating protocol itself encompasses more sports than just hockey and any other kinematics-based helmet testing protocol that outputs X, Y and Z-direction kinematics could also be adapted to this pipeline seamlessly.

There are limitations of this study. As is the case with brain injury, the understanding of what constitutes as a definitive concussive or sub-concussive scenario is still an uncertainty and therefore the reliance on only CSDM as the singular predictor of brain injury is a limiting factor. Although CSDM is a validated DAI predictor in the GHBMC model, other predictors have been shown to be equally as effective or have exhibited different advantages in the GHBMC and other computational head and brain models. Kleiven et al. have shown that pressure is a good predictor for mTBI and that while rotational motion is effective in perpetuating strain response, it does very little in terms of contributing to pressure response [44]. Therefore, future studies using this dataset could include more examination and analysis of other predictor methodologies that would encompass all kinematic factors and therefore view a larger scope of the brain predictor metrics. Another limitation of this study is the inherent limitation with finite element head models that are validated against brain-skull relative motion, as it was recently determined to possibility not be fully sufficient in determining accurate strain prediction outputs [126, 127]. Validation of head models against experimental brain strains in addition to brain-skull relative motion was suggested and will be further explored in future studies.

A limitation arises with the validity of this testing methodology, as while the side and top impacts have some tangential contact with the head forms, the rear and frontal impacts go through the center of gravity and hence do no provide that tangential factor. While we acknowledge this as a limitation what this study explores is how this widely used and accepted experimental testing methodology is related and potentially lacking in its prediction of the brain's response, particularly in terms of brain strain. The Hockey STAR helmet testing protocol uses real world data as the exposure metric, validating some of the linear and rotational acceleration values, meaning that the conditions could be assumed to be realistic in hockey, and hence the evaluation of these helmets is appropriate, or at least consistent as a comparison tool.

2.6 Conclusions

We developed a novel computational brain injury prediction pipeline that was based on validated industry used methodologies and computational models to evaluate the

concussive and sub-concussive mitigating potential of hockey helmets. The helmet industry, and those of football and hockey are committed to innovating for changing consumer behaviors and provide helmets that are safer, especially in mTBI or concussive impacts. What this paper helps to provide is a stepping stone for the current limitation of some of the state of the art testing procedures and an approach into how to quickly and automatically test new metrics that could involve machine learning or artificial neural networks to predict kinematic injury thresholds to help design future helmets. This preliminary study focused on understanding and showcasing which traditional helmet testing output kinematics are most correlated to brain injury, as per the CSDM metric, and provided initial insight into the effects of direction on brain injury and how well individual helmets can mitigate these effects. Rotational velocity is a significant contributor and predictor of brain strains and future helmet testing protocols need to include this telling metric. This study has also provided some initial reporting that future innovations in helmet design need to consider impact direction when attempting to limit brain strains. Future studies will delve deeper into understanding the underlying factors that influence the success of a specified helmet in mitigating brain strains and analyze more statistically significant relationships between specific kinematic mechanisms and the level of injury a real-world subject might experience.

2.7 Acknowledgement

1. We acknowledge funding provided through the NSERC ENGAGE program in partnership with Bauer Hockey Ltd, Blainville, Quebec, and Canada Research Chairs program.

Chapter 3

3 Investigating injury metrics in predicting brain damage and evaluating hockey helmets

3.1 Abstract and key terms

Abstract *Understanding what qualifies as a concussion and how to prevent or mitigate this devastating injury is still in need of more exploration. This study used one of the most common concussion prediction testing methodology in the sport of hockey, known as the Hockey STAR, to assess 6 different helmet models. Using one of the most state of the art and validated FEHMs, GHBMC, the concussion mitigation potential of the different helmets were tested and the validity of the STAR helmet testing protocol was assessed against widely used kinematics-based traumatic head injury prediction criteria and compared to strain based injury predictors. This novel study showed that while the level of STAR varied greatly between different helmets (113.0 %), the level of strain in the brain was consistent with changes of less than (10.8 %), indicating variances in the injury mitigation capabilities of different helmets when being evaluated by two approaches. This study concluded that the main factor of this discrepancy is the lack of a rotational velocity component in the STAR equation, which correlated much more highly to MPS and CSDM metrics than linear or rotational acceleration. Furthermore, this study evaluated recently proposed evaluation methods such as UBrIC and DAMAGE. Finally, this study introduced an ANN based injury predictor which used rotational velocity and linear acceleration to predict MPS at a* R^2 *of 0.988, which could provide helmet manufactures an efficient tool to quickly test the concussion mitigation potential of their helmets.*

Key terms: Concussion, Brain Injury prediction, Strain-based assessment

3.2 Introduction

3.2.1 Background

The mild traumatic brain injury (mTBI), is quickly becoming one of the most critical global health issues. With over sixty-nine million individuals experiencing TBI every year, there is a growing urgency from academia and industry to provide validated and tested solutions to this ever-growing problem [1]. One of the prevalent issues that arises from sustaining this form of injury is the seemingly random onset of varied post injury symptoms and the widespread inability to rehabilitate these injuries and return the affected individuals back to their regular day-to-day life. The concussion, one of the most common pathologies of mTBIs is on the forefront of research and media alike. Typically victims of diagnosed concussions experience a multitude of symptoms both in the short-term (unconsciousness, headaches, cognitive impairments, dizziness, etc.) and long-term such as neurodegeneration and in some cases death [3]. Researchers are limited in their ability to diagnose and assess the level of injury, due to inherent limitations, the skull is opaque and hence limits visual view of the brain, and this leads to confusion and varying opinions on what mechanical mechanism is the primary factor in concussion occurrence.

Organized sport is one area where the research into mTBI, and, concussive and sub-concussive impacts are growing and providing novel insights into prevention and mitigation, especially on developing new helmets. This environment provides several important benefits over other primary concussion sustaining environments such as random falls or automobile accidents; (1) A controlled and monitored location (video accident reconstruction), (2) individual protective equipment (individual telemetry systems) and (3) a competitive and physical situation where athletes are encouraged to tackle and hit opposing players. In some sports, such as American Football and Ice Hockey, the use of physical contact is a primary mean of gaining a competitive advantage. These sports are made up of mostly adolescent aged individuals where the outcome after sustaining a concussion is debilitating to the evolving brain. One of the primary methods that these sports looks to mitigate the risks associated with TBI is using a protective helmet. These helmets however were not originally designed to reduce the risk of sustaining a concussion but were designed as the first line of protection from

mechanical loading that leads to common injury types such as lacerations, abrasions, fractures and other surface level forms of tissue disruptions [66]. There is an urgent need for helmet technology to be improved to assist in energy absorption to reduce the forces leading to more mild injuries such as the concussion.

Manufacturers have been conducting experimental testing on helmets mounted onto dummy head form. The tests modes include linear-impactor-induced, pendulum-based, and gravity-guided impacts to the head in a laboratory setting. In the sport of hockey, the standards for the level of protection in helmets is governed by three different organizations; The Hockey Equipment Certification Council (HECC) [128]. The Canadian Standards Association (CSA)[129], and the International Organization for Standardization (ISO)[130]. All three standards have similar pass/fail criteria mainly targeted towards the reduction of the probability of sustaining catastrophic head injuries. These current testing protocols are geared towards high energy linear impacts to the head and dummy but not for more mild or concussive like impacts.

3.2.2 Kinematic relationships to brain injury

The use of head injury metrics to predict the probability of sustaining a brain injury are usually calculated based on the resultant kinematic responses of the head during and immediately following an observed impact. One of the earliest metrics proposed to provide a link between resultant kinematic and brain injury was that of Lissner and Gurdjian et al. widely known as the Wayne State Tolerance Curve (WSTC) [131, 132]. This equation explored the relationship between the linear acceleration and duration of an impact and how that effected the head injury. The data provided by the WSTC was and still is the basis of many widely used and cited injury metrics such as the Gadd Severity Index (GSI) which uses linear acceleration, and impact duration and is effective at quantifying severe skull fractures and severe brain injuries, but has limitations in its ability to predict the risk of more mTBI’s such as the concussion [72]. Another commonly used prediction metric is the Head Injury Criterion (HIC) which is based on the WSTC and is calculated by averaging the integrated curve of the time history of the resultant acceleration over a specified time interval with a power of 2.5,

and finding the maximum HIC value, with HIC_{15} being the most adopted with a time interval of 15ms [133] .

These early linear-acceleration-based injury prediction metrics were then expanded on with the inclusion of rotational motion to incorporate the deformation of the brain typically associated with common pathological injuries such as diffuse axonal injury (DAI). These new metrics were better suited to provide better assessments of more mild injuries such as concussions. The development of the Generalized Acceleration Model for Brain Injury Threshold (GAMBIT), became one of the first criterions that took into effect both linear and rotational kinematics[78]. The Brain Injury Criteria (BrIC) was then developed to examine the predicting potential of angular velocity, which theoretically provides a clearer image of an impact as it inherently includes duration and overcomes the limitations of using only translational acceleration [79].

These different injury criterions continued to develop and encompass more details including real world head impact data, an example of this is the Head Impact Telemetry Severity Profile (HITsp), a weighted composite score which takes into account; linear acceleration, rotational acceleration, impact duration and impact location through the use of HIC and GSI [134]. The introduction of FEHM such as the GHBMC model led to the introduction of new injury metric which used second order mechanical system to behave similarly to the brain deformation response to angular head motion. Two of these metrics, particularly the Universal Brain Injury Criterion (UBrIC) and the Diffuse Axonal Multi-Axis General Equation (DAMAGE), utilize rotational kinematics and compare their correlation to typical FEHM response outputs such as CSDM and MPS in order to estimate the probability of sustain injuries such as DAI [85, 86] [19, 88].

The Summation of Tests for the Analysis of Risk (STAR) formula and safety testing methodology recently developed by Rowson et al., is based on similar ideologies. Allows for a novel helmet testing procedures that looks to mitigate some of these inertial effects by examining the rotational forces applied to the helmeted head in low and medium energy level impacts [64, 66]. This STAR testing methodology utilizes the kinematic principles of linear acceleration, rotational acceleration and head impact

exposure, a metric based on male and female collegiate player's impact location and severity over several seasons [66], to provide a resource for consumers to make educated decisions on purchasing helmets which are perceived as most likely to mitigate concussive risk. The STAR Helmet rating system, in theory, should provide a conclusive rating to assess the safety of a specific helmet, acting to keep helmet manufactures truthful and innovative with their research and development into new and innovative concussion mitigation technology, benefiting consumers. While considered an improvement over traditional helmet assessment methodologies it has its inherent limitations. The issues with these kinematics-based metrics is that they treat the head and brain as a rigid mass, with no inclusion of the deformation and potential strains that affect the brain. Table 5 lists widely used injury metrics.

Table 5, kinematics-based injury metric equation summary

Injury Metric	*Equation*
1. GSI	$GSI = \int a(t)2.5dt$
2. HIC	$HIC = \max_{t_1, t_2} \left\{ (t_2 - t_1) \left[\frac{1}{t_2 - t_1} \int_{t_1}^{t_2} a(t)dt \right]^{2.5} \right\}$
3. GAMBIT	$GAMBIT = \left[\left(\frac{a_{max}}{a_{cr}} \right)^2 + \left(\frac{\alpha_{max}}{\alpha_{cr}} \right)^2 \right]^{\frac{1}{2}}$
4. BrIC	$BrIC = \sqrt{\left(\frac{\omega_x}{\omega_{xC}} \right)^2 + \left(\frac{\omega_y}{\omega_{yC}} \right)^2 + \left(\frac{\omega_z}{\omega_{zC}} \right)^2}$
5. UBrIC	$UBrIC = \left\{ \sum_i \left[\omega_i^* + (\alpha_i^* - \omega_i^*) e^{\frac{\alpha_i^*}{\omega_i^*}} \right]^r \right\}^{\frac{1}{r}}$
6. DAMAGE	$DAMAGE = \beta max_t \{ \vec{\delta}(t) \}$
7. STAR (Hockey)	$Hockey\ STAR = \sum_{L=1}^{4} \sum_{\theta=1}^{3} E(L, \theta) * R(a, \alpha)$

3.2.3 Computational models and strain-based relationship to brain injury

The development of computational finite element models allowed researchers to explore micro-level injury outcomes with the implementation of macro-level kinematic inputs, thus providing a more detailed and encompassing assessment of human brain response. These finite element head models (FEHMs) provide a level of exploration into the head that allows for accident reconstruction and the ability to analyze the brain response to mechanical loading at a level of detail which is superior to dummy head form and surrogate cadaveric model experimental testing. Various physical parameters such as coup pressure, countercoup pressure, von Mises stress, shear stress, and tensile strain could now be assessed to predict the level of brain injury [89]. Researchers are beginning to understand the potential of these FEHM and the demand for validated and accurate models is exploding. More than 10 different highly tested and validated, three-dimensional FEHM have been developed in industry and academia over the last decade alone, with varying levels of anatomical features and complexities present [59, 94, 97, 114-117].

These FEHM have allowed for a more in-depth look at the brain's response to impact and with this newfound assessment method, a slew of new brain injury metrics, some of which provided a more accurate prediction of the injuries associated with more mild impacts, were developed. Looking into the strains in the brain, a direct mechanical metric which quantifies deformation on brain tissue also known as the "stretching" of the brain, has direct correlation to common traumatic brain injury pathologies such as DAI [56]. Using a strain-based injury metric such as maximum principal strain (MPS), is one method of determining the outcome of a traumatic head impact scenario. Based on MPS, several more encompassing metrics were developed, cumulative strain damage measure (CSDM) provides a volume based correlation of the extent of damage that could be attributed to DAI, and this metric predicts DAI by calculating the MPS level at a volume fraction of the FEHM [79].

3.2.4 Objectives

This study looks to combine laboratory dummy experiments and FEHM techniques and attempts to better understand how effective the different brain injury prediction criteria are for determining the effect of a helmeted head during typical hockey impact scenarios. This group believes that some of the more modern helmet assessment techniques such as that of STAR could be updated to include more expansive brain injury predictors such as strain which is highly correlated to angular velocity. The use of a previously developed novel start-to-finish kinematic to brain injury pipeline, allows for instantaneous comparison of modern injury prediction metrics, and the scope of this work is to provide new data to help helmet manufactures create and design a new generation of helmets that are better suited to dealing with the devastating effects of the concussion.

3.3 Materials and Methods

3.3.1 Experimental setup

To re-create an industry standard method for physical helmet evaluation, this study based its helmet testing procedure on that of Hockey STAR. This methodology of assessing the biomechanical performance of hockey helmets differs from traditional methods provided by other standardization organizations as it primarily looks to recreate some of the rotational kinematics associated with head impacts. The Hockey STAR equation, equation 1, includes several unique metrics that pertain specifically to the sport of Ice Hockey. The L represents the location of impact (rear, side, front or top) and the θ represents different impact energy levels. These levels were determined in the original methodologies by the angle of the pendulum arm of the impactor. The E represents exposure, the number of times a player is expected to receive an impact in a season. Finally, R is the risk of concussion as a function of linear (a) and angular (α) acceleration. One of the purposes of this study is to examine whether the variable R is a sufficient and accurate assessor of the correlation between the kinematic outputs of a traumatic impact and the true level of injury response of the brain.

Rather than a pendulum as the STAR methodologies originally called for, a pneumatic impactor was used as it allows for more consistent impacts transferred to the

head-form and less of a safety risk in testing [62]. Like the original laboratory testing procedure; 3 impact energy levels (low, medium and high) with impact speeds of 2.6 m/s, 4.6 m/s and 6.0 m/s respectively, and 4 impact locations (front, rear, side and top), were recreated to assess the viability of each helmet sample. Each helmet was hit twice with the impactor (19.94 kg) per direction per impact speed per trial, with 4-5 helmet samples for each helmet model type. In this study 6 different helmet models were tested. In total each helmet went through an average of 112 impacts for a total of 672 impacts with corresponding kinematics. The helmets were fitted onto a medium size NOCSAE head-form mounted on a Hybrid III 50th percentile neck with 3 Endevco 7264C-2KTZ-2-240 (Meggitt, Bournemouth airport, Dorset, United Kingdoms) accelerometers for linear acceleration, and 3 rotational velocity channels of the DTS6DX Pro (Diversified Technical Systems, Seal Beach, California, USA) mounted in the center of mass of the head form. Two Endevco Model 136 amplifiers provided excitation voltage and signal conditioning. The kinematic data of each helmet impact; linear acceleration, rotational acceleration and rotational velocity, were collected at 20 KHz with a filter chain of hardware CFC1000 filter at amplifier for all channels, software CFC1000 filter on linear acceleration and software CFC155 filter on rotational velocity. A custom script was then developed to export the data into a spreadsheet including X, Y and Z axis data.

3.3.2 Computational Model

The finite element model used in this study to simulate the physical testing impacts was the Global Human Body Model Consortium (GHBMC) head model [59]. This validated model of the human brain and skull is based on computed tomography (CT) and magnetic resonance imaging (MRI) scans of a healthy adult male brain of average height and weight. This model allows for a biofidelic computational model to simulate and interpret the mechanical stresses and strains associated with traumatic impact. The GHBMC model, as seen in Figure 12, allows for the quantification and visualization of the mechanical soft-tissue materials metrics in key anatomical regions such as; the corpus callosum, thalamus, cerebellum, brainstem and basal ganglia. In this model a linear visco-elastic material was used in both the gray and white matter with the skull modelled as an elastic plastic material. In total the GHBMC head and brain model contains 62

components of bone and soft-tissue, 61 unique material properties and 270,552 total elements (beam, shell and solid), and is validated against intracranial pressure and brain displacement data [118, 119].

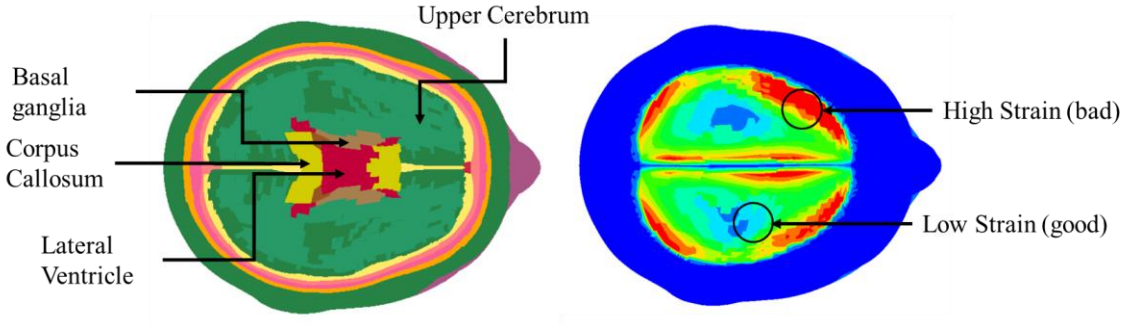

Figure 12, GHBMC Model in its normal configuration, anatomical features given different colors for visual representation, on right, typical MPS patterns exhibited in traumatic head impact, red is considered bad or high strain while green/blue is considered low to no strain which is good.

When setting up the model, the direction of the kinematics was reoriented to a 23-degree offset above the horizontal Y- axis to mimic the sensor setup in the original dummy head form. An initial dataset of an impact in 3 different impact energy levels in a single direction based on a single helmet sample was provided to determine an optimized time of impact to allow for both analysis of the moment of maximum principal strain as well as allowing for efficiencies regarding computational time and resources. The kinematic curves used in this study were determined through an initial testing round, the overall time of simulation (80ms) was used based on the peak strain responses of a test impact (t = 200ms) where peak max principal strain (MPS)was included along with subsequent inertial response. The simulations were then completed on a Lenovo workstation (2 X Intel Xeon GOLD 5118 Processor (12 cores @ 2.3GHz), 128 GB DDR4 Memory) using LS-DYNA, finite element program, (Livermore Software Technology ANSYS LSTC, Livermore, CA, USA) with simulation time equivalent to ~2 hours per simulation at NCPU = 2, for a total computational time of ~1344 hours. Each simulation was then analyzed in LS-PrePost and checked over for any logical errors.

3.3.3 Analysis Methods

An in-house script was used to calculate common head injury prediction criteria (Chapter 2). Each of the 672 impact scenarios was assessed for peak kinematics in the X, Y and Z direction to determine resultant peak kinematics as well as injury prediction metrics, summarized in table 1. The kinematic data was automatically processed to calculated common injury metrics such As HIC_{15}, GSI, GAMBIT, BrIC, UBrIC and DAMAGE. This retrofitted pre-processing pipeline required the introduction of a rotational matrix about the Z-Axis to align with the Frankfort horizontal plane as the sensor position was at a 23-degree offset above the horizontal (Figure 13).

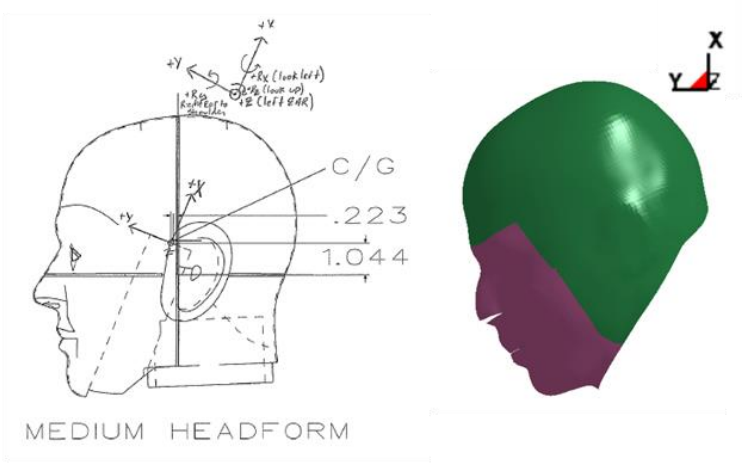

$$RotMatrix\ (z) = \begin{bmatrix} \cos(23) & -\sin(23) & 0 \\ \sin(23) & \cos(23) & 0 \\ 0 & 0 & 1 \end{bmatrix} \quad (8)$$

Figure 13, comparison of schematic of dummy head form with accelerometer placement and modified GHBMC model at 23 degree offset to account for prescribed motion

Along with analyzing the preprocessed kinematics, the post-processed strains were also analyzed using an automated extraction method. The post processing pipeline looks to take the simulated GHBMC model and extracts the element data output (ELOUT) file. This process acts as a batch script to utilize a custom in-house script [120] and extract the MPS of each element and the total volume of the brain and calculate the CSDM of the

brain at varying levels to provide a glimpse into the perceived level of sub-concussive and concussive injury likelihood. All files in a folder can be examined with a single click, and hence 672 individual CSDMs (5% to 25% threshold) along with average MPS and MPS critical 1% and 5% were examined in this experiment. Each of the peak head impact kinematics along with their associated peak resultant kinematics were assessed for their correlation to the brain response assessment metrics (CSDM5-25, Average MPS, Top 1 % and 5% MPS) to determine their linear relationship and overall effect on the brains strains that lead to mTBI.

The physical testing produced results like what were to be expected from the STAR methodology, providing evidence of the accuracy of the repeatability of this experiment. Peak kinematics were recorded in the X, Y, and Z directions with their mean values and standard deviations provided in the table below. These peak kinematic were then input into the STAR equation and compared to the STAR scores that were listed on the Virginia Tech Helmet Rating website (Virginia Polytechnic Institute and State University, Blacksburg, VA, USA).

Table 6, breakdown of a typical helmet impact, in this example Helmet A with a Low impact Energy is shown

Helmet	*Energy*	*Impact Direction*		*LinX*	*LinY*	*LinZ*	*RPLA*	*RotvX*	*RotvY*	*RotvZ*	*RPRV*	*RotaX*	*RotaY*	*RotaZ*	*RPRA*
A	Low	Front	Mean	22.97	64.41	4.36	67.77	1.22	0.93	21.17	21.20	585.66	471.36	2285.03	2299.34
			N	10	10	10	10	10	10	10	10	10	10	10	10
			Std. Dev.	0.62	1.87	1.38	1.97	0.40	0.10	0.28	0.28	169.23	63.63	117.85	122.18
		Rear	Mean	11.63	53.34	4.64	54.23	0.82	0.88	24.98	25.00	483.57	417.77	2857.35	2878.12
			N	10	10	10	10	10	10	10	10	10	10	10	10
			Std. Dev.	0.92	3.85	0.79	3.75	0.39	0.20	1.30	1.29	26.77	104.40	134.65	139.80
		Side	Mean	9.53	14.65	68.29	69.70	3.03	18.23	4.93	18.88	926.90	4018.35	784.19	4135.50
			N	10	10	10	10	10	10	10	10	10	10	10	10
			Std. Dev.	0.24	1.41	1.60	1.55	0.36	0.35	0.35	0.25	159.90	217.67	76.49	233.69
		Top	Mean	24.32	6.11	38.18	44.73	8.76	14.69	2.65	14.94	1810.89	1902.11	936.29	2547.55
			N	10	10	10	10	10	10	10	10	10	10	10	10
			Std. Dev.	1.72	1.61	3.51	3.51	0.72	0.82	0.23	0.71	169.48	156.33	131.48	145.47
		Total	Mean	17.11	34.63	28.87	59.11	3.46	8.68	13.43	20.00	951.75	1702.40	1715.72	2965.13
			N	40	40	40	40	40	40	40	40	40	40	40	40
			Std. Dev.	6.75	25.17	27.00	10.71	3.25	7.99	9.92	3.77	547.07	1489.05	899.05	732.79

Each prediction metric was then imported into a master spreadsheet where the data for each of the 672 impact scenarios was stored. Using IBM SPSS statistics 26 (IBM, Armonk, New York), data was analyzed for statistically significant correlations and data trends with tools such as bivariate Pearson correlation, hierarchical linear regression and Artificial Neural Networks (ANNs).

For this study a new method was developed to attempt to provide more instantaneous strain metrics through the introduction of an ANN surrogate. We devised a hockey specific artificial neural network (ANN) injury prediction tool which provides a strain-based outputs for input 9 input parameters (peak; rotational velocity, linear and rotational acceleration in the X, Y and Z directions). The ANN was produced in SPSS using a Multilayer Neural network perception with 80-20 training testing partition. This ANN was produced using 5 helmet samples as training and testing for the model (576 impacts) and excluding 1 helmet (96 impacts) from the training for additional testing and validation. This final helmet was then put through the ANN algorithm with only the input kinematics and the predicted ANN output strain parameters including CSDM and MPS were compared to those determined by the GHBMC model. This relatively large dataset and well laid out input and output parameters, allowed for an in-depth analysis and the ability to train and test the dataset for machine learning techniques.

3.4 Results

3.4.1 Kinematics

The calculated STAR scores in this study produced a percent difference between this study's linear impactor tests and the original star methodologies pendulum-based tests that were on average 13.78 % higher. Using bivariate two tailed Pearson coefficient correlation, highly correlated and statistically significant parameters were flagged, a representation of the different kinematic measures and strain measures is shown in Figure 14. When examining the output strain related metrics, the most correlated input kinematic parameter was resultant peak rotational velocity (RPRV). It is correlated highly with CSDM5-25 with an average $r = 0.92$ ($P < 0.01$) and correlates highly, $r = 0.96$ ($P < 0.01$), with $MPS_{average}$, MPS 1% and MPS 5%. Looking at resultant peak linear acceleration (RPLA) the correlation while significant is decreased with an $r = 0.604$ ($P < 0.01$) for averaged CSDM5-25 and r values of 0.66, 0.58 and 0.54 ($P < 0.01$) for $MPS_{average,}$ MPS 1% and MPS 5% respectively. Resultant peak Rotational Acceleration (RPRA), was the least correlated to strain metrics of the three with $r = 0.51$ ($P < 0.01$) for averaged CSDM5-25 and $MPS_{average,}$ MPS 1% and 5% ($r = 0.58$, 0.47 and 0.40 $P < 0.01$) respectively.

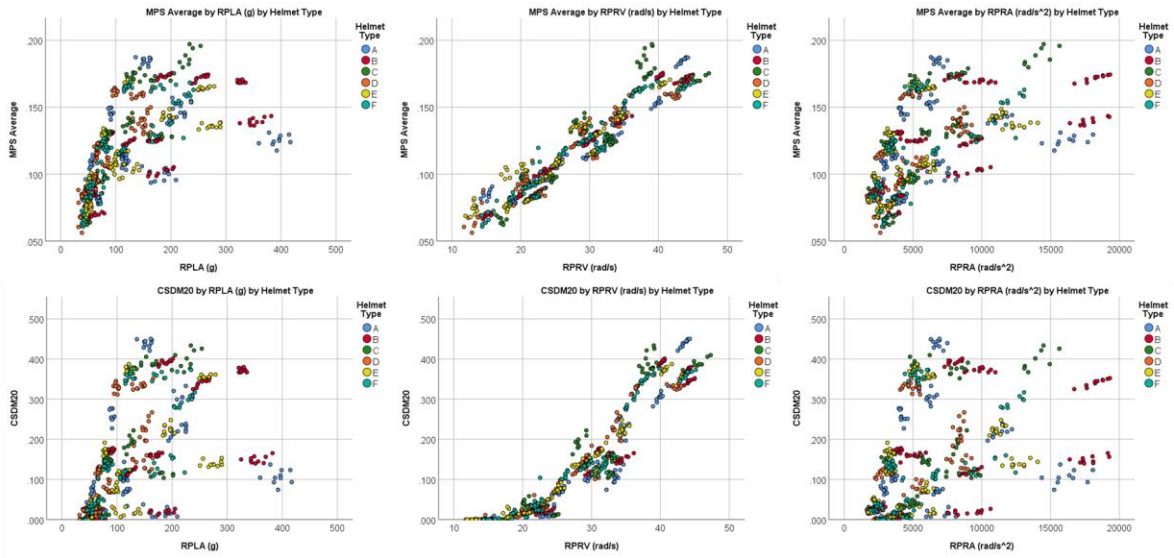

Figure 14, comparison of different raw peak max resultant kinematic, top row is compared to MPS average bottom row is CSDM 20 and from left to right is RPLA, RPRV and RPRA.

3.4.2 Comparison of Different Injury Metrics

The different injury metrics (GSI, HIC_{15}, GAMBIT, BrIC and UBrIC and DAMAGE) were assessed based on the strength of their relationship to the different strain-based metric (CSDM5-25, $MPS_{average}$, $MPS_{5\%critical}$ and $MPS_{1\%critical}$), shown in Figure 15. The velocity based injury prediction criteria, BrIC ($r = 0.914$ $P < 0.001$), UBrIC $_{MPS}$ ($r = 0.916$ $P < 0.001$), and UBrIC $_{CSDM}$ ($r = 0.922$ $P < 0.01$) preformed significantly better than the linear and rotational acceleration based metrics GSI ($r = 0.582$ $P < 0.001$), HIC_{15} ($r = 0.702$ $P < 0.001$), GAMBIT ($r = 0.564$ $P < 0.001$) and even outperformed DAMAGE ($r = 0.882$ $P < 0.001$). When compared to the FEHM strain outputs all injury metrics outperformed the STAR incidence rating ($r = 0.186$ $P < 0.001$), however this could be due to the way that STAR is calculated where all directions experience different exposures in combination.

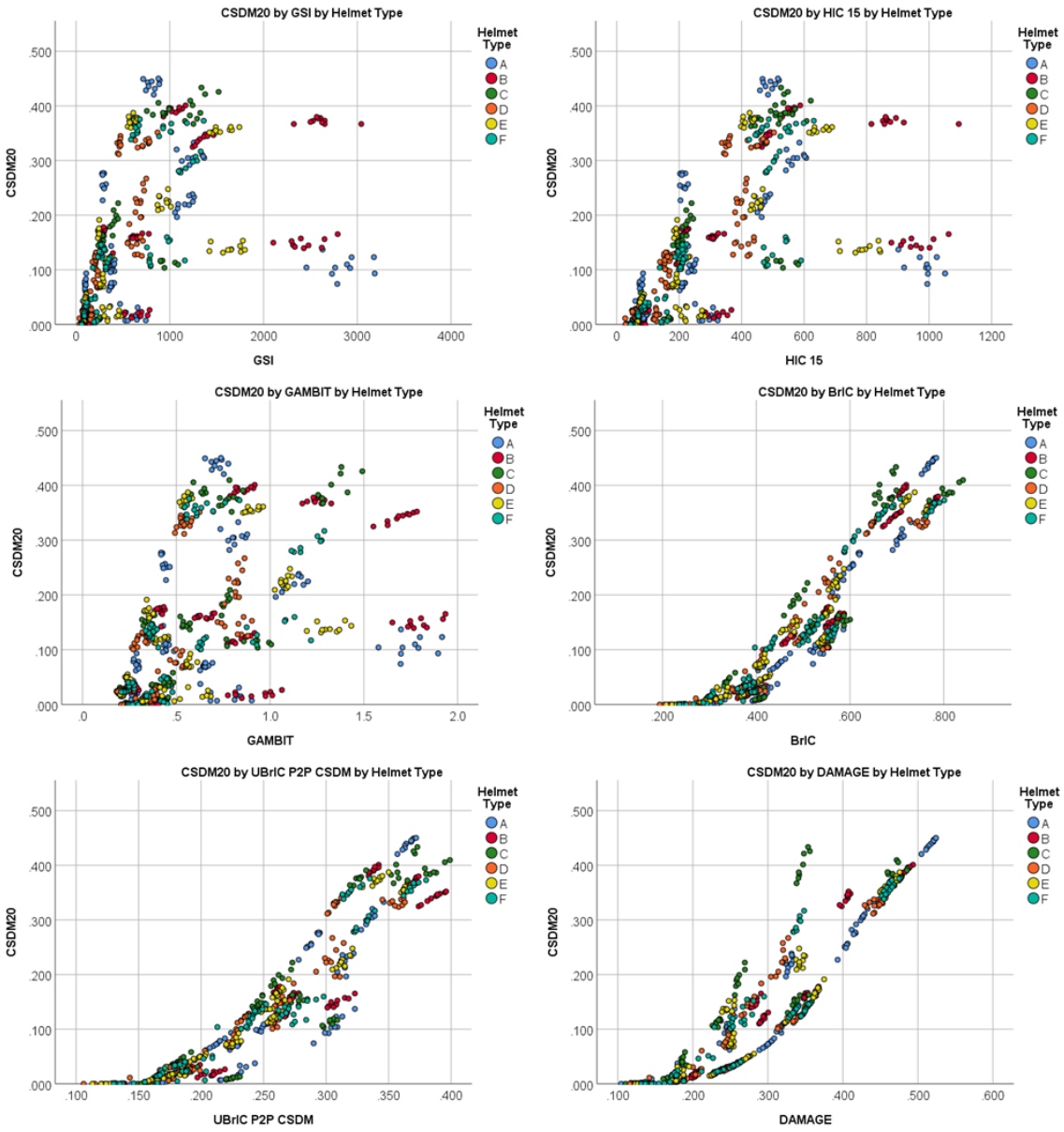

Figure 15, comparison of different injury metrics to CSDM 20, colors indicate helmet models.

3.4.3 STAR VS Strain results

The STAR equation was then assessed vs the different strain metrics that were correlated to brain deformation responses such as MPS $_{average,}$ MPS $_{critical}$ 1% and 5 % and the different CSDMs (Figure 16). The relationship between the STAR rating and the different strain parameters was not strongly correlated. While there were decreased in

overall strain, average MPS for 0 star equal to 0.123 compared to 0.114 for a 4-star helmet, a percent difference of only 7.6%, does not seem to justify the perceived difference between a 0 STAR rating and a 4 STAR rating. The difference between a 3 to a 4 stars rating was even more miniscule and was almost the same in terms of average MPS response.

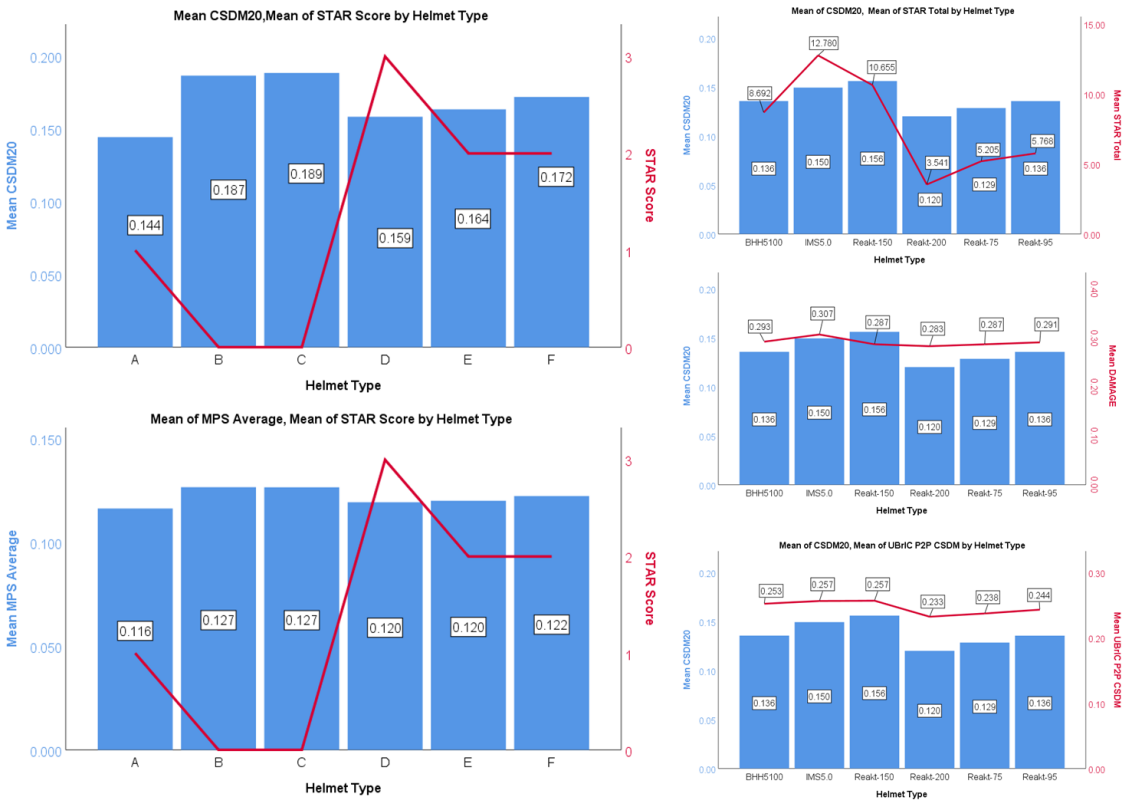

Figure 16, showing average strain and comparing it to STAR (red line), showing that while the difference between a 0 star rated helmet and a 3 star rated helmet is minimal in terms of strain the correlation between strain and a simple velocity based injury prediction method is much larger.

3.4.4 Directional performance

There were interesting differences in the performance of the different directions. Rear impact had the largest MPS average, 0.133 ± 0.031 (n = 168) followed by frontal impact, 0.122 ± 0.033 (n = 168), side impact, 0.118 ± 0.033 (n = 168) and finally top impact, 0.101 ± 0.026 (n = 168). Looking more in-depth into each direction, as shown in

Figure 17, some helmets such as helmet C preformed worse in side impacts resulting in a higher strain (0.142 ± 0.038 n = 24) than front (0.127 ± 0.036 n= 24) or rear impacts (0.133 ± 0.034 n =24). While helmet A and helmet B performed differently in frontal and rear impacts where helmet A showed a difference of 14.7 % in strain values whereas helmet B only showed a 3.86 % difference in mean MPS $_{average.}$

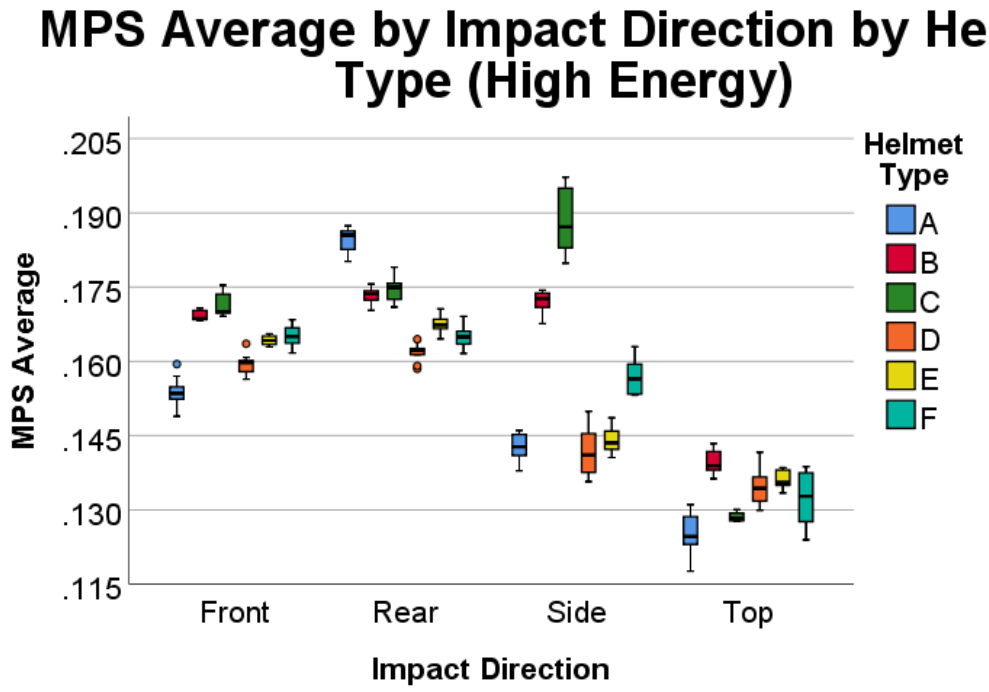

Figure 17, boxplots representing the performance of each helmet, in terms of impact direction and energy level, in this example 'High', each helmet preformed slightly differently in how they fared under each impact loading scenario, however trends emerged such as strain being least effected by top impacts and rear impacts producing the most strain, on average.

3.4.5 Helmet performance

Based on average MPS the helmet that performed best based across all impact direction and energy types was helmet D with a mean MPS $_{average}$ of 0.113 ± 0.030 (n =120). The worst preforming helmet across all impact directions and energy levels for MPS $_{average}$ was Helmet C, MPS $_{average}$ = 0.125 ± 0.0373 (n = 96). The percent difference

of the strain levels of these two helmets was approximately 10.1%, meaning that overall of the 6 different helmet models, based on this helmet testing methodology, the best preforming and worst preforming helmets, both at varying levels of STAR protocol and relative consumer perspective had a performance boost of 10%, with the best performing helmet having a reduced strain of 5.2% of the mean $MPS_{average}$ across helmets and the worst preforming helmet having an increased mean $MPS_{average}$ of 4.9%.

When comparing those performance differences with those of the STAR methodology, there is a different picture of how effective each helmet performed relative to one another. While Helmet D is still the best performing helmet with a STAR score of 3.54 ± 0.19 which equates to a 3 Star helmet, but borders on 4 Star, which is considered a very good helmet for mitigating concussive risks. Helmet B was determined to be the worst preforming helmet according to STAR with a score of 12.78 ± 0.18 which equates to a 0 Star helmet rating and is 113.2% worse in terms of overall STAR rating differences. Figure 18 shows the differences between that of the STAR rating system and the MPS from the GHBMC FEHM, there is an evident disparity between not only the way that the helmets are ranked and the difference in overall concussion mitigating metrics between the two methods.

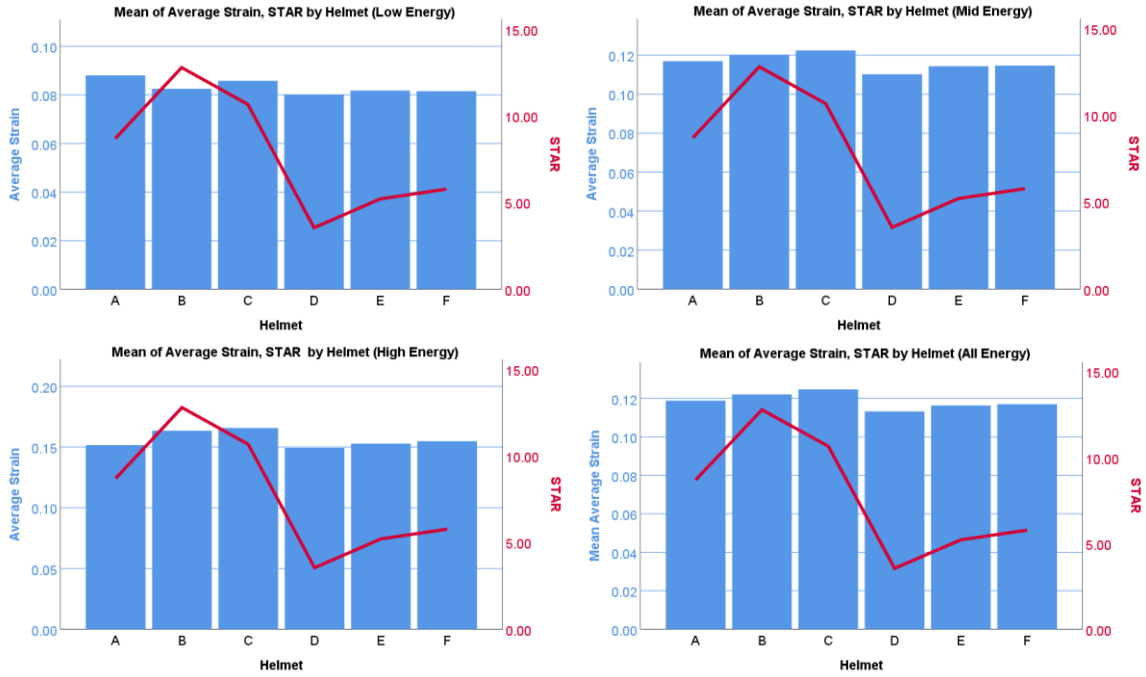

Figure 18, helmet performance comparison between strain-based brain response metric, Average MPS and kinematic based performance metric, STAR. From top left to bottom right, low energy, mid energy, High energy and average energy. Chart is used to show discrepancy between the strain reducing effects of helmets and their relative STAR score. STAR recommends only helmets that are 4 or 5 stars rated, with 5 stars equal to a score of 2.0 and lower and 4 stars equal to a score of 3.5 and lower.

When comparing individual helmet performance there is little difference between comparable models in terms of overall visual strain plot differences. Setting the threshold fringe level of MPS to 0.25 the strain contours in coronal, mid-sagittal and transverse planes are almost identical for a similar impact direction and loading energy level (Figure 19). That is partially the reason that elemental based strain outputs and statistical analysis were important for this study as they provide clearer helmet differences.

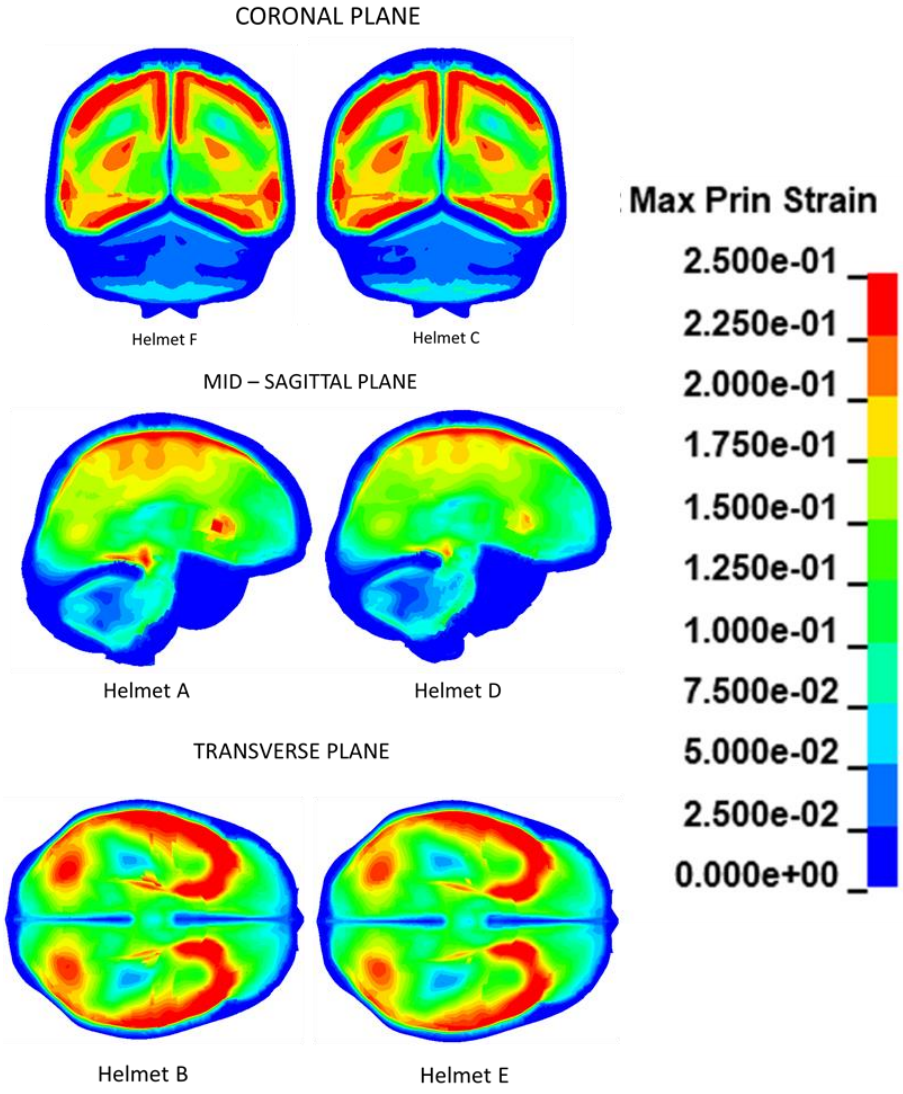

Figure 19, comparison of strain plots between different helmet models, the strain plots appear very similar hence the need to investigate the values in more detail.

3.4.6 Use of ANN

We devised a hockey specific artificial neural network (ANN) injury prediction tool which provides a strain-based output for input rotational velocity and linear and rotational acceleration. The tested model had a total of 672 cases with 80.4% (540) of the cases used as training and the other 19.6% (132) of the cases used for testing, all impact scenarios were deemed valid by the software. with an average percent difference of 2.86% and strain error rates of over 10% only 1.49% of cases (n =10/672) and a R^2 = 0.985 (Figure 20). Using input

parameters; linear acceleration, rotational acceleration and rotational velocities in XYZ (9 inputs) the hypothesis is that the ANN could predict average MPS and CSDM values that would normally have to be first simulated by GHBMC models. In comparison of time, ANN took approximately 0.04s to train, while GHBMC models took approximately 22 hours for 12 with a workstation running at NCPU =2 for each scenario (total NCPU =24). In Figure 20, the bottom two graphs show the ability of this tool to be used in future surrogate uses. The linear regression value R^2 was 0.987 for the excluded helmet. This helmet only included the peak kinematics as inputs and produced convincing strain outputs. In this example CSDM20 was compared.

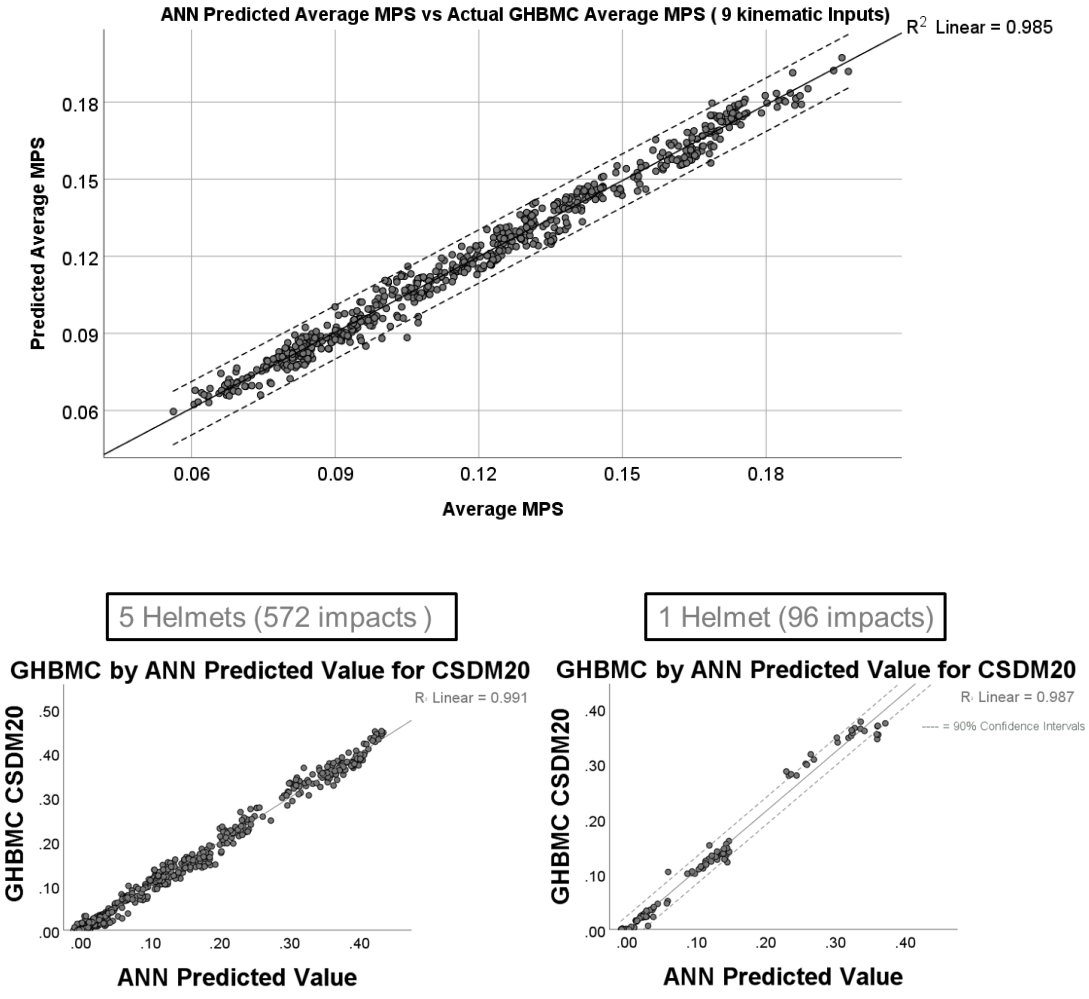

Figure 20, scattered plot graph of the 672 impact scenarios actual average MPS and predicted average MPS, this study helps to create a framework for instantaneous

injury prediction of 97.14% confidence with only linear and rotational acceleration and rotational velocity as inputs. Linear line of best fit with an R^2 of 0.985 and the dashed lines representing 95% confidence interval. Without the inclusion of rotational velocity prediction decreases to 93.52 % with 20.68% (139/672) of cases differing by over 10%.

3.5 Discussion

3.5.1 What are the most effective injury criteria in determining the concussive mitigating potential of Ice Hockey helmets?

We were able to show in this study the significant advantages that rotational velocity-based injury prediction criteria such as, BrIC, UBrIC and even RPRV have over linear acceleration and rotational acceleration based metrics such as HIC, GSI, GAMBIT, DAMAGE and STAR, which have limitations in their ability to predict the brain's deformation response to an impact. Rotational velocity metrics have produced higher correlations to brain strains in several recent studies and their inclusion into any helmet assessment protocol should be incorporated immediately [52]. In this study we validated their importance, with a large dataset that showed statistically significant correlations to common computational related injury prediction metrics such as CSDM and MPS which have been shown to provide a reasonable assessment of the brains level of injury and are shown to be related to common mild traumatic brain injury pathologies, in particular DAI. While this study does have its limitations, including the absence of axial strain through the embedding of an axon fiber component in the FEHM, this study still uses a widely validated state of the art model that provided a reduced computational cost for large data acquisition.

3.5.1.1 Exploring DAMAGE injury metrics in more detail

The recent introduction of the DAMAGE injury metric provided a new injury prediction criterion which was based on strain outputs from the GHBMC model and relied on linear and rotational acceleration as inputs. Our results indicated that it was important to look beyond the Pearson correlation of DAMAGE which was r = 0.882 and explore how well it correlated in terms of directional performance. An interesting finding was that DAMAGE very highly correlated highly in the Front and Rear impact directions (R^2 =

0.979 and 0.963 respectively) yet suffered a bit in correlation in the Top and Side Impacts (R^2 = 0.855 and 0.870 respectively) (Figure 21). One possible explanation for this reduction in correlation could be the tangential kinematics associated with the Side and Top Impacts, which as stated in the Hockey STAR methodology are impacted not through the COG like the Front and Rear impacts and hence the resulting brain response is less correlated to the linear accelerations that each impact produces. This again could provide as more definitive proof that rotational velocity-based metrics such as BrIC and UBrIC are superior in injury prediction.

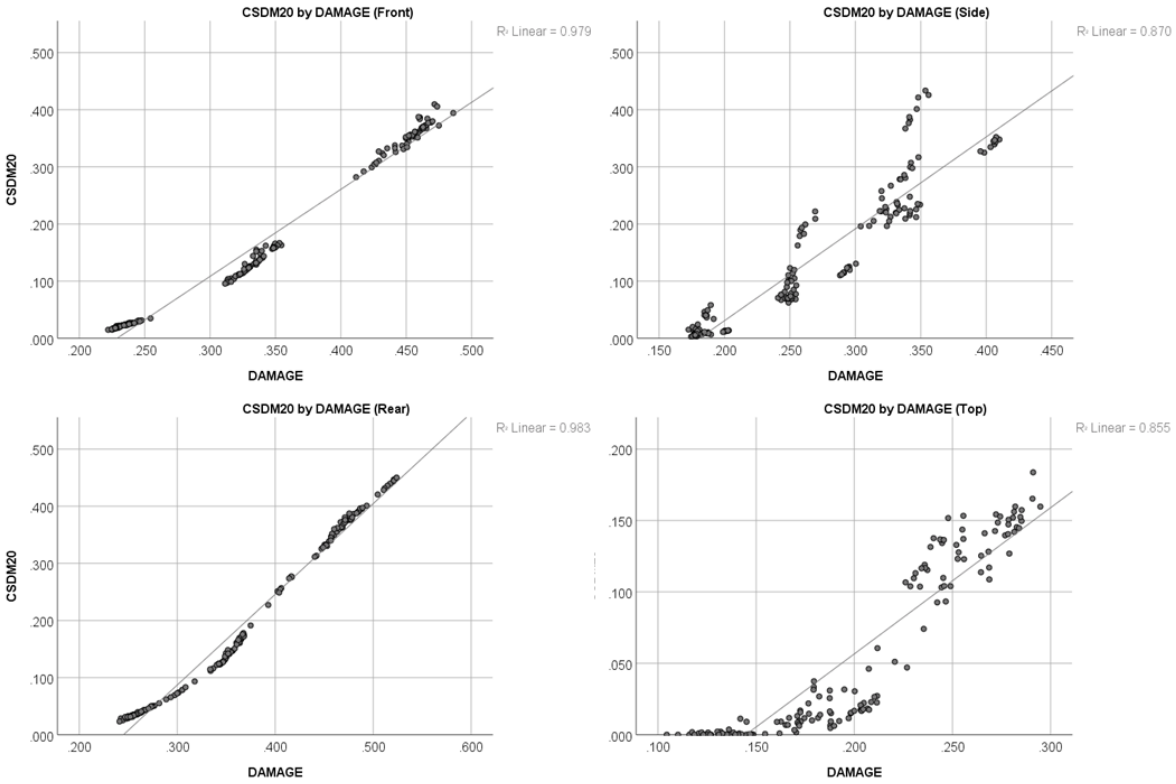

Figure 21, comparison of DAMAGE correlation to CSDM20, Front, Side, Rear and Top impacts. DAMAGE is derived from strain outputs of the GHBMC model which is most likely the reason for it having good correlation to the strain results of this experiment

3.5.2 Comparison of helmets and impact directions – compare to the brains preferred direction of motion

Comparatively the helmets performed similarly when exploring their strain reducing ability, while some helmet performed slightly better overall, Helmet C, the differences were small. Exploring the areas of injury rather than the brain as a whole or including the axial strain metric could be some next steps that provide a clearer image of the differences and concussion mitigating potential of the different helmet models, but based on the GHBMC FEHM and common injury prediction criteria the helmets preformed similarly without enough of a variance to determine that a particular helmet model is marginally better than a another for reducing brain strain and rotational based kinematics. This is most likely based on the helmet industry as a whole designing helmets and materials with a goal of reducing linear and rotational acceleration, which based on this study is a mistake.

This study also examined the directional differences of helmet impacts. Other studies have shown that an impact directed at a specific region results in larger brain deformation, even with similar impact energies [52, 62, 86, 122, 124]. While it is presumed that the direction that causes the highest brain strains is the axial rotational direction, in this particular experiment about the x-axis, this study showed that rear and frontal impact or impacts that would affect the flexion/extension direction produced the highest strains consistently, with the highest overall average strain produced by helmet C with a side (axial rotation + lateral bending) impact. This is interesting especially combined with our previous analysis showing that an axial rotation produced much higher brain strains compared to flexion/extension with the same magnitude of head rotation[52]. While this testing methodology has some obvious limitations, particularly in its inclusion of more tangential impact directions that would induce higher axial rotation kinematics, it cannot be ruled out that the helmets themselves have either geometric or material differences that directed impact energy away from the higher danger impact directions into lower danger directions.

3.5.3 STAR Methodology could use some updating

Based on this study the STAR helmet safety rating protocol has some major limitations when it comes to predicting the effectiveness of different helmet models in mitigating concussive impacts. Whereas we determined a relatively minute difference in the helmet models in terms of strain reduction, STAR reported significant differences in the helmet's performances. For example, for Hockey STAR Rowson et al. explained that a difference between a 12.809 star rated helmet and a 7.098 star rated helmet would equate to 44.6 % less likelihood of sustaining a concussion [66]. In our study, similarly rated helmet A (STAR = 8.692) and helmet B (STAR = 12.780) only showed a percent difference in strain by way of CSDM20 of 9.79%.While there are studies that have reported relationships between linear and rotational acceleration to TBI, the STAR rating could use some updating, specifically with the addition of rotational velocity. This will allow for potential consumers to make a more educated helmet purchasing decisions, one that is supported by brain strain response. While the methodology itself has been brought into question, specifically with it not being fully encompassing of tangential impacts, the equation itself appears to be a more major point of error in the assessment capabilities of the testing protocol.

Showing that there are major limitations with the use of rotational acceleration and linear acceleration to predict the strains in the brain, in the form of MPS and CSDM, leads us to believe that the STAR safety rating protocol and specifically the STAR equation needs to be updated. We propose the use of rotational velocity kinematics, as evident by its strong correlation to the different brain response metrics to better predict the effectiveness of a helmet and its ability to mitigate concussive impacts.

3.5.4 Use of ANN and future research

The ANN predicted strains proved to be more highly correlated to both $MPS_{average}$ and CSDM20 than any of the literature prediction criteria (Figure 22). For $MPS_{average}$ the predicted values from the ANN had an R^2 of 0.962, compared to 0.895 which was the R^2 of UBrIC MPS peak to peak, the most correlated of the injury prediction metrics. The same story can be seen in CSDM20 where the ANN outperformed all other criteria, with

an R^2 of 0.991 which was 0.122 larger than the second closest metric. These results in combination with the effectiveness of predicting strain metrics such as CSDM20 seem to justify the use of ANNs as surrogate models in future studies that look to utilize this pipeline. The ability to have a start to finish prediction of different brain injury metrics both kinematics-based and strain based in a matter of minutes post impact could be important indicators of injury level and prove to be a valuable research tool. With more testing and data input in the future this model will only become more accurate and would lead the way into providing instantaneous brain injury response based on a validated helmet testing methodology and a validated state of the art computational head model. This chapter highlights the in-depth analysis that could be done using current state of the art FEHM, though there exists limitation in terms of the physical dummy testing and the complete biofidelity of the computational model as highlighted in the previous chapter, these results show novel insights into the role of the hockey helmet in mitigating brain injury. The next step for this research is to try to target one of these limitations, with improvements to the FEHM and new methods of examining mTBIs the ability to determine subtle changes in the brains structure could unlock the door into understanding concussions and providing insights into improving hockey helmet design.

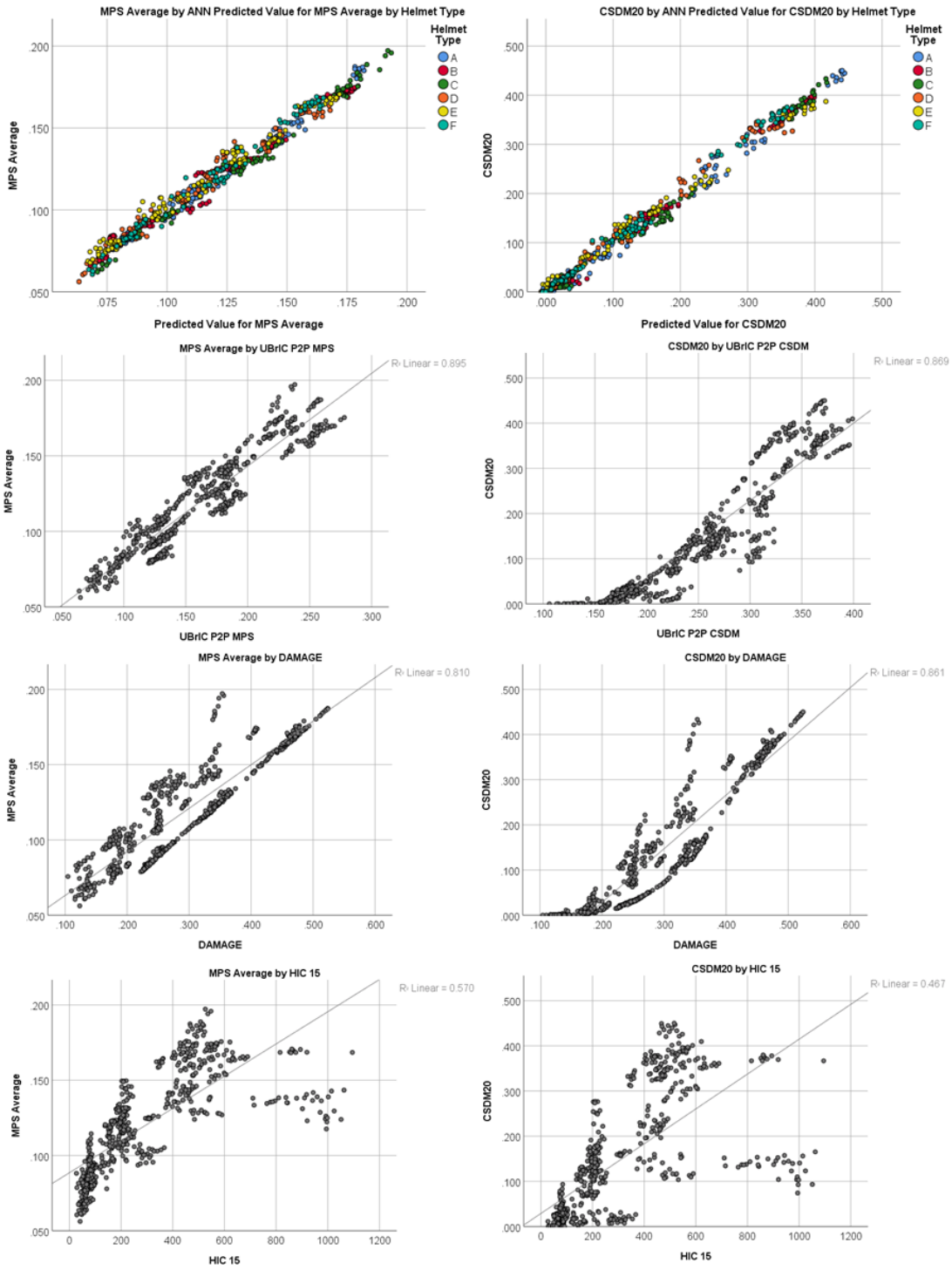

Figure 22, ANN comparisons of MPS average and CSDM20 to some of the more recent injury prediction criteria (UBrIC and DAMAGE) as well as the most well-known HIC15.

Chapter 4

4 Development of Multiple Parcellated Axon Fiber FE models for TBI symptom diagnosis

4.1 Abstract

The growing need for an accurate assessment of mild traumatic brain injuries in the determination of concussion protocol requires the exploration of new technologies. The use of Finite Element Modelling has provided a computational approach to recreate loading and impact conditions without the need to recreate impacts physically. This study delves into a novel computational approach to better understand the mechanisms of the deep-brain responses associated with concussions through the generation of a validated parcellated axon fiber tractography atlas embedded head and brain model. This study examined shortcomings of previous literature pertaining to the subject area, while creating a detailed 1-D beam model using 3T and 7T diffuse tensor imaging. The model was compared to that similar literature models, as well as validated using brain skull displacement studies, determining that difference in strain was exhibited and that the overall model generation workflow was possible, validated and repeatable. This anisotropic axon embedded model will be a useful tool in future studies and industry as a better predictor of the mesoscopic ($\approx$ 1mm) white matter structure of the brain and is a step forwards in uncovering the mystery of the concussion.

4.2 Introduction

The mild traumatic brain injury (mTBI) is a prevalent and debilitating injury that is shown to lead to a host of negative short and long-term health related symptoms [135]. These classified “minor” brain injuries, affecting an estimated 1.6 - 3.8 million people the United States (US) annually, are difficult to diagnose using standard neuroimaging techniques, and result in a large portion of those affected reporting a wide variety of symptoms for months post injury known as post-concussion syndrome (PCS) [136, 137]. There exists a knowledge gap between researchers and doctors on how to accurately assess the severity of the injury and determine the proper rehabilitation protocol to return

patients to their normal daily function [103]. The first step to assess the different levels of injury is through the development of repeatable and validated injury recreation methodologies to better understand the mechanisms associated.

4.2.1 Experimental history

Historically, physical dummy models were used to measure the linear and angular kinematics associated with head impacts to aid in the creation of injury criteria to assess the damage of such injuries quantitatively [138]. The issue with these methodologies is that they do not allow for researchers to investigate the in-vivo brain response of how brain reacts to such impacts, especially with the complicated nonlinear and anisotropic behaviors of soft tissues in the human brain [60]. Throughout the 1970s, 80s and 90s numerical models were created that were able to do just that, investigate and attempt to simulate the response of the brain to real world traumatic impact scenarios. However, these models were simplistic in nature and were inaccurate in their simulation of complex impact scenarios [59].

New models have been created over the past several years have provided more accurate predictions of brain response and have allowed for reliable predictions of mechanical response and an accurate description of the constitutive behavior of the viscoelastic and hyper-elastic soft tissue responses [15, 56, 60, 103, 105, 139-144] .

4.2.2 Diffuse axon injury and new models

The strains derived from the impact to the head are found to cause different injury outcomes such as diffuse axonal injury (DAI) [55]. These types of injuries, specifically the ones associated with the axon fibers of the brain are the focus of this study as it has been proven that there is a specific injury threshold at this axonal level [57]. The study completed by Bain et al. 2001, showed through the stretching of the optic nerve of a guinea pig that a functional injury was present at a strain threshold for sensitivity and specificity measuring in at 0.21 [43]. Strains at the axonal level are believed to be a predominant driving force in the negative outcomes associated with traumatic brain injuries and concussions in humans [58]. While other studies have looked in depth at the response of the brain to traumatic head impact [138], few studies have looked at the axon

fibril networks dynamic response in real world impact scenarios. Studies such as those completed by Giordano et al. and Wright et al. focused on the validations of a computational model that treated white matter as an anisotropic, hyper-elastic material based on DTI to determine a threshold or probability of DAI [55, 60]. Both studies determined that strain in the direction of the fibers (axonal strain) is a better predictor of injury then a generalized max principal strain (MPS), anisotropic equivalent strain (AESM) and cumulative strain damage measure (CSDM). More complex models involving the entirety of the brain and axonal fiber tracts were developed by T.H. Garimella and R.H. Kraft (2017) [103]. A Patient specific methodology was used to create a fiber tractography finite element model to calculate axonal strains and for real time tracking and the mechanical response of the axonal fiber tract under different head impact, scenarios. The study determined the influence of impact direction to the extent of axonal injury, with lateral impact loading considered to be the most dangerous [103]. A second, more recent study completed by Wu et al. (2019) attempted to create a statistical axon fiber model of a large population and utilize the model as a prediction tool an improvement on the already validated GHBMC head and brain model. The two studies above are summarized in Table 1 and will be referenced as literature validations throughout this paper, as they are currently the only two explicit axon fiber models to our knowledge.

Table 7, comparison of different explicitly embedded tractography models.

Group	*DTI info Tract*	*Number of fibers*	*Average Fiber length*	*Element type*	*Number of elements*	*Axon diameter (mm)*	*Material*	*Element Size (mm)*
H. Garimella & R. Kraft [103]	Siemens Trio Tim 3.0T MRI	17001	43.735 +- 23.329	Truss	161,811	1.12 +- 0.08 [145]	Ogden Hyperelastic ρ =1040kg/m^3 μ = 35.64 kPa α = 6.101 and D = 9.1 e-10 Pa^{-1} K = 2.2 GPa [140]	5
T. Wu et al. (Panzer) [141]	Siemens 3T Skyra scanner [146]	4556	78.6 +- 38.24	Cable	104,866	Based on FA values	Hyper viscoelastic user defined, Holzapfel - Gasser-Ogden (HGO) [147, 148]	2.5
Gerber (Kraft) [142]	Siemens Trio Tim 3.0T MRI	2994	22.5	Truss	2994 (block of fibers)	1.0	Ogden Hyperelastic ρ =1040 kg/m^3 μ =2.5 kPa α = 4.5 D =9.1 e-10pa-1 [140]	3.4

4.3 Methodology

4.3.1 Baseline model

The idea behind this study was to utilize a pre-existing and validated finite element head model and attempt to improve it by incorporating new analysis features and more anisotropic behaviors. Therefore, the baseline model chosen was that of the global human body model consortium (GHBMC) head model, which has been used extensively in the automotive and safety industry for TBI and mTBI research [59, 141]. The GHBMC head model is derived from computed tomography (CT) and magnetic resonance imaging (MRI) of 35 cadaveric subjects to create the accurate geometry of an adult 50^{th} percentile male [59]. The head model is made up of 270,552 elements, with 62 different bone and soft tissue components, including important anatomical features such as; the skull, bridging veins, cerebrospinal fluid and membranes along with the

cerebellum, brainstem, corpus callosum, thalamus and ventricles. This model was validated for robustness of model prediction using intracranial pressure data, relative skull-brain displacement and skull and facial bone impact responses. This model is still considered one of the most state-of-the-art FEHMs for brain strain and pressure prediction [97]. The GHBMC model was used in this study as the master system, loads were applied to its center of gravity and the response of the brains white matter composition was relayed to the axon fiber 1D elements. The new model was examined against the original unchanged "baseline" model and compared in terms of overall strain response changes as well as time dependent displacement changes, such as those provided by Hardy et al. 2001 & 2007 [118, 119].

4.3.2 Axon fiber tractography

The tractography for this model was extracted using a common and widely accepted 3D tractography extraction methodology known as DTI, which is based on DWI, a modality of MRI [13, 20]. Two different models were developed, requiring slightly differing development processes to produce high quality finite element parcellated axon fiber tractography models, an explanation of the pipeline generation process is shown in Figure 23. These models were then individually embedded into the GHBMC head model, hence creating the first explicit parcellated finite element axon fiber model, which allows for specific tract injury prediction and introduces anisotropic behavior to the GHBMC model.

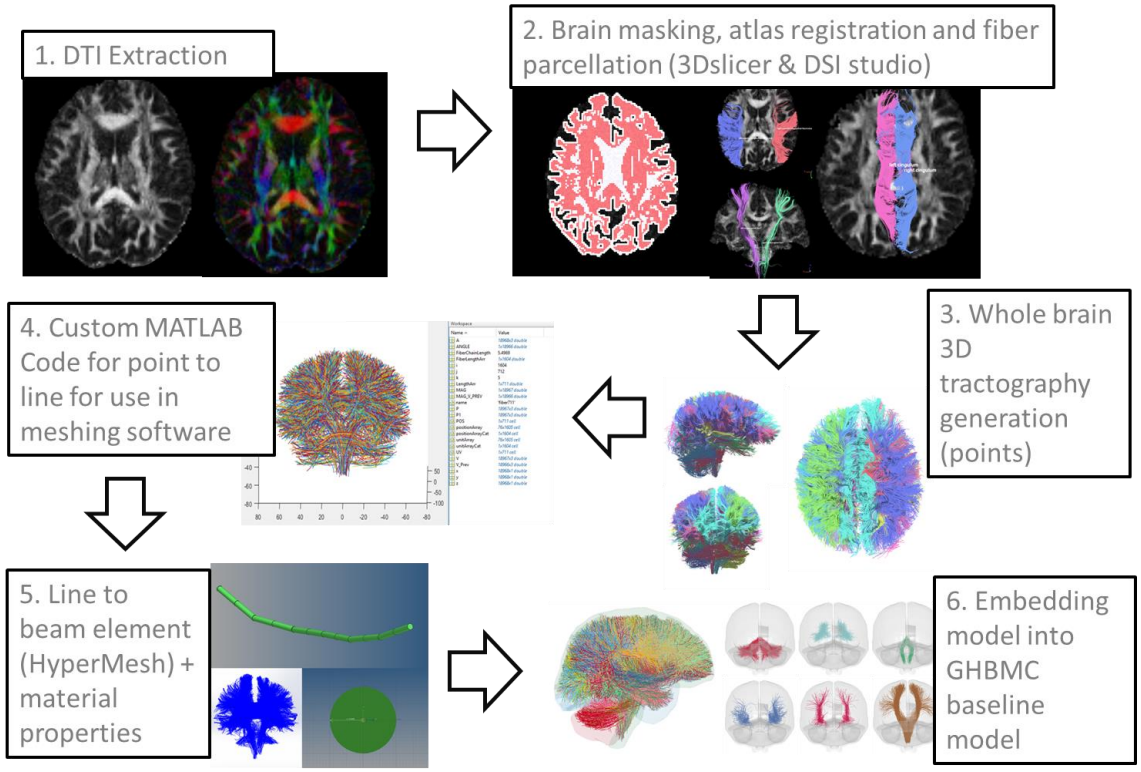

Figure 23, process flow of explicitly embedded axon fiber model from the (1) DWI to DTI (2) brain masking and parcellation (3) tractography visualization, (4) MATLAB point to line to IGES file, (5) Hyper Mesh 1-D beam FE generation (6) anatomical embedding in GHBMC model and final generated model.

4.3.2.1 HCP group dataset parcellated tractography model

Using a pre-existing, anatomically curated white matter atlas parcellated tractography model, developed and validated by the O'Donnell Research Group (ORG), a novel automated FE pipeline was created [35]. The atlas for this model was generated based on 100 healthy human scans from the human connectome project (HCP), and tested on 584 diffusion MRI scans across genders, ages (1-82) and health conditions [146]. This is one of the most consistent and comprehensive automated white matter tract-based parcellations to date with 58 deep white matter tracts and 198 short and medium range tracts for a total of 800 fiber clusters to allow for whole brain connectivity analysis [149]. Another benefit of this atlas is it being open sourced and publicly available [150, 151], available on GitHub (San Francisco, California, United States) and utilizing the free and

open source software 3D Slicer for image analysis and scientific visualization. The curated population based anatomical fiber tracts used in this study are derived from the SlicerDMRI platform using the ORG-Tracts-MRB and ORG-800FiberClusters files to visualize the 800 fiber clusters and break those down into 41 predetermined tracts from the ORG-88FC-100HCP atlas [35]. A visual representation of some important anatomical tracts and the distribution of average fiber lengths and number of fibers in our generated model are shown in Figure 24.

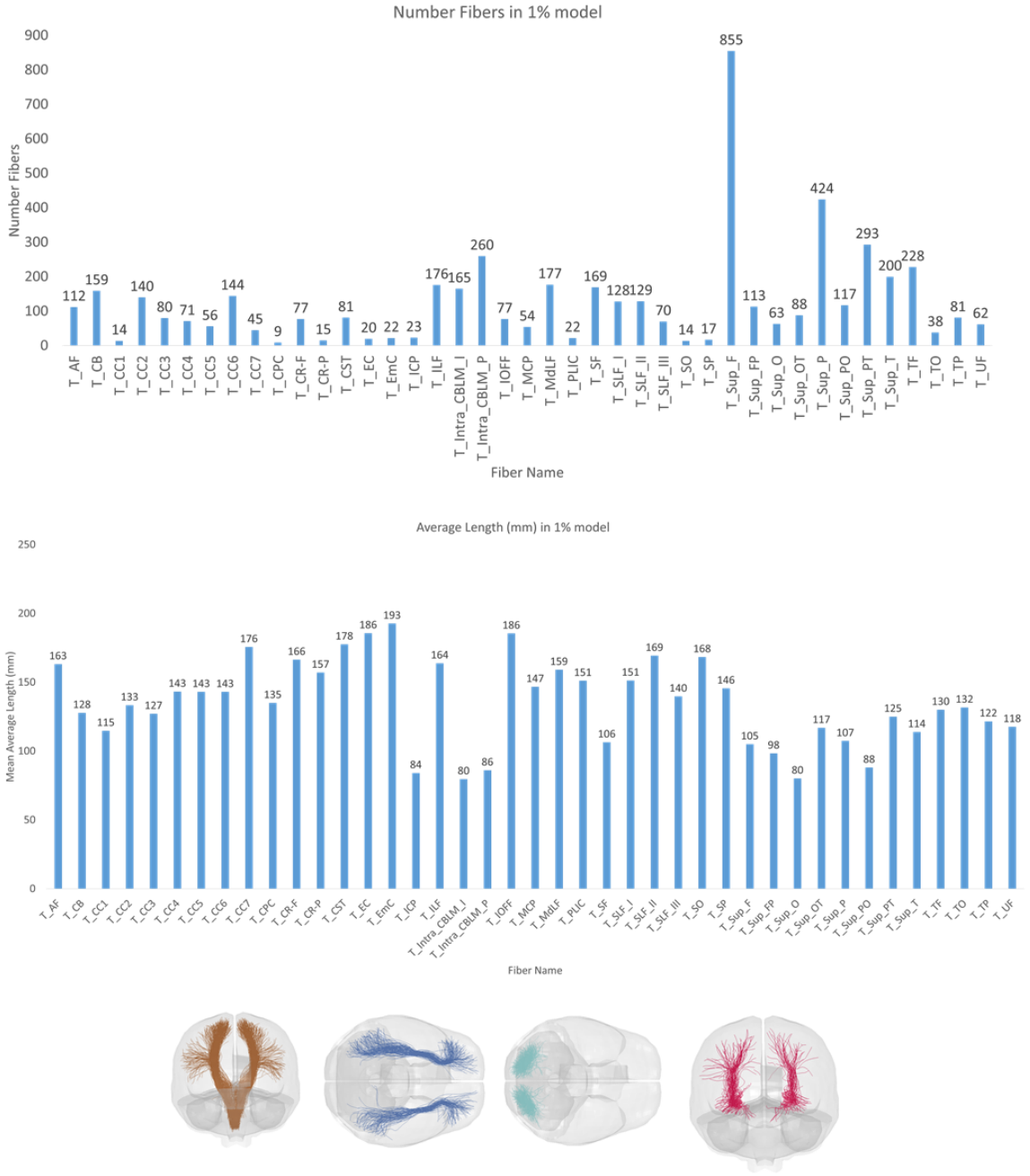

Figure 24, breakdown of number of fibers in 1% tract (top), Average mean fiber length in each tract (bottom) and outcome of beam elements inside head model. This pipeline allows for different metrics of fibers to be quickly and easily calculated.

4.3.2.2 Subject specific model

The DMRI used for this study was provided by the Western Universities Center for Functional and Metabolic Mapping and represents a single, healthy, 23-year old female patient. Although there are differences in the general size between male and female brains, this study was not focused on the anatomical difference but more on validating the overall process flow for this type of model. The fibers were generated and visualized using DSI studio (www. dsi-studio.labsolver.org), a tractography software tool that maps brain connections, with the overlaying atlas to determine the anatomical parcellation of the fibers being that of HCP-842 [146]. This software is considered a golden standard for fiber tracking and visualization, achieving the highest (92%) valid connections over 96 different methods (54% average) [152]. The diffusion images were acquired on a SIEMENS Investigational Device 7T scanner using a 2D EPI diffusion sequence. Echo time was 59ms, and repetition time was 6700ms. A multishell diffusion scheme was used, and the b-values were 1000 and 2000 s/mm2. The number of diffusion sampling directions were 30 and 60, respectively. The in-plane resolution was 1.6 mm. The slice thickness was 1.6 mm. The b-table was checked by an automatic quality control routine to ensure its accuracy [153]. The diffusion tensor was calculated. A deterministic fiber tracking algorithm [154] was used and fiber direction was determined using tri-linear interpolation [155]. A seeding region was placed at whole brain. The fa threshold was 0.141. The angular threshold was randomly selected from 15 degrees to 90 degrees. The step size was randomly selected from 0.5 voxel to 1.5 voxels. Tracks with length shorter than 18 or longer than 300 mm were discarded. A total of 50000 seeds were placed, repeated fibers within 1 voxel size were deleted as well as further manipulated with the in- house fiber generation script, provided as supplementary material.

4.3.3 Model Calibration and Validation

To validate this model, several similar studies were examined to assess their ability of determine model response compared to real world examples. As this is a preliminary study where the goal was to prove the viability of a parcellated axon fiber model, comparison to the baseline model was paramount and hence all validations were assessed based on that of the original GHBMC model results.

To assess the material properties and model response, a simplistic 3x3 solid model with embedded fibers was created using HyperMesh. This model was based off of work completed by Gerber et al. with solid elements modelled as Kelvin-Maxwell viscoelastic, the same material as white matter in the GHBMC model and the axon fibers modelled as Elastic MAT type 1 in LS-DYNA as well as MAT 6 viscoelastic and MAT 27 Mooney-Rivlin hyperelastic in an attempt to recreate accurate brain – fiber stress strain response [142]. These simulations where run to 1.5 times of stretch with a baseline (no fiber model) and fiber included models.

The first step in the calibration and validation process was to create a 3x3x3 (27 elements in total) simplistic model to determine the effect of different axon material properties, constraint type, and 1d element property type (Figure 25). This was also a quick way to test out the effects of axon diameter on stress-strain relationships and understand the overall effects that constrained axon fibers have on providing anisotropy to the isotropic brain material. For the solid elements, the same material properties as those in the original GHBMC model were used, this being a *MAT_KELVIN-MAXWELL_VISCOELASTIC on LS-DYNA. This model was based on that used by Gerber et al., and hence the dimensions (24mm) and number of axons used (100) were recreated accordingly. Each simulation given a prescribed motion set in the Z-translational acceleration to simulate a tensile loading scenario. A 1.5 times of stretch was applied meaning an additional 12 mm in the z-direction was applied to the top nodes of the model, while the bottom nodes were fixed in the z-direction, this was applied over a 1200ms time, each simulation took approximately 1 minute with additional time added for axon embedded models.

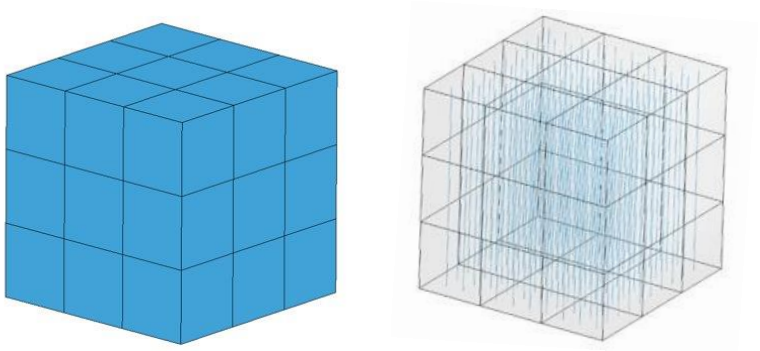

Element type	Material	Properties
Solid	Kelvin-Maxwell Viscoelastic [53]	ρ = 1060 kg/mm^3 κ = 2.19 GPa G_0 = 7.5 kPa G_I = 1.5 kPa λ = 0.0125
Beam	Elastic [95]	ρ = 1040 kg/mm^3 E = 63.3 kPa ν = 0.499
Truss	Mooney-Rivlin [148]	ρ = 1040 kg/mm^3 C_{10} = -1.034 kPa C_{01} = 7.803 kPa K = 2 GPa

Figure 25, the 3x3 simplified model to efficiently test material and property modification on left is the solid material model, on the right is a look inside the model to shows the 1D beam axon fibers. Also included is a description of the material properties tested for the solid material and beam materials.

Following the initial simulated tensile test studies multiple fiber embedded models were simulated to assess the bio fidelity of the axon-based model, when compared to the original GHBMC model. This was done using a study that is widely referenced for validating FE models completed by Hardy et al. (2001) [98, 103, 141, 142] which look to measure the relative brain-skull displacements under high- rate impacts in human cadavers using embedded radiopaque, neutral density targets (NDT) [118]. The baseline GHBMC model has already undergone these simulations, with the impact direction, duration and magnitude being inputted into LS-DYNA as time-history curves through a *PRESCRIBED_MOTION boundary condition [59]. Two scenarios where chosen, based

on widely referenced FE studies, NDT C755-T2 and NDT C383-T3 which simulated frontal and rear impacts and were compared to both the GHBMC baseline model result and experimental model result.

4.3.4 Finite element model generation

Although the subject specific and population-based models differed on how they were extracted, the process of converting the individual points of those models into 1-D beam elements for finite element analysis was similar. Points were imported into a custom MATLAB script that allowed for a visualization of individual fibers along with quantification of fiber dimensional characteristics. A tractography breakdown like the one used in this study is summarized in table 9. This in-house script also allowed for the conversion of the 3D tractography data obtained into line and points that could be imported into HyperMesh as IGES files and generated into 1D Hughes-Liu with cross section integration (ELFORM 1) beam elements and Truss (ELFORM 3) 1D elements. The beam elements are 5mm in element length, as per Garimella et al. [103], this was chosen to reduce overall number of elements, for computational efficiency. A unique cross section diameter of the beam element, representing the axons, was determined for each level of detailed axon models based on volumetric conservation of the relative ratio of axon fibers volume to total brain volume.

Table 8, tractography model breakdown

Tract Name	*Brain 1 percent*
number of tracts	6500
tract length mean (mm)	90.07
tract length SD (mm)	48.04
tracts volume (mm^3)	49592
fa mean	0.45
md mean	0.65
ad mean	0.99
rd mean	0.47
ha mean	31.57
Axon diameter mean	0.67
Axon SD	0.43

For both the population-based and subject-specific models, different numbers of fibers and therefore elements were used to determine the parametric differences in models will optimizing overall computation time. The 1D beam elements were then given a simple elastic material property based on a recommended Ogden Hyper-elastic substitute provided by Garimella et al. [103], as well as different viscoelastic and hyper-elastic models to determine optimal model response. LS-DYNA does not allow for Ogden Hyper-Elastic materials to be applied to beam elements hence a replacement material had to be found[11]. For this study the simplicity of an elastic material was important as it provided a repeatable uncomplicated material that could be modified with relative ease and was validated by Garimella et al. as a suitable replacement to Ogden Hyperelastic, producing on average a difference of only 3.4% strain values [103]. Table 9 shows the material properties of the elastic model which showed similar strains in relation to the brain in other literature studies, other materials, mainly a Mooney-Rivlin hyperelastic and a viscoelastic material modelled around white matter properties were also tested, however showed significant inaccuracies in the models response to impact.

Following the completion of this initial parametric study the fully detailed fiber axon model was embedded into the GHBMC baseline head model through anatomical location estimations and constrained as embedded elements using the LAGRANGE_IN_SOLID keyword in LS-DYNA. Techniques like this have been employed previously to model rebar-reinforced concrete composites, and model response appeared to be more accurate with this type of constraint over *BEAM_IN_SOLID, especially for Hughes-Liu beams (ELFORM1), which allow for better visualization of strain response as well as allow for shear strain and stress response which is not possible with ELFORM3 Truss elements [141]. This constraining method should ensure that the baseline white matter and the fiber axons will have the same accelerations and velocities under loading. The models were then simulated as a PRESCRIBED_MOTION at the COG of the head with a *DEFINED_CURVE which is simulated as parabolic acceleration at 5 krad/s^2 to simulate a typical mild traumatic impact to the head [63]. This six-degree-of-freedom (DOF) kinematic curve was accelerated for 5ms and decelerated for 5ms before given an additional 10ms to represent any strains that result from the “lagging” inertial effects. Once the process was validated to providing repeatable results

a more complete representation of the displacements and anisotropic effects of the model was simulated based on previous brain-skull displacement experiments.

4.3.4.1 Testing model response and fiber sensitivity

The purpose of this project was to determine the ability to produce a parcellated axon fiber FEM. This model is not available to the best of our knowledge and hence its ability in injury diagnosis and in neuroscience applications is significant. Three landmark tracts were chosen, based around the idea of fiber tract orientation (commissural, association and projection) with differences to tract damage level assessed. The commissural tract chosen was the (CC), this tract was assessed for its average axial strain and cumulative strain damage measure axon (CSDMa) which was set at 0.20 as per Bain et al. the same was done for the projection fiber tract (CST) and the association fiber tract (SLF I) [43]. A simplified prescribed rotational acceleration of 5000 rad/s^2 was applied to the GHBMC model along different axis. This resulted in three different head motions Lateral Bend (LB), Axial Rotation (AR) and Flexion (FL), each of which will look to provide a better image of how the axons react to different impact direction along with how the brain responds to its preferred direction of motion.

4.3.5 Data analysis

All simulations were performed with LS-DYNA (V971 R8, double precision, LSTC, Livermore, CA) using a Lenovo P920 Thinkstation (24 Core, Intel XEON Gold 5188 CPU @ 2.3GHz (2 processors), 128 GB RAM). All kinematics were applied to the center of gravity of the head model. A custom MATLAB code was also developed to provide post processing comparison metrics such as CSDM, $MPS_{average}$, MPS top 1 % and 5 % and MPS 50^{th} 75^{th} and 95^{th} percentile and maximum axial strain (MAS). All statistical analysis was completed using SPSS 26 and Excel.

4.4 Results

4.4.1 Calibration results

Based on the initial simplistic model the best combination of element type, constrain type and material properties was determined to be an elastic material,

constrained Lagrange in solid with 1D Beam elements. Based on stress strain curves as well as visual confirmation with the stress plots and strain plots, Figure 26, that combination of parameters provided the most consistent patterns in respect to the original baseline material. Also compared were the axial strain responses, with a Lagrange in solid beam element providing a more consistent representation of axon strains, based on previously validated models in literature [103, 141, 142], with similar strain levels as the solid elements constraining it.

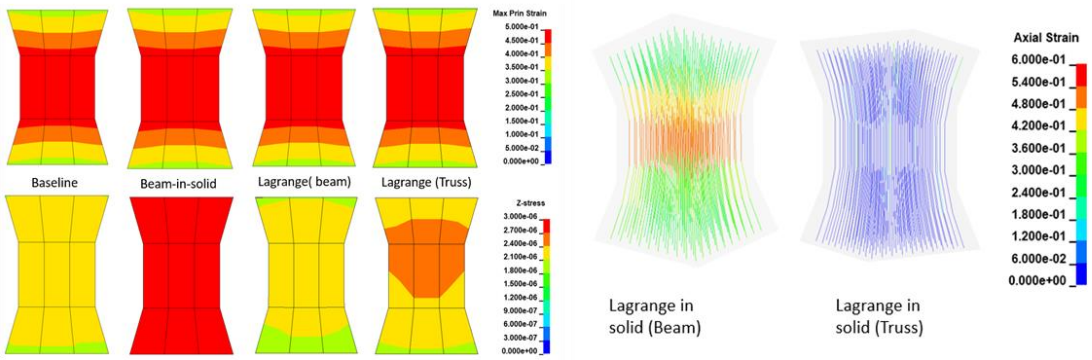

Figure 26, calibration model showing the different strain and stress patterns of the different models baseline, beam in solid with included axon constrain and lagrange in solid with included axon constrain, also shown is the difference in axial strain behavior between beam and truss elements.

4.4.2 Final models

The generation of the models was successful, with a full process flow pipeline generated to take DICOM images from D-MRI and transform it into a fully parcellated and anatomically accurate axon fiber finite element head model. These models can discretely showcase the axial strain as well as the shear strain present individual fiber tracts, with region-based output of maximum axial strain (MAS) and cumulative strain damage measure of axon (CSDMa) able to be quantitatively assessed. Visual confirmation of the strain response of both the original brain solid elements and the new beam axon elements is shown in Figure 27. The relative strain outputs, including CSDM and different MPS measures show that the difference in model response is below the 10% percent difference.

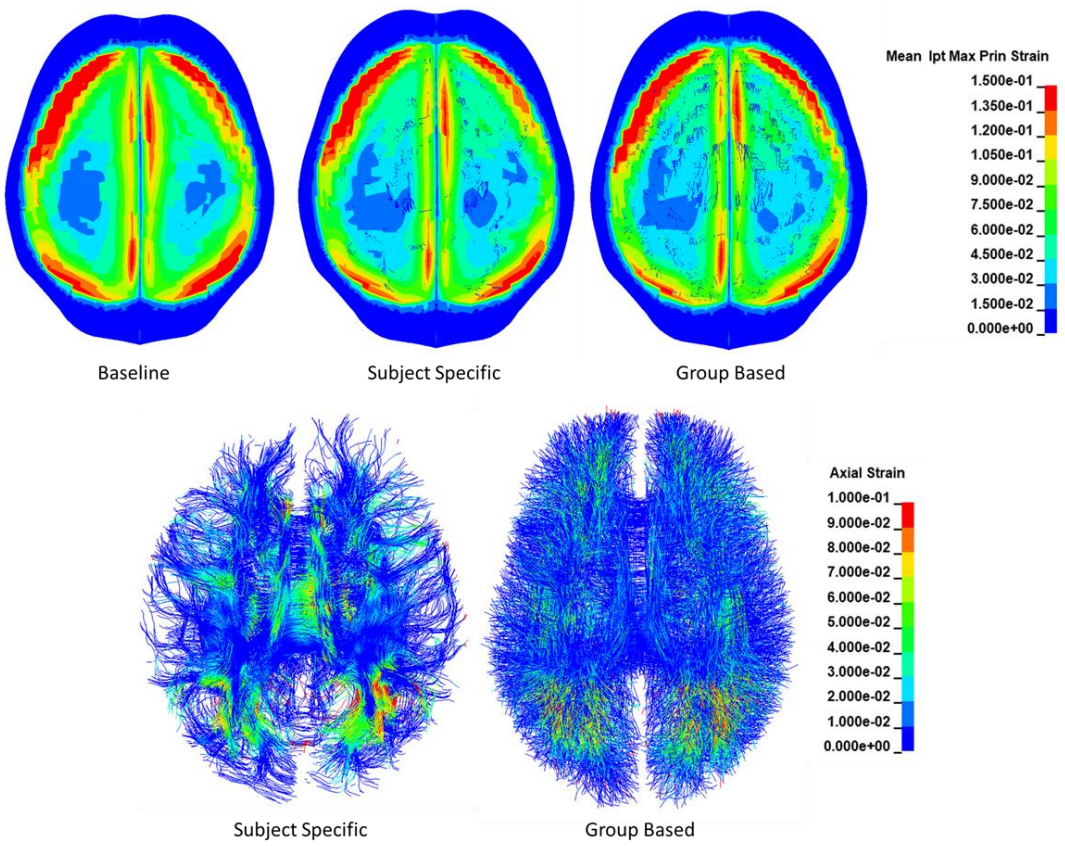

Figure 27, comparison of tissue-based strains in baseline vs the fiber embedded subject specific and group-based models.

Also shown is the validation study completed, with comparison between the baseline model, the experimental Hardy results and the new axon embedded model shown (Figure 28). The primary results of this validation study are that the relative displacement curves are slightly muted in the axon embedded model, which is to be expected as there is additional volume and material stiffness added to the brain model.

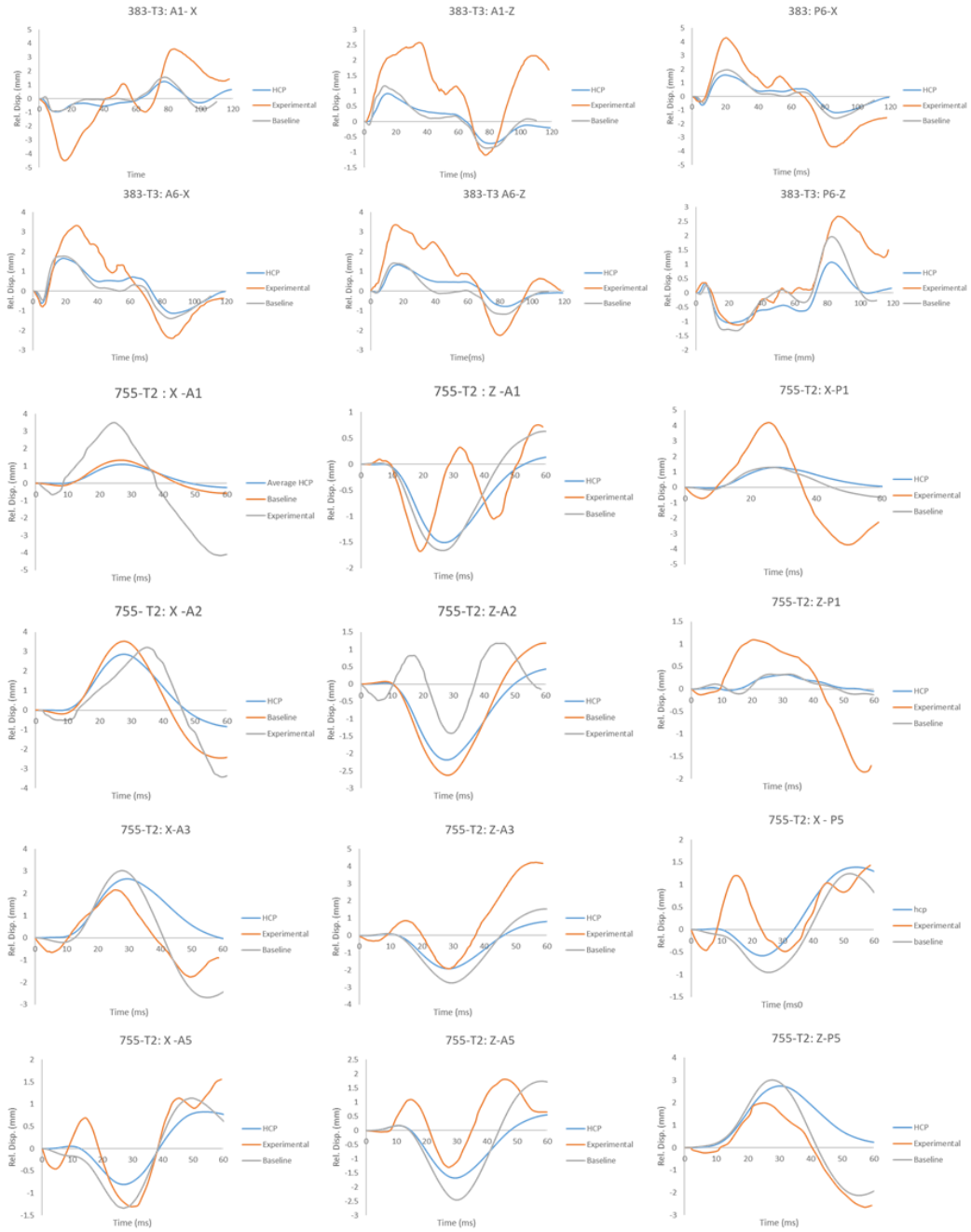

Figure 28, brain skull relative displacement charts comparing Hardy et al. cadaveric head experiments with the baseline GHBMC model and the new axon embedded GHBMC Model. Two experimental cases were examined (383-T3 and 755-T2) representing front and rear impacts.

4.4.2.1 HCP population-based model

The model chosen to represent the population-based HCP fiber tractography was considered the "1 percent" model, this model was generated through down sampling the original fiber tractography in 3DSlicer from 650,000 individual fibers to around 6,500 fibers, to allow for decreased computational expense. These fibers represent the myelinated long tract fibers which represent approximately 20% of all axon fibers in the brain. A volumetric conservation equation was used to retain overall axon volume in the brain to approximately 2% of brain volume, this was based on total fiber length (approximately 150,000km) and axon diameter (average is approximately 0.7 micrometers) [156]. This final model included 0.2mm diameter fibers representing 0.00043% of estimated total number of fibers in the average male brain while accounting for 2% of the total brain volume. Following the validation, CSDM5-25 along with average maximum principal strain and MPS5% and MPS1% were recorded and compared to the baseline model to confirm model response accuracy. The new axon embedded model exhibited a slightly stiffer model however all fall within the previously mentioned 10% range.

Table 9, baseline model vs group-based axon model vs subject specific axon model Strain comparison

755-T2	*Baseline*	*Group Based*	*Subject Specific*
CSDM5	0.790	0.757	0.759
CSDM10	0.378	0.295	0.326
CSDM15	0.095	0.087	0.084
CSDM20	0.024	0.033	0.027
CSDM25	0.003	0.008	0.005
MPS average	0.085	0.079	0.079
MPS 5%	0.195	0.203	0.196
MPS 1%	0.241	0.258	0.248

The total computation time for the Axon embedded model compared to the baseline model was approximately 1.75X longer, however, it now provides more insight into fiber directional damage and specific fiber injury, which was previously not possible. These models are now able to visualize strain patterns in individual parcellated axon fiber tracts.

4.4.2.2 Subject-specific model

In this study the subject specific parcellated model was developed more for validation of processes, for future research, although it opens the door for interesting exploration of the injured brain. The parcellated subject specific model was also validated against the baseline model (Table 9) with comparable outcomes to that of the population-based model. Using DSI studio a model was developed to mirror that of the HCP model, with 6500 fibers that were distributed over 73 different tract clusters, this model allowed for the differentiation of the left and right hemispheres. Therefore, the axon diameter was like that of the population-based model. Overall, the computation time was comparable to the HCP model with a total time of 20 hours at NCPU = 4 for the 62.224ms simulation time of the HARDY 755-t2 impact duration.

4.4.3 Tract specific strain response (typical impact)

The results, along with their respective visualize strain plots are shown in Figure 29, and tables 10 (tissue-based metrics) and 11 (axon-based metrics). Of note is the increased presence of CSDMa10 in the CC tract (0.14 compared to 0.042 (CST) and 0.025(SLFI)) during lateral bend and CSDMa5in the CST tract (0.3 compared to 0.21 (SLFI) and 0.16 (CC) during flexion loading. We hypothesize that this is due to the anisotropic response of the new model, where strains acting along a specific direction can now be visualized in the FEHM.

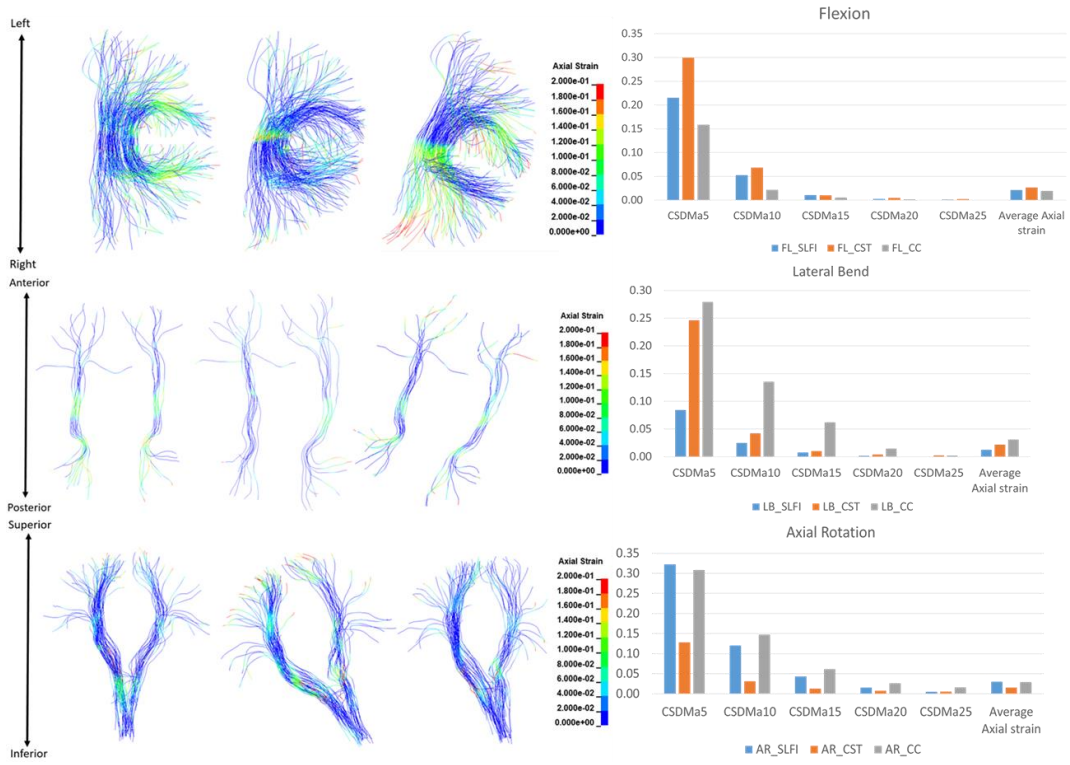

Figure 29, axial strain visualization of the 3 specified parcellated tract clusters along with the CSDM $_{axon}$ and average MAS during each loading condition.

Table 10, comparison of tissue-based metrics of 3 impact directions

Row	*Axial Rot.*	*Flexion*	*Lateral Bend*
CSDM5	0.940	0.913	0.870
CSDM10	0.735	0.651	0.538
CSDM15	0.526	0.345	0.287
CSDM20	0.346	0.166	0.136
CSDM25	0.221	0.079	0.064
MPS Average	0.190	0.131	0.117
MPS5%	0.493	0.325	0.298
MPS1%	0.580	0.410	0.351

Table 11, comparison of axon-based metrics of different directions lateral bend (LB), axial rotation (AR) and Flexion (FL)

CSDM Threshold	*CSDMa5*	*CSDMa10*	*CSDMa15*	*CSDMa20*	*CSDMa25*	*Average Axial strain*
LB_SLFI	0.0842	0.0250	0.0079	0.0015	0.0001	0.0124
LB_CST	0.2462	0.0423	0.0101	0.0040	0.0024	0.0217
LB_CC	0.2793	0.1354	0.0621	0.0146	0.0021	0.0309
FL_SLFI	0.2152	0.0527	0.0109	0.0028	0.0014	0.0213
FL_CST	0.2995	0.0684	0.0104	0.0049	0.0024	0.0267
FL_CC	0.1585	0.0218	0.0054	0.0015	0.0003	0.0196
AR_SLFI	0.3223	0.1203	0.0434	0.0156	0.0052	0.0301
AR_CST	0.1283	0.0313	0.0128	0.0077	0.0057	0.0156
AR_CC	0.3081	0.1477	0.0618	0.0268	0.0162	0.0292

4.5 Discussion

4.5.1 Exploration of brain strains in parcellated model (different strain thresholds)

Two validated embedded models were generated that provided a novel parcellated construction while utilizing new and previously explored methodologies to generate one of the most biofidelic FEHM to date. This study was successful in providing evidence of the connection between axial strain and the brains MPS while also showcasing the differences between isotropic strain patterns and the anisotropic patterns exhibited by the embedded axon fibers, a more accurate representation of the human brain as mentioned by Garimella et al and Wu et al. With the use of new analysis metrics such as CSDMa and MAS average, different tracts could be compared and analyzed for potential injury risk, one of the goals of this study. While other groups have developed similar models, mainly Wu and Garimella, the introduction of specific tract analysis through the use of a pre-existing brain atlas shows a new direction that computational biomechanical analysis of head injuries could pursue, mainly injury prediction not through general threshold level but through regions most likely affected.

4.5.2 Validation of model's viability a potential use as exploratory tool

Axial strain is a validated method to determine brain injury level, Hajiaghamemar et al, compared axonal based injury prediction metrics such as MAS to other tissue based injury metrics and determined that it had outperformed typical brain metrics such as MPS and CSDM in predicting traumatic axonal injury (TAI) [157]. The improved injury prediction capabilities and the ability to validate impacts with those seen in specific sports and their resultant injuries studies such as Bain et al. indicate an injury likelihood of 50% from axonal strains of 0.18 or greater [16, 43] [44] will allow for future studies to use this threshold with our in-house developed CSDMa to determine the extent of axon injury. The level of injury which could result in permanent damage, leading to short- and long-term cognitive impairments and neurodegenerative diseases due to DAI. These new axon embedded models have shown that while tissue based strain results where similar in some models as a whole , the specific location of strain differed, with the parcellated model this was taken a step further where injury along the tract was able to be discerned and hence the exact location of potential lesion was determined.

It is well understood that rotational motion leads to what are known as diffuse injuries [158]. The strain patterns that were exhibited in the different impact directions shows that the idea of a singular definition of a concussion could be misconstrued, while the saying "no two concussions are the same" holds up, the knowledge gap to group those concussions into symptom based categories could provide a better idea of how to better protect the brain and help treat concussion patients.

4.5.3 Advancing computational brain models for better understand injury mechanisms

The developed models exhibit several prominent advantages that helps the field. While advantageous to use one of the most commonly used and validated models as the baseline model, GHBMC, the addition of explicitly embedded axon fiber tracts extracted from DTI to add another level of mesoscopic detail to the model, an improvement on models such as that of the SIMon, KTH model. Ji et al. have stated that this higher level of detail, especially when considering the anisotropic strain parameters derived from axial strain

produces significant advantages when correlating FEHM strain outputs and concussive events in sport [17].

The addition, the inclusion of two separate models, easily generated from a partially automated DTI to FE pipeline, provides advantages over other comparable explicit axon embedded models such as that developed by Garimella et al. which is a subject specific based axon model incorporated into a subject specific and relatively untested head model or that developed by Wu et al. which was constructed with the HCP population based model and GHBMC head model, but is limited as it does not include the detail of beam elements along with the atlas based parcellation included in this model.

4.5.4 Limitations

This preliminary study does have its limitation however, the first, which applies to all DTI derived axon tractographies is fundamental ambiguities inherent in tract reconstruction based on orientation information alone, which need to be considered when interpreting tractography and connectivity results [152]. While DTI has improved, limitations with the accuracy of tract prediction, especially in crossing fibers is still prevalent. The comparative nature of this and subsequent studies does reduce the overall negative effect of this limitation as the models are compared with similarly derived DTI models, all of which are at a reduced tract density percentage.

Another limitation of this study is the use of 1D beam elements with an elastic material behavior. While this material provides efficient simulation and a reduced computational cost it does differ from the gold standard Ogden hyperelastic material used by other groups, primarily Wu et al. and Garimella et al. However, the use of this material and its material properties were reported to be sufficient as an Ogden hyperelastic replacement in beam by Garimella et al. who reported that MPS differed by only less than 5% and the percent of “damaged axons” only differed by 2.1% [103].

4.5.5 Conclusion

This study provided the preliminary setup and development process of future studies that will look to explore the relationship between the mechanical loading inside the head

immediately post impact and the associated functional changes of the brain that leads to the varying post-concussion symptoms and the idea that “ no to concussions are alike”.

This study is the first, to our knowledge of combining researched human brain atlas with high resolution 7T MRI and a highly validated FEHM to create a novel tool for the future of traumatic brain injury reconstruction and concussion prediction. The use of this tool looks to assist in future helmet-based studies as well neuropsychological studies to combine an engineering approach to exploring brain injury with neuroscience.

Chapter 5

5 Predicting the typical mTBI injury patterns to the brain's functional network exhibited in ice hockey for post-concussion syndrome assessment

5.1 Abstract

Post-concussion symptoms such as cognitive impairment, decreased motor function and sensory sensitivity results in the decreased quality of life of mild traumatic brain injury (mTBI) victims. Innovations in imaging technology and the rise of computational head models to predict the brain responses to impacts has provided new insights into how to better protect the brain and how to potentially mitigate the risk of receiving a concussion. While understanding the effects of an impact to the brain is important, linking those brain responses to real world functional magnetic resonance imaging data, could be the bridge between quantitative injury prediction and qualitative injury outcome diagnosis measures. In this study, a novel three-dimensional parcellated axon fiber model, derived from diffuse tensor imaging (DTI), was developed and embedded inside a validated sate of the art computational model, the global human body model consortium (GHBMC) head model, to provide unique insight into the deep brain microscopic response and the effect of typical hockey impacts on different axon fiber clusters. In this study, 12 impact kinematic curves (80-ms duration impact), representing typical hockey impacts at 4 impact directions, 3 energy levels and 6 different helmet models (n =672), were simulated using this state-of-the-art model. Impact kinematics was assessed for their injury probability level using peer reviewed brain injury prediction criteria such as; Gadd Severity Index (GSI), Head Injury Criterion (HIC15), The Generalized Acceleration Model for Brain Injury Threshold (GAMBIT), Brain Injury Criteria (BrIC), Universal Brain Injury Criterion (UbrIC) and Diffuse Axonal Multi-Axis General Evaluation (DAMAGE). Following the simulation each impact was post-processed with validated injury assessment methodologies such as average maximum principal strain ($MPS_{Average}$), cumulative strain damage measure (CSDM), MPS 1% and

5% critical values, and axial strain. Along with those assessments a new injury assessment measure was proposed, the cumulative axon strain damage measure (CASDM) to assess axon fiber clusters relative damage. Of the 12 kinematic impacts, the rear impacts were chosen for in-depth analysis, as it aligned with the reported impact location of the concussed test subjects. As the background research was previously completed at Western University, studying real-world youth resting state functional magnetic resonance imaging (RS-MRI) following hockey impacts, the Superior Longitudinal Fasciculus (SLF) tract showed particular high levels of axial diffusivity (AD) which has been shown to correlate to diffuse axonal injury (DAI) [8, 21]. Patients in those studies also completed regular testing of $SCAT_3$ to assess post-concussion symptoms associated with PCS[159]. Our model showed a similar injury pattern of axial strain to that of the connectivity impairment in the RS-FMRI dataset, resulting in a preliminary validation of the model's prediction capabilities. This data was then further analyzed to confirm the typical function of each affected tract and how this can affect a victim's post-concussion symptoms. The functions associated with the tracts are; the facilitation of cognitive processes, spatial-attention deficits and connection of high and low order auditory processing. Superior Longitudinal Fasciculus tract experienced CSDM10 of 0.053 and 0.051 in the rear and frontal impact which was approximately 2 times that of those experienced in the side and top impacts. These findings align with those reported in the study, while other findings align with symptoms reported in the $SCAT_3$ results. This study helps to bridge the gap between some of the mechanical responses inside the brain and their related symptomatic responses that patients experience. The goal of this and future studies is to gather a large enough dataset where the potential to diagnose a concussive injury could be done more precisely and effectively and lead to new advancements in rehabilitation methodologies to increase patient outcome and improve their quality of life quickly.

5.2 Introduction

5.2.1 Background and problem

The traumatic brain injury (TBI) is amongst the most predominant injury types in terms of case fatalities, long term implications, and injury occurrence/ re-occurrence [160]. This injury type is broken down into three similar but varying levels of injury severity mild, moderate and severe, according to the Glasgow coma scale (GCS) [161]. The mild traumatic brain injury (mTBI) is a significant burden on patients, their families and the health care system, as it is the most common reported at approximately 80% of hospitalized TBI instances [135]. While the diagnosis and mitigation of these injuries continues to be the focus of academic research, the rehabilitation and long-term negative effects that this injury type presents to a large portion of its recipients remains a challenge. Approximately 10 – 25 % of mTBI patients, while reporting recovery of initial symptoms, exhibit the persistence of other functional impairments such as cognitive, emotional, somatic and behavioral disturbances, a presence of any singular or combination of these symptoms is generally referred to as post-concussion syndrome (PCS) [162]. Cognitive impairments generally refer to issues with ones working memory and executive functions, both of which have specific tests that can test for subtle differences. Somatic symptoms usually refer to how a patient feels, typical examples include nausea, dizziness, headache, blurred vision, auditory disturbances and fatigue. As for emotional or behavioral problems, changes to a person's typical mood are noticed by themselves or surrounding individuals with typical examples including disinhibition, emotional lability and post-traumatic stress disorder (PTSD) [163]

5.2.2 Post-Concussion symptoms

With concussions constituting a large portion of sports related injuries, particularly in physical sports such as hockey, rugby, football and soccer the prevalence of PCS in adolescent athletes is concerning. Babcock et al. reported that 29.3% of adolescent (age 5-18) mTBI patients admitted to the emergency department, experienced some form of PCS, with the most common persistent symptom being headaches, resulting with patients to miss between 1-3 weeks of school[164]. The difference between this

injury type and other typical sports injuries such as broken bones or torn ligament is the inability to return to daily norms quickly, particularly in school environment, leading to future academic complications.

5.2.3 Axon fiber models and computational models

To understand the outcomes of a concussion, it is important to first understand the mechanisms that result in injuries that constitutes as concussions. Typically, impacts to the head or body that result in rotational motion to the skull and brain kickstart a chain of responses that lead to damage to the brains soft jelly-like tissue. Brain tissue, made up of grey and white matter, stretches during rotational motions leading to damage. These injuries are known as diffuse injuries, which are the most common pathology in mTBIs, with diffuse axon injuries (DAIs) exhibited to lead to axonal degeneration [139]. Being the second most common cause of fatality in TBIs and the most prevalent injury pathology across mild to severe TBIs, the presence of DAI is an excellent metric for concussion prediction. It has been shown that there is a 50% risk of DAI at 15% of axonal strain which marks it as a telling metric for concussion prediction [139]. The potential of this metric in determining concussion risk has led to several groups to create detailed axon embedded FEHMs to calculate axonal stretch through the axial strains predicted in computational simulations [103, 141]. Bain et al. reported similar findings and stated that axonal strain of between 0.18 -0.21 has a 50% likelihood of resulting in permanent axonal tearing and therefore impairment [43].

5.2.4 Typical hockey impact and the concussed player

A research study that looks to track the post-concussion brain changes in hockey players was competed at Western University by Manning et al. [8]. In the study, 17 bantam-aged (11-14) male hockey players that were diagnosed with concussions and a control group of 26 age-matched players were recruited. The study then evaluated the concussed players over time (24-72 hours after an injury) using a variety of advanced MRI techniques and compared that data to the control group (Figure 30). This study provided a basis of typical brain changes evaluated through imaging modalities in concussed players and hence will provide evidence to the validation of this research methodology for the typical

hockey impact kinematics and typical hockey injuries sustained from these impact situations.

In this study clinical measures, diffusions metrics along with resting state network and region to region functional connectivity patterns were analyzed. The results indicated that tract specific spatial statistics revealed a large region along the SLF with significant decreases in diffusivity measures, correlating with clinical cognitive deficits [8].

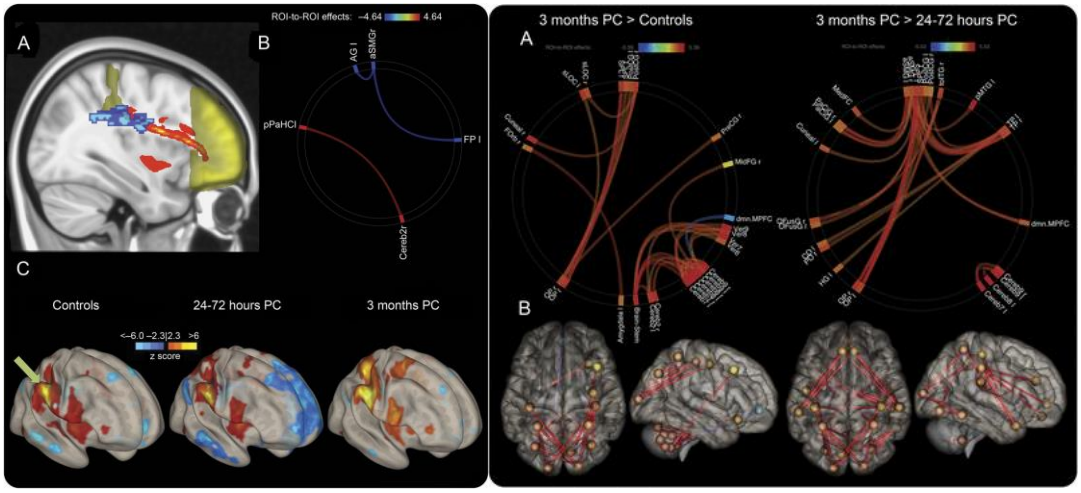

Figure 30, left, rs-fMRI changes in concussed subjects brain, showing activity area in SLF, Right, network connections in different regions in brain, concept derived from connectograms (images taken from Manning et al. 2018 Neurology manuscript)

5.2.5 Comparison of tissue-based injury metrics and axon-based injury metrics of helmets

Several outcomes that this paper looks to explore are (1) what is the typical hockey concussion brain response and what prediction metrics or the new axon-based metrics best explains it, (2) what are some of the brains "hot spots", and how does typical brain injury patterns in tissue compare to axon damage and finally (3) can this detailed FEHM provide evidence to some of the typical PCS symptoms exhibited by hockey players who have experienced concussions and does this match with functional imaging studies of concussed players brain changes.

5.3 Methods

5.3.1 Creation of Kinematic representative curves

The Hockey STAR experimental hockey helmet evaluation methodology was used in this paper as the basis of the laboratory testing parameters. This laboratory testing method, was designed to recreate real-world, concussion-like, impact conditions in the sport of ice hockey, to evaluate and identify the differences in the ability of hockey helmets to reduce concussion risk [66]. The laboratory testing matrix is made up of 3 different energy levels and 4 different impact locations equating to 12 individual testing scenarios for each helmet. To determine the magnitude of different impact energies, data from two different studies encompassing impact data from men's, women's and youth ice hockey players was used[165]. One of these studies, following male and female collegiate ice hockey players over 3 seasons, recorded 37,411 impacts, and recorded linear and angular kinematics, using a helmet mounted sensor array, as well as differences in exposure by sex, player position and session type(game or practice) [165]. The Hockey STAR experimental procedure used a pendulum-based impactor, striking a medium NOCSAE head form mounted on a Hybrid III 50^{th} percentile neck at varying levels of speeds (energies). This experiment used a pneumatic impactor with output velocity speeds designed to align with those generated by the pendulum arm angles of 40° (low), 65° (medium) and 90°(High), with 2.4 m/s, 4.8 m/s and 6.0 m/s respectively. These impact magnitudes were then focused on the helmeted dummy head at 4 different impact locations, two aligned with the center of gravity of the head form (front and rear) and two non-centric or tangential with the COG (side and top). For each impact scenario a minimum of 2 different helmets of each model are to be tested with each helmet tested twice for each of the 12 impacts for a total of 24 impacts on each individual helmet. A representation of a typical impact testing scenario can be seen in Figure 31. In total 6 different helmet models were tested, producing 672 individual impacts that conveyed the typical kinematic of a lab produced real world hockey impact. This was explained in more detail in previous chapters.

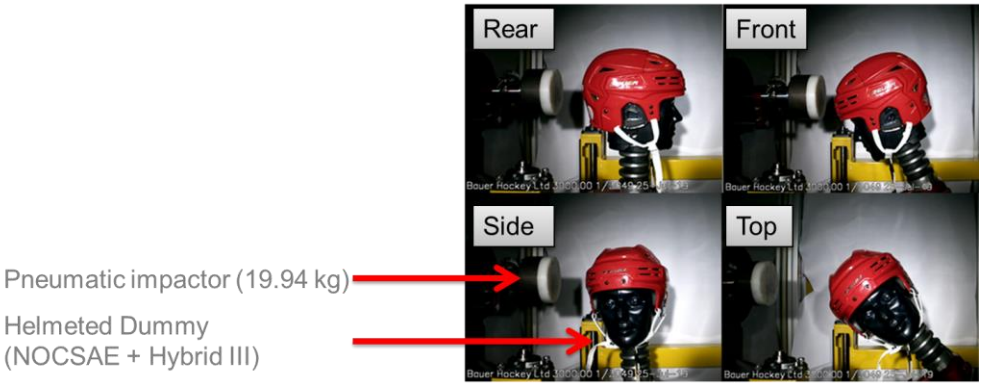

Figure 31, representation of a typical helmet setup for physical experiment. Side and Top impacts were non-centric.

For this study, a new MATLAB processing script was developed to take the previously generated 672 individual helmet impacts, categorize and average them. These were then organized based on impact location and energy to create 12 representative curves of what a hockey player would be most likely to experience in-game (ex. Mid-level impact to rear of head). These 12 impacts provide the typical helmeted head kinematic response over 80ms post impact and will be used along with a validated FEHM to model typical injury patterns exhibited by ice hockey players.

5.3.2 Explicit embedded axon fiber model

A modified, explicitly embedded, parcellated FEHM based around The Global Human Body Models Consortium (GHBMC) head model was used in this study as the functional injury predictor and PCS assessor. The model generation procedure was explained in detail in the previous chapter; however, highlights of the model include its new human brain atlas-based segmentation and parcellation of DTI derived axon fiber tractography extracted from 100 healthy subjects from the human connectome project (HCP). The automatically created white matter atlas parcellated 3D tractography model was developed and validated by the O'Donnell research group (ORG), and includes 58 deep white matter tracts, and 198 short and medium range tracts for a total of 800 fiber clusters broken down into 41 predetermined and labelled tracts found in the ORG-88FC-100HCP atlas [35].

The atlas segmented axon fiber tractography was then individually converted into 41 respective FE 1D beam models to create a group-based axon fiber model that was constrained in the GHBMC model by a Lagrange in solid constraining method in LS-DYNA. This model, embedded inside the GHBMC model, is shown in Figure 32 along with individual tracts, a total of 6500 fibers were used to provide a high enough level of anatomical detail while still reducing the computational expense that the additional 220,000 elements imposed. This embedded model underwent preliminary validation based both on brain-skull displacements derived from cadaveric studies completed by Hardy et al. as well as strain based comparison studies from the original baseline model developed by Mao et al. [59, 118].

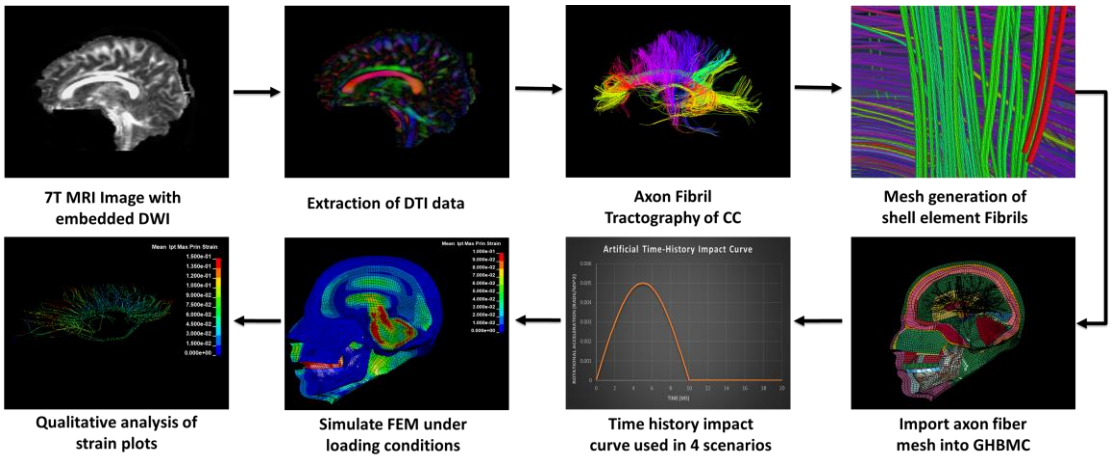

Figure 32, process flow for explicitly embedded GHBMC axon Model

5.3.3 Analysis Methods

Using the in-house script, post- processed tissue and axon strain metrics were assessed along with pre-processed kinematics-based metrics. The kinematics injury assessors used for injury comparison rely on linear and rotational accelerations and rotational velocity and have been widely used as TBI injury predictors. These metrics include GSI, HIC_{15}, GAMBIT, BrIC, UBrIC and DAMAGE. The strain-based injury predictors rely on the correlations between mechanical strain and tissue damage, which include CSDM, MPS and different variations. For axon injury predictors, individual tracts will be assessed with both MAS and a new threshold metric that works off CSDM,

which is named in this study as $CSDM_{axon}$. This metric will assess percent of axon damage, and axons elements which have exceeded predetermined injury thresholds for permanent functional damage [43].

5.3.3.1 Analysis and post-concussion symptoms prediction based on axon damage patterns

Using neuroscience concepts such as connectomics and connectograms along with the injury pipeline, this study looked to compare the highest damaged fiber clusters vs typical PCS symptoms. This study also looked to determine any additional correlation between individual tract damages for different impact magnitudes and directions, using SPSS V26 (IBM). All post-processing of the FEHM was done with LS-PREPOST V4.3.

Example uses of this pipeline and future research potentials were provided with a comparison to rs-fMRI literature studies which have examined post-concussion imaging of a helmeted hockey player. A comparison of the injury pattern exhibited by the player and those exhibited by the model could predict the injury location the player had while potentially predicting some of the players possible symptoms and provide a tool for researchers and medical professionals to look for and assess those injury patterns of PCS in impacted players. The subjects tested for this study included 17 male adolescent bantam aged players (age 13.3 ± 0.6 years) who were diagnosed with a concussion based on observed mechanism of injury followed by the onset of typical concussion symptoms. The design of this study has been described previously by Daley et al. [159]. The benefit of using this study as a reference point is both its relatively large concussive group size, but as well the tedious attention to detail that was described in diagnosing and gathering clinical data on the concussed players. Players also completed a Sports Concussion Assessment Tool -3rd edition ($SCAT_3$; 13-14 years of age) [166] which provided concussed individuals somatic, cognitive and behavioral post-concussion symptoms.

Table 12, breakdown of n =11 adolescent hockey players $SCAT_3$ results [159, 166]

Self-reported symptom	***# of concussion patients with symptoms (n = 11)***	***% of concussion patients with symptoms***
Headache	10	91
Dizziness	9	82
Pressure in head	9	82
Sensitivity to light	9	82
Don't feel right	9	82
Difficulty concentrating	8	73
Fatigue or low energy	8	73
Sensitivity to noise	8	73
Feeling slowed down	8	73
Drowsiness	7	64
Balance problems	7	64
Trouble falling asleep	7	64
Difficulty remembering	6	55
Neck Pain	5	45
Blurred vision	4	36
Feeling like in a fog	4	36
Confusion	4	36
Irritability	3	27
Nausea or vomiting	2	18
More emotional	1	9
Sadness	1	9
Nervous or Anxious	1	9

For this study 4 different tracts representing different orientation of fibers as well as different typical functions associated with damage to those tracts were chosen. These tracts (table 13), where analyzed in further detail for MAS as well as $CSDM_{axon}$ ranging from 5 -25 % strain. All tracts were analyzed with a medium level energy impact to recreate an impact that would border on being concussive and non-concussive and hence would provide detail in how an individual could be affected by each impact scenario. [165, 167, 168].

Table 13, description of different fiber tracts to be assessed

Tract Name	*Tract location and anatomical orientation*	*Tract function and symptoms when impaired due to damage*
1. Cingulum Bundle (CB)	Association tract connection located in parietal, temporal, and frontal lobes of cortex, above CC and under cingulate cortex (made up of five regions).	Executive control, emotion, pain, episodic memory, and cognitive functions, damage associated with Alzheimer's disease, schizophrenia, depression, PTSD, OCD and autism spectrum disorder [24, 25].
2. Corpus Callosum (CC)	Commissural tract connecting cortical regions of both hemispheres through corpus callosum.	Interhemispheric interaction, damage leads to inhibited transfer of somatosensory information and learning processes between sides of cerebral cortex, decline cognitive function [26, 27].
3. Corona-radiata-frontal and parietal (CR-F & CR-P)	Along brainstem projection tract.	Motor and sensory patterns, loss of motor function and muscle weakness, damage leads to sever motor and sensory deficits (faciobrachial or brachiocrural and hemihypethesia) [29].
4. Superior Longitudinal Fasciculus (SLF)	Major association fiber pathway connecting the postrolandic regions to frontal lobe, made up of four components	Facilitates cognitive processes; attention, memory emotion and language as well as a connection for working memory, damage to left SLF is language disorders, right SLF spatial attention deficits [32]

5.4 Results

5.4.1 Kinematic curves + typical tissue metrics

The pipeline successfully generated the 12 representative curves for input into the axon embedded FEHM, an example of these curves, with impact duration times of 80ms is shown (Figure 33).

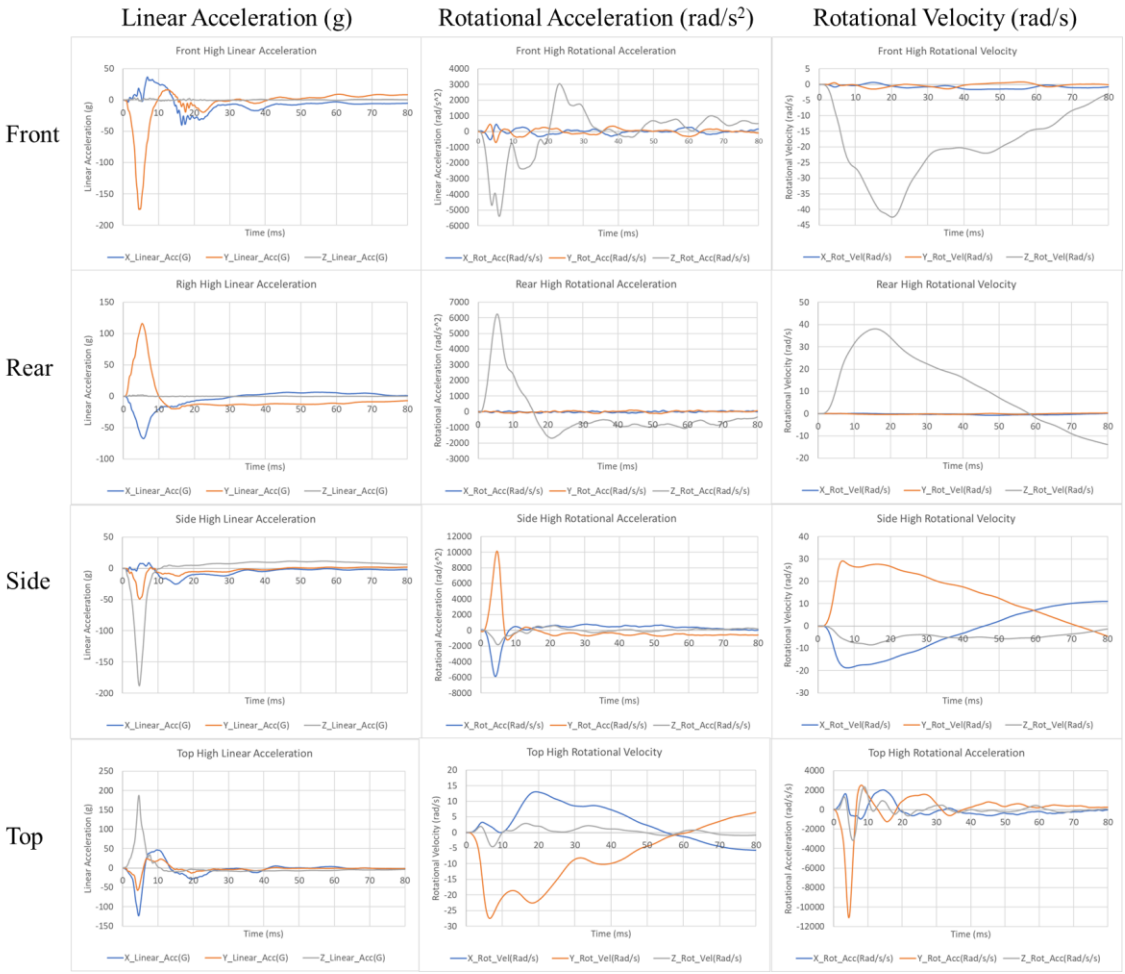

Figure 33, representative curve examples of 'High' Impact scenarios

The breakdown of these curves and their respective peak kinematics is provided in Table 14. The largest linear accelerations are produced in the a_z direction of the side impacts with 187.9 g in the high energy impact. However, the largest overall peak resultant linear acceleration is in the high energy level top impact with a value of 230.50 g. For rotational velocity the largest velocities are produced in the Front High direction with an average of ω_z = 42.44 rad/s, this is also the direction and impact energy with the highest resultant peak rotational velocity with 42.45 rad/s. In the rotational acceleration kinematic, again, side impacts with high impact energy produced the largest rotational velocity with α_y = 11482.30 rad/s^2, while also producing the highest Resultant peak rotational acceleration of 11677.27 rad/s^2.

Table 14, numerical values for peak kinematics of 12 representative curves

	Front			*Rear*			*Side*			*Top*		
Measure	Low	Mid	High	Low	Mid	High	Low	Mid	High	Low	Mid	High
$a_{x\ (g)}$	14.55	31.31	60.68	7.59	12.93	23.34	8.36	15.63	27.65	21.39	64.25	135.25
$a_{y\ (g)}$	48.11	91.39	168.08	52.20	79.05	132.96	11.78	25.29	48.43	2.01	6.89	13.13
$a_{z\ (g)}$	0.91	1.28	3.01	1.36	1.47	2.08	54.12	101.21	187.90	38.85	90.93	187.44
PRLA (g)	50.26	96.55	175.98	52.56	79.70	133.94	55.32	104.43	194.33	43.37	110.60	230.50
$\omega_{x\ (rad/s)}$	0.69	0.93	1.43	0.21	0.25	0.69	3.51	6.07	9.72	5.37	7.01	8.89
$\omega_{y\ (rad/s)}$	0.95	1.22	1.67	0.30	0.39	0.40	17.64	24.78	33.90	12.07	17.67	26.14
$\omega_{z\ (rad/s)}$	21.68	31.00	42.44	21.42	29.33	38.11	4.60	6.47	8.48	1.69	2.84	4.61
RPRV (rad/s)	21.69	31.00	42.45	21.42	29.33	38.11	18.26	25.66	34.83	13.16	19.10	27.83
$\alpha_{x(rad/s^2)}$	142.35	179.87	294.22	74.40	74.87	83.07	716.51	1269.77	1989.36	1239.25	2482.57	4517.04
$\alpha_{y(rad/s^2)}$	184.91	304.02	815.16	81.19	88.66	122.77	3612.39	6420.68	11482.30	2317.77	4979.71	10256.86
$\alpha_{z(rad/s^2)}$	1658.92	3232.39	5401.99	2510.16	3797.96	6254.36	646.87	1127.54	1810.94	606.20	1565.04	3155.06
RPRA (rad/s^2)	1659.71	3232.70	5408.31	2510.25	3798.06	6254.71	3717.43	6588.53	11677.27	2583.66	5515.74	11182.80

Along with the curve generation injury metrics were generated, these include GSI which had the highest score of 1152.76 in the Top High impact, HIC_{15} with the largest score of 593.94 in the top impact, BrIC with a largest score of 0.75 in the High Front impact, GAMBIT with a highest score of 1.14 in the top high impact, UBrIC MPS peak to peak of 0.25 in the High Front impact, UBrIC CSDM peak to peak of 0.36 in the High front impact, and DAMAGE of 0.46 in the High Rear Impact and an example DAMAGE score of 0.34 for a High Side impact of a typical hockey helmet.

Table 15, kinematics-based injury prediction metrics summarizing the 4 impact locations and 3 energy levels.

	Front			*Rear*			*Side*			*Top*		
Injury Metrics	Low	Mid	High	Low	Mid	High	Low	Mid	High	Low	Mid	High
GSI	90.53	290.88	957.75	97.63	250.71	660.29	89.93	304.12	998.85	67.22	297.19	1152.76
HIC 15	71.02	201.28	523.37	79.94	195.58	446.54	69.41	193.69	454.32	51.55	189.63	593.94
BrIC	0.38	0.55	0.75	0.38	0.52	0.68	0.29	0.42	0.58	0.22	0.32	0.45
Gambit	0.20	0.39	0.68	0.26	0.39	0.65	0.35	0.62	1.12	0.25	0.56	1.14
UBrIC MPS p2p	0.13	0.18	0.25	0.13	0.17	0.22	0.09	0.13	0.19	0.07	0.10	0.15
UBrIC CSDM p2p	0.18	0.26	0.36	0.18	0.25	0.32	0.16	0.23	0.32	0.12	0.17	0.25
Incidence STAR	0.08	0.14	0.47	0.19	0.05	0.17	0.53	1.64	2.20	0.04	0.26	0.10
DAMAGE	0.23	0.33	0.45	0.25	0.35	0.46	0.18	0.26	0.34	0.13	0.19	0.25

Following the simulation of the 12 representative curves in the axon embedded GHBMC model in LS-DYNA (smp_s_R10.0), where each simulation took approximately 38 hours with NCPU =2, tissue-based strain metrics could be extracted using the ELOUT file. These now provide representative injury outcomes from an impact, meaning a Top Low impact in a hockey game would produce a CSDM20 of 0.1 or approximately 10% of the brains volume would see a stretch of over 20% its original shape. For CSDM the most consistently high CSDM seen in the simulations was that of Front impacts with an average CSDM 5-25 across low- high of 0.378, 0.004 higher than Rear impacts. Front and rear impacts also have large MPS average across the board while Rear impacts have the high MPS 95th percentile. A full breakdown is provided in table 16.

Table 16, tissue-based strain metrics of the simulated impacts

	Front			*Rear*			*Side*			*Top*		
Strain Metrics	Low	Mid	High	Low	Mid	High	Low	Mid	High	Low	Mid	High
CSDM5	0.75	0.86	0.93	0.78	0.88	0.93	0.69	0.85	0.94	0.59	0.79	0.92
CSDM10	0.31	0.57	0.74	0.32	0.56	0.74	0.24	0.47	0.66	0.14	0.33	0.56
CSDM15	0.09	0.27	0.50	0.10	0.26	0.46	0.06	0.18	0.37	0.01	0.10	0.25
CSDM20	0.03	0.12	0.29	0.04	0.11	0.25	0.01	0.07	0.17	0.00	0.01	0.10
CSDM25	0.01	0.05	0.15	0.01	0.05	0.13	0.00	0.02	0.08	0.00	0.00	0.03
MPS $_{Average}$	0.08	0.11	0.15	0.08	0.11	0.15	0.07	0.10	0.14	0.06	0.09	0.12
MPS5%	0.20	0.29	0.39	0.21	0.29	0.38	0.17	0.24	0.31	0.15	0.20	0.27
MPS1%	0.26	0.37	0.50	0.27	0.37	0.49	0.20	0.28	0.37	0.17	0.23	0.30
MPS 50th	0.17	0.24	0.32	0.17	0.23	0.30	0.15	0.21	0.27	0.13	0.18	0.24
MPS 75th	0.11	0.15	0.21	0.11	0.15	0.20	0.10	0.13	0.18	0.09	0.12	0.15
MPS 95th	0.07	0.10	0.14	0.08	0.11	0.14	0.06	0.09	0.12	0.06	0.08	0.11

5.4.2 Axon injury results

The $CSDM_{axon}$ and MAS differs with the different impact directions as well as impact magnitudes. Figure 34 provides comparisons of the CSDMa values of the different tracts as well as MAS average values. Of note, across all impacts the CRF tract appeared to be most damaged in terms of $CSDM_{axon.}$ Moreover, the CC sustained the highest $MAS_{average}$ in the non-centric top impact with $MAS_{average}$ = 0.021, 33% more than the second largest $MAS_{average}$ values seen in CRF and CRP tracts.

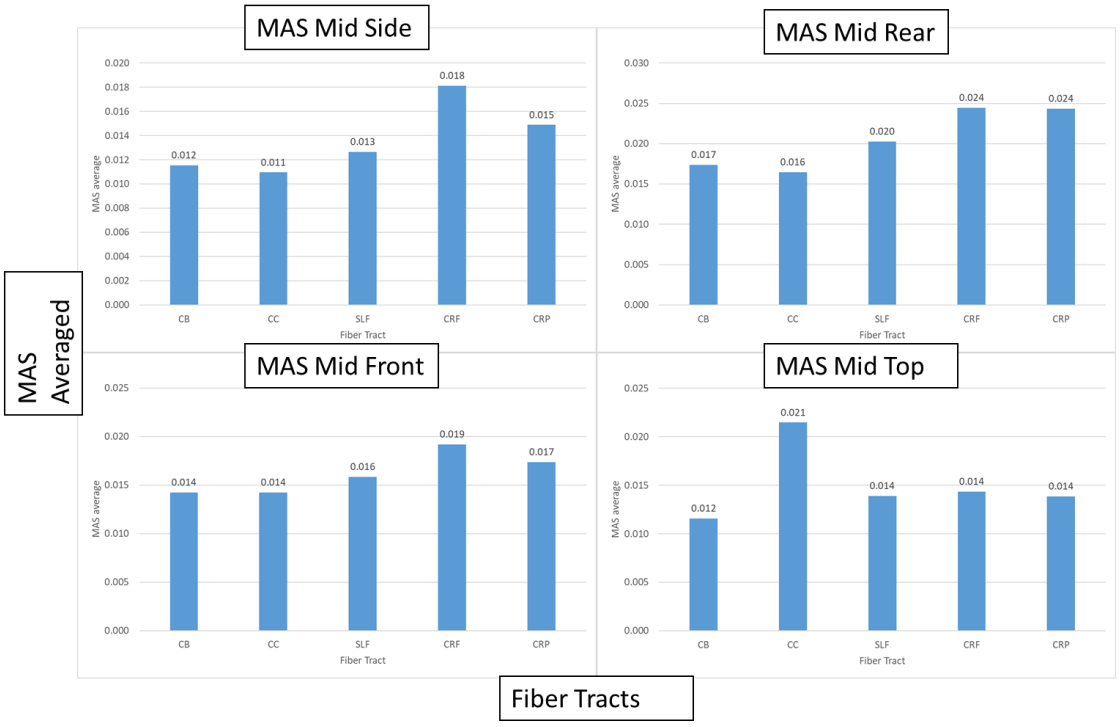

Figure 34, charts visualizing the differences in fibers MAS Average. Left to right, CB, CC, SLF, CRF and CRP.

5.4.3 Relation to real world concussion subjects

We then compared the specific tracts shown to have changes in their axial diffusivity, mean diffusivity, Fractional anisotropy and rs-fMRI in the Manning et al. study with the axial strain plots extracted from LS-PREPOST. Figure 35 visualizes these changes while showing specific regions of the tract where high strain concentrates. One observation that was reported was the obvious differences in high strain locations, with frontal and rear impacts showing varying locations along the tract of high strain concentrations. CST was also included in these strain plots to align with the Manning et al. and Daley et al. studies.

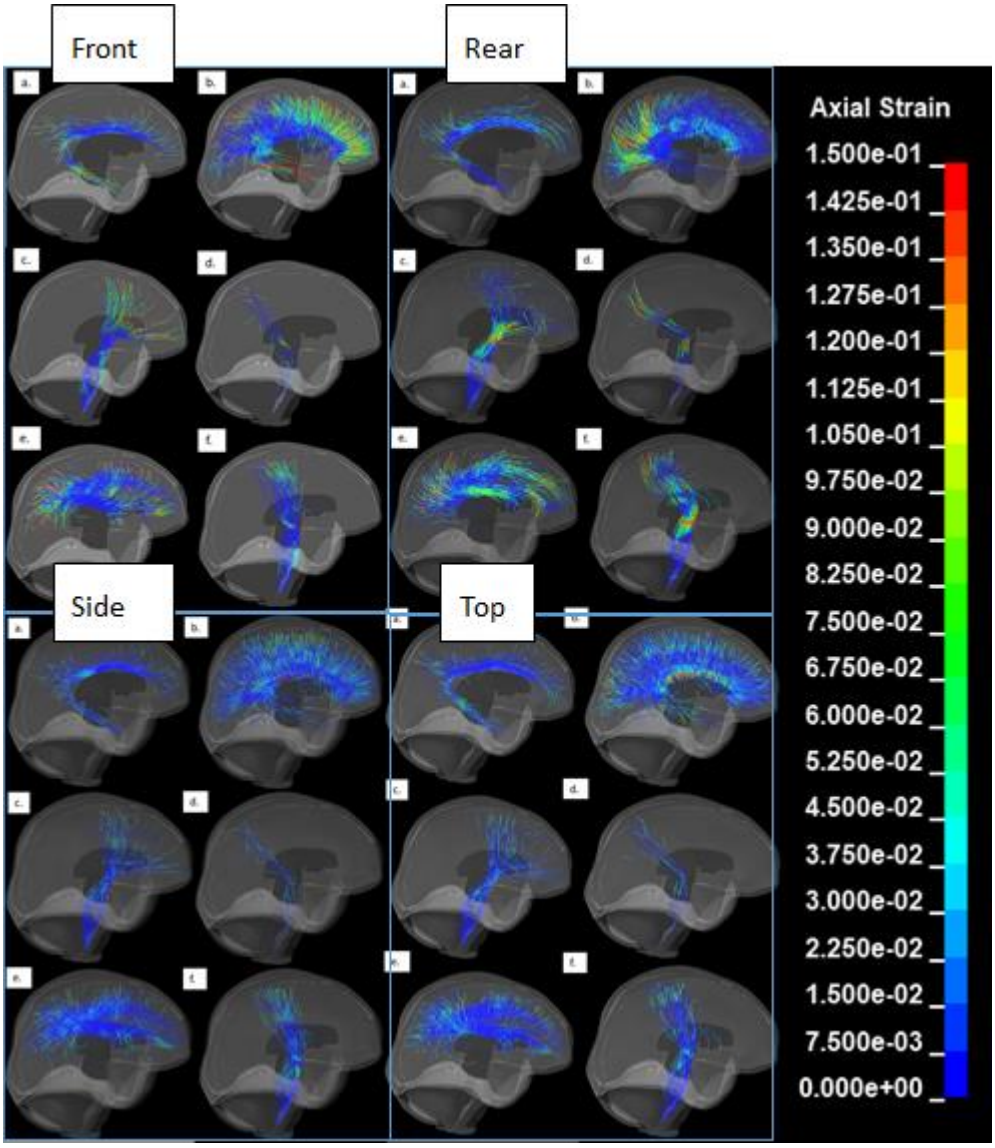

Figure 35, strain patterns of different landmark fiber axon tracts (a.) CB (b.) CC (c.) CR-F (d.) CR-P (e.) SLF (f.) CST

5.5 Discussion

5.5.1 Representative curve validity

It is important for the curves that are used to prescribe motion to the axon embedded model to be accurate to real world scenarios, so that they can recreate those real-world impacts and therefore provide reasonable data. Several studies have looked to determine peak impact kinematics during practices and games in-season, Mihalik et al.

captured 12,253 head impacts over 151 games and 137 practices and determined average linear and angular kinematics [168]. They reported that head impacts reported during game resulted in higher rotational accelerations than in practices and that directional effects were also present with 'Top' impacts resulting in higher linear accelerations but lower rotational accelerations and side impacts resulting in the largest rotational accelerations. Wilcox et al. completed a similar study recording 37,411 impacts over 3 seasons [165]. Their results provided average frequency of impacts per season for male and female collegiate players, 95th linear acceleration for male players equaling (41.6 g) and rotational impacts (4424 rad/s^2). Their study reported rear impacts resulted in the largest 95th percentile peak linear accelerations (45.2 g) while side and rear impact resulted in the largest 95th percentile peak rotational accelerations of 4719 rad/s^2. These two studies helped foster the idea for head impact exposure metrics and weighted factors for injury predictions such as those seen in UBrIC and STAR [66, 86]. In this study, the average peak resultant linear accelerations of approximately 50 g were seen in the low energy impacts while peak resultant rotational accelerations of around 5000 rad/s^2 where exhibited in mid to high level energy impacts except for top impacts which exhibited RPRA of over 10000 rad/s^2 in high level energy impacts. Our reasoning for these discrepancies is twofold, first, while providing accurate readings, the hybrid III fixed neck in the testing dummy is passive, not active, as one would see in a real world situations of one bracing themselves for impact, this would mean that the neck could be less of a factor in decelerating the head in our experimental procedure. Secondly, most studies recording these impacts (both concussive and non-concussive) are mostly made up of normal 'non-injury' impacts. These impacts can be assumed to be much lower than those experienced in concussive situations.

5.5.2 Typical post-concussion symptoms

One outcome of this study was the obvious advantages that are exhibited by the inclusion of axon fiber tractography in computational head models. While tissue-based strain metrics provide researchers an understanding of the overall probability of brain injury or concussive likelihood it has inherent limitations in attempting to predict or describe potential injury outcomes of the concussed individual [47, 51, 55, 86]. While

both are representative of DAI in the brain, the parcellated axon fibers provide a new tactic that could be implemented for future brain research. In this study it has been shown that Rear impacts prove to show significant MAS in landmark tracts such as the SLF tract, validated by comparison to manning et al. study. For Manning et al.'s diffusion results, there were significant main effect for group differences in the CST, cingulum and SLF (F =4.18 $p < 0.05$), with a large region of the SLF shown to have significant MD, RD and AD changes even at 3 months post-concussion [8].The SLF tract known to facilitate cognitive processes; attention, memory emotion and language as well as a connection for working memory [26], symptoms exhibited in over 55% of concussed subject [159], could provide a new tool for impact location prediction as well as symptom prediction of impact location is known. These strain patterns line up both in terms of tracts showing high MAS as well as the specific location of injury determined by rs-fMRI changes in the SLF as well as the CST, where high strain (damage) to the lower portion of the tract was also observed in Manning et al. study [8]. Another point of note was the consistently high axial strain exhibited in the CR-F tract, where damage to this tract and the CR-P tract leads to severe motor and sensory deficits, all of which were again exhibited by the majority (64%) of concussed cases, as stated by the $SCAT_3$ results [29]. Moreover, Top impacts proved to have high MAS in the CC which was also present in the visual strain plots for frontal and rear impacts at a fringe level of 0.15 MAS, damage in the CC leads to inhibited transfer of somatosensory information and learning processes between sides of cerebral cortex, decline cognitive function [26, 27], this somatosensory damage could explain the headache and dizziness exhibited by 91% of the concussed hockey players an again provides some connection between the simulated impact and those experienced by the players.

5.5.3 Limitations of model and future improvement

This study provided a starting point for future research involving imaging modalities, concussion assessment testing such as that of $SCAT_3$ and axon embedded FEHM. While inherent limitations exist with diffusion MRI imaging modalities, mainly potential inaccuracies with crossing fibers [14, 152], the level of detail feasible with modern computing power, should render this limitation minute. One area which could be an

interesting future approach, would be to replace this studies group-based HCP model with a subject specific model, particularly that of a 13-year-old male, in order to better recreate the axonal tracts that would be anatomically connected to different brain regions. Another point to consider for future research is the variance in axonal diameter, in this study uniform axon thickness was used, however as Liewald et al. observed, different axon tracts have wildly varying axon diameters [156]. For example reported diameter of a cadaveric brains right SLF tract was 1.34 μm while the CC tract was 0.74 μm, so while their average diameter is close to the 1 μm used in this study, as reported in a the preceding chapter, axon diameter especially when its doubled could have a relatively large effect on brain anisotropy.

The goal of this research, particularly this study is to provide clinicians and other non-engineering researchers the tools to be able to better assess brain injuries in-order to take steps in mitigating the sports concussion.

Chapter 6

6 Conclusion and future work

The need to continue the exploration of the mild traumatic brain injury in a collaborative research environment is paramount to its decline as a societal catastrophe. This chapter looks to highlight the work that was completed over the two-year master's thesis research while examining what research is now possible with this work as a base.

A literature review to encapsulate the latest work in the field of concussion research and the methods of which state of the art FEHM are developed, tested and used to predict concussion probability was described in the first chapter. This literature review and background research provided a starting point to help develop the topics and research plan of this thesis, from understanding through experimentation the mechanisms that are most correlated to concussion to providing new tools to help predict and diagnose concussions through symptom-based approaches. Exploration of imaging techniques such as DTI, to provide a secondary level of detail, while understanding the limitations of these modalities and the benefits that their use could provide in bridging the gap between computational models and patient outcome post injury is an important part of the research process.

6.1 Summary

This thesis encapsulates my work over the past 2 years, it follows a chronological breakdown through the chapters to understand the mechanisms that effect the risk of concussion and how to potentially reduce those risks.

6.1.1 Understanding injury mechanism

Starting with the development of an automated injury prediction pipeline to prepare, simulate and post-process large amounts of data using a state of the art FEHM. This pipeline allowed for the confirmation of the role that rotational motion has in increasing concussion likelihood through brain responses such as engineering strain. The

utilization of this pipeline to explore how different impact directions and magnitudes cause differing brain responses through metrics such as CSDM and MPS is critical in providing a base of understanding what increases concussion likelihood. This chapter focused on the development of a physical experimentation procedure, testing 6 different helmet models, at 3 different impact energies at 4 different impact locations, following that described by STAR to provide an assessment of which kinematics affect output brain strain the most. The understanding that strain is a prominent indicator of concussion likelihood, with its connection to typical concussion pathologies such as DAI, provided a starting point for future chapters to explore this injury mechanism.

6.1.2 Deeper dive into brain injury, purpose of the helmet

Following up on the development of the initial strain-based injury prediction processing pipeline, the addition of several other important kinematic based metrics were added to provide a better understanding of the overall correlation that well used and accepted injury prediction criteria have with the strain-based brain response. Using the data collected from the 672 impacts simulated with the GHBMC head model, several key criteria including GSI, HIC, GAMBIT, BrIC, UBrIC and DAMAGE were assessed based on their statistical correlation to brain response metrics such as MPS and CSDM. Along with assessing the different kinematic measures a more detailed examination of the effect of varying levels of helmet technology was also assessed. The 6 different helmet models ranged both in terms of price and in terms of the technology and R&D that was put into their development. Different materials and different helmet geometries designed to mitigate concussive impacts by reducing linear and rotational accelerations were implemented into the newer and more expensive helmet models, with the perception that they were safer. This hypothesis was considered proven by the rating received by the STAR hockey helmet rating system, the leading consumer focused helmet ranking. The STAR rating gives a score of between 0 and 5 stars, where 5 stars is considered excellent in terms of concussion mitigation potential and 0 stars considered not recommended. This rating system is widely referenced in by media outlets and is the foremost source of consumer information when determining the safety of a helmet when making an informed purchasing decision. This chapter looked to test this rating system with the kinematics-

based criteria to determine if its rating is correlated to helmet effectiveness in reducing brain strains, a metrics associated with concussion prediction. This chapter was then concluded with the introduction of a new kinematics-input, strain-output artificial neural network algorithm to take the total information of the linear and rotational velocity and acceleration accelerometer outputs and the strain measures extracted from the GHBMC model to train a dataset of 672 impacts and produce the most encompassing concussion prediction measure. This chapter highlights the limitations that arise with the baseline GHBMC model and the limitations that arise from using strain as the only metrics to correlate computational injury severity with real world patient outcome.

6.1.3 Development of a new and improved model

Following the understanding of the inherent limitation of tissue based strain outputs and the advantages of anisotropic brain material representation, along with the need to explore the connection of injury patterns exhibited in computational models to real world injury scenario and concussion symptoms, the need for a new, more detailed FEHM was proposed. This model looks to connect tissue based injury associated with the strain response in computational models with the axon based injury metrics that would provide directional effect insights as well as provide insights to correlate FEHM to imaging modalities that look at structural and functional changes, such as DTI or RS-FMRI. This chapter highlights the process of developing and validating two novel axon fiber tractography explicitly embedded into a validated FEHM. These two models, one being population based and a second being a subject specific model extracted from DWI in 7T MRI scans, both included a novel feature, individually parcellated axon fiber tracts that provide a new approach of analyzing FEHM injury response. The process for model generation and an exploratory experiment on directional effects of impact on differently directed axon fibers was completed, leading the way for more detailed work on the effects of real world traumatic head impact on the tractography clusters and how the damage presented in these axons relates to the real world post-concussion symptoms experienced by mTBI victims.

6.1.4 Exploring models functionality, the future of brain research

Taking the work completed in each of the previous chapters and combining their outcomes leads to this final content chapter. Using the axon embedded GHBMC model in combination with 12 impact representative curves based on 672 impact scenarios recreating a typical hockey level impact provides a prescribed motion that represents different impact energies and different impact locations to the head. These 12 curves were treated as inputs for the GHBMC group-based axon embedded head model to create an encompassing study that provides details into the brain's microscopic anatomy post injury. These results were then compared as a preliminary measure to injury patterns exhibited by a concussed hockey player, with the effect of each impact scenario both in terms of direction and magnitude compared to determine which tractography cluster was most damaged and relate it to what typical symptoms could be exhibited by the simulated injured player. This exploratory study exhibited a combination of the different preceding chapters of this thesis and exhibits the potential use of the automated pipeline, injury criteria calculation, axon model development and parcellated human brain atlas to develop a useful tool for future researchers in concussion injury analysis.

6.2 Conclusions

6.2.1 Best metrics for injury prediction

Several outcomes that were in line with some of our original hypothesis were exhibited by the results analyzed in this thesis. The first prevalent outcome which pertained to determining the best metrics for injury prediction was the significant advantage of using rotational velocity as a predictive kinematic than both linear and rotational acceleration when it comes to strain prediction. As stated, resultant peak rotational velocity was the most correlated with the different tissue-based strain predictors, more so than linear or rotational acceleration. *Our hypothesis, that peak linear velocity predicts more accurately due to its inclusion of impact duration, proves to be true based on our FEHM, which leads us to concluding that future predictive criteria, such as that of STAR, should be updated to include rotational velocity as a kinematic input for predicting probability of a concussive scenario.*

Even when combining linear and rotational acceleration into an ANN training algorithm RPLV outperformed in its linear relationship to CSDM and MPS measures. When comparing past injury criteria, even some recently developed ones, those that contained velocity in the equation outperformed those that contained linear and rotational acceleration. The increased adoption of machine learning and deep learning methods for the analysis of big data and use as a forecasting/predictive tool is another method that we believe concussion prediction could be improved. Combining some of the most state of the art computational simulation practices that provide a large amount of data with a large amount of inputs, such as which direction an impact occurs from, what the magnitude of the impact was and what are its peak kinematics allows for improved predictive capabilities that greatly outperform current injury prediction criteria. *An outcome of this study that was not originally hypothesized but proved to be valuable in future research was the importance of ANN and other machine learning methodologies as an efficient predictive tool to help in impact reconstruction and big data summarization.*

6.3 Future studies

6.3.1 Future research

The methods and models developed over this research project prove to have the capabilities to provide a basis for future innovative research in the field of computational biomechanics and impact biomechanics. These models, particularly the explicit parcellated tractography models, that combine engineering principals with imaging and neuroscience for segmentation and atlas registration, are widely accepted as the proper method going forward in the field of injury prediction [105]. This project encompassed multiple engineering principals from background research to design of experiment to model development, iteration and testing to provide an answer for the original hypothesis and prove the novelty and impact of this research. Future group members now have new tools such as the automated injury prediction pipeline which allows for the automatic pre-processing and post-processing of large quantities of data to allow for more industry partnerships. Encapsulating the different injury prediction metrics of the field into this pipeline allows for the simple comparison of accepted metrics and the combination or exploration of new metrics.

The development of new parcellated tractography embedded FEHM's is another step towards the future as it provides the first atlas based segmented FE DTI derived axon model to this authors knowledge. The development of model's framework and generation pipeline also allows for future studies exploring the effects of impacts to different tractography clusters to improve the predictive capabilities of computational models through the improvement in biofidelity and microscopic detail. Potential future research involving rodent DTI could also allow for a more cohesive connection from injury to simulation to animal cognitive impairment which could result in more groundbreaking research.

This research looks to provide new evidence of helmet effect on mitigating brain strain and the effects post-concussion symptoms. With 6 different helmet models and over 670 individual impact cases analyzed using a multitude of different injury prediction criteria as well as some of the most highly detailed FEHMs understanding the role of the helmet and how different geometries and materials provide concussion mitigating effects has been given a preliminary examination. Understanding if specific helmets reduce localized strain better than others and how that could relate to common symptoms post-concussion, could help drive the answer to questions such as what concussion thresholds are and what quantifiable differences exist between similar concussive and non-concussive impacts.

Future incorporation of more machine learning techniques such as ANN and deep learning to assist in large data analysis and visualization along with neuroscience tools such as The Virtual Brain (TVB), where there are possibilities to construct personalized virtual brains to recreate tract lesions extracted from the axon embedded FEHM [169]. This future work would improve patient diagnosis for physicians or allow for app-based concussion prediction tools based on helmet or mouthguard embedded accelerometers. While we understand that these models have their limitations and do not represent the human head 100%, the ability to recreate some of these impact scenarios, with FEM and highly detailed and validated models provides new insights into the human condition. While this model was based on that of an adult 50^{th} male, future models encompassing a wider range of subjects including older adult, adult female, and child human models as well as primate and rodent models could provide new insights and outcomes that could

drive innovation in the field of concussive injury rehabilitation, diagnosis and ultimately prevention.

6.3.2 Novelty, significance, and impact of work

1) Development of a fully automated start to finish injury prediction and analysis pipeline that calculates important injury risk criteria, pre-processes a FEHM, and post-processes said FEHM to extract important engineering metrics that are considered essential in TBI assessment.

2) Developed a pipeline for the generation of the first explicitly embedded parcellated axon fiber FEHM, this pipeline and model was proven to be an effective predictor of injury location and looks to be a better tool for comparison to imaging modalities for accident reconstruction.

3) Analyzed injury metrics suitable for predicting concussion in Ice Hockey, using literature data and our own experimental procedure which included 672 individual impacts, recreated with validated processes.

4) Combined engineering, imaging and neuroscience principals to create a full start to finish process for the assessment of future protective equipment and technologies through looking at axonal-fiber related loading. Future collaborations within Western University and industry partners could benefit from this computational suite, what we believe could benefit concussion research for years to come.

References

1. Dewan, M.C., et al., *Estimating the global incidence of traumatic brain injury.* Journal of Neurosurgery, 2019. **130**(4): p. 1080-1097.

2. Taylor, C.A., et al., *Traumatic Brain Injury–Related Emergency Department Visits, Hospitalizations, and Deaths — United States, 2007 and 2013.* MMWR. Surveillance Summaries, 2017. **66**(9): p. 1-16.

3. Baugh, C.M., et al., *Chronic traumatic encephalopathy: neurodegeneration following repetitive concussive and subconcussive brain trauma.* Brain Imaging and Behavior, 2012. **6**(2): p. 244-254.

4. Kolb, B. and I.Q. Whishaw, *Fundamentals of human neuropsychology*. 2009: Macmillan.

5. Mao, H., *Modeling the head for impact scenarios*, in *Basic Finite Element Method as Applied to Injury Biomechanics*. 2018, Elsevier. p. 469-502.

6. Fonseca-Azevedo, K. and S. Herculano-Houzel, *Metabolic constraint imposes tradeoff between body size and number of brain neurons in human evolution.* Proceedings of the National Academy of Sciences, 2012. **109**(45): p. 18571-18576.

7. Herrick, C.J., *The Anatomy of the Nervous System from the Standpoint of Development and Function.* Science, 1921. **54**(1400): p. 409-411.

8. Manning, K.Y., et al., *Multiparametric MRI changes persist beyond recovery in concussed adolescent hockey players.* Neurology, 2017. **89**(21): p. 2157-2166.

9. Irimia, A., et al., *Circular representation of human cortical networks for subject and population-level connectomic visualization.* NeuroImage, 2012. **60**(2): p. 1340-1351.

10. Van Horn, J.D., et al., *Mapping Connectivity Damage in the Case of Phineas Gage.* PLOS ONE, 2012. **7**(5): p. e37454.

11. Huisman, T.A., et al., *Diffusion tensor imaging as potential biomarker of white matter injury in diffuse axonal injury.* American Journal of Neuroradiology, 2004. **25**(3): p. 370-376.

12. Niogi, S.N. and P. Mukherjee, *Diffusion tensor imaging of mild traumatic brain injury.* The Journal of head trauma rehabilitation, 2010. **25**(4): p. 241-255.

13. Arfanakis, K., et al., *Diffusion Tensor MR Imaging in Diffuse Axonal Injury.* American Journal of Neuroradiology, 2002. **23**(5): p. 794-802.

14. Wilde, E.A., et al., *Diffusion tensor imaging of acute mild traumatic brain injury in adolescents.* Neurology, 2008. **70**(12): p. 948-955.

15. Colgan, N.C., M.D. Gilchrist, and K.M. Curran, *Applying DTI white matter orientations to finite element head models to examine diffuse TBI under high rotational accelerations.* Progress in biophysics and molecular biology, 2010. **103**(2-3): p. 304-309.

16. Ji, S., et al., *Group-Wise Evaluation and Comparison of White Matter Fiber Strain and Maximum Principal Strain in Sports-Related Concussion.* Journal of Neurotrauma, 2014. **32**(7): p. 441-454.

17. Ji, S., et al., *Group-wise evaluation and comparison of white matter fiber strain and maximum principal strain in sports-related concussion.* Journal of neurotrauma, 2015. **32**(7): p. 441-454.

18. Kraus, M.F., et al., *White matter integrity and cognition in chronic traumatic brain injury: a diffusion tensor imaging study.* Brain, 2007. **130**(10): p. 2508-2519.

19. Margulies, S.S. and L.E. Thibault, *A proposed tolerance criterion for diffuse axonal injury in man.* Journal of biomechanics, 1992. **25**(8): p. 917-923.

20. Basser, P.J., J. Mattiello, and D. LeBihan, *MR diffusion tensor spectroscopy and imaging.* Biophysical journal, 1994. **66**(1): p. 259-267.

21. Manning, K.Y., et al., *Longitudinal changes of brain microstructure and function in nonconcussed female rugby players.* Neurology, 2020: p. 10.1212/WNL.0000000000009821.

22. Bernal, B. and A. Ardila, *The role of the arcuate fasciculus in conduction aphasia.* Brain, 2009. **132**(9): p. 2309-2316.

23. Catani, M. and M. Mesulam, *The arcuate fasciculus and the disconnection theme in language and aphasia: history and current state.* cortex, 2008. **44**(8): p. 953-961.

24. Bubb, E.J., C. Metzler-Baddeley, and J.P. Aggleton, *The cingulum bundle: Anatomy, function, and dysfunction.* Neuroscience & Biobehavioral Reviews, 2018. **92**: p. 104-127.

25. Wu, Y., et al., *Segmentation of the cingulum bundle in the human brain: a new perspective based on DSI tractography and fiber dissection study.* Frontiers in neuroanatomy, 2016. **10**: p. 84.

26. Hinkley, L.B., et al., *The role of corpus callosum development in functional connectivity and cognitive processing.* PLoS One, 2012. **7**(8): p. e39804.

27. van der Knaap, L.J. and I.J. van der Ham, *How does the corpus callosum mediate interhemispheric transfer? A review.* Behavioural brain research, 2011. **223**(1): p. 211-221.

28. Kamali, A., et al., *Diffusion tensor tractography of the human brain cortico‐ponto‐cerebellar pathways: a quantitative preliminary study.* Journal of Magnetic Resonance Imaging, 2010. **32**(4): p. 809-817.

29. Kumral, E. and G. Bayülkem, *Spectrum of single and multiple corona radiata infarcts: Clinical/MRI correlations.* Journal of Stroke and Cerebrovascular Diseases, 2003. **12**(2): p. 66-73.

30. Sterr, A., et al., *The role of corticospinal tract damage in chronic motor recovery and neurorehabilitation: a pilot study.* Neurorehabilitation and neural repair, 2010. **24**(5): p. 413-419.

31. Lang, C.E. and M.H. Schieber, *Reduced muscle selectivity during individuated finger movements in humans after damage to the motor cortex or corticospinal tract.* Journal of neurophysiology, 2004. **91**(4): p. 1722-1733.

32. Wakana, S., et al., *Fiber tract–based atlas of human white matter anatomy.* Radiology, 2004. **230**(1): p. 77-87.

33. Agarwal, N., *Functional Anatomy of the Major Tracts*, in *Neuroimaging: Anatomy Meets Function*. 2018, Springer. p. 101-110.

34. Kanamaru, Y., et al., *Cerebellar pathways in mouse model of Purkinje cell degeneration detected by high-angular resolution diffusion imaging tractography.* The Cerebellum, 2017. **16**(3): p. 648-655.

35. Zhang, F., et al., *An anatomically curated fiber clustering white matter atlas for consistent white matter tract parcellation across the lifespan.* NeuroImage, 2018. **179**: p. 429-447.

36. Morales, H. and T. Tomsick, *Middle cerebellar peduncles: Magnetic resonance imaging and pathophysiologic correlate.* World journal of radiology, 2015. **7**(12): p. 438.

37. Seo, M., E. Lee, and B.B. Averbeck, *Action selection and action value in frontal-striatal circuits.* Neuron, 2012. **74**(5): p. 947-960.

38. Pulsipher, D.T., et al., *Thalamofrontal circuitry and executive dysfunction in recent‐onset juvenile myoclonic epilepsy.* Epilepsia, 2009. **50**(5): p. 1210-1219.

39. González, H.F., et al., *Thalamic arousal network disturbances in temporal lobe epilepsy and improvement after surgery.* Journal of Neurology, Neurosurgery & Psychiatry, 2019. **90**(10): p. 1109-1116.

40. Qin, W. and C. Yu, *Neural pathways conveying novisual information to the visual cortex.* Neural plasticity, 2013. **2013**.

41. Cho, D., et al., *Differential modulation of thalamo-parietal interactions by varying depths of isoflurane anesthesia.* PloS one, 2017. **12**(4).

42. Helmchen, C., et al., *Disappearance of central thalamic pain syndrome after contralateral parietal lobe lesion: implications for therapeutic brain stimulation.* Pain, 2002. **98**(3): p. 325-330.

43. Bain, A.C. and D.F. Meaney, *Tissue-Level Thresholds for Axonal Damage in an Experimental Model of Central Nervous System White Matter Injury.* 2000. **122**(6): p. 615.

44. Kleiven, S., *Predictors for traumatic brain injuries evaluated through accident reconstructions*. 2007, SAE Technical Paper.

45. Zhang, L., K.H. Yang, and A.I. King, *A proposed injury threshold for mild traumatic brain injury.* J. Biomech. Eng., 2004. **126**(2): p. 226-236.

46. Patton, D.A., A.S. McIntosh, and S. Kleiven, *The biomechanical determinants of concussion: finite element simulations to investigate tissue-level predictors of injury during sporting impacts to the unprotected head.* Journal of applied biomechanics, 2015. **31**(4): p. 264-268.

47. McAllister, T.W., et al., *Maximum principal strain and strain rate associated with concussion diagnosis correlates with changes in corpus callosum white matter indices.* Annals of biomedical engineering, 2012. **40**(1): p. 127-140.

48. Viano, D.C., et al., *Concussion in professional football: brain responses by finite element analysis: part 9.* Neurosurgery, 2005. **57**(5): p. 891-916.

49. Yoganandan, N., et al., *Influence of angular acceleration–deceleration pulse shapes on regional brain strains.* Journal of biomechanics, 2008. **41**(10): p. 2253-2262.

50. Zhao, W. and S. Ji, *Brain strain uncertainty due to shape variation in and simplification of head angular velocity profiles.* Biomechanics and modeling in mechanobiology, 2017. **16**(2): p. 449-461.

51. Post, A., et al., *Peak linear and rotational acceleration magnitude and duration effects on maximum principal strain in the corpus callosum for sport impacts.* Journal of biomechanics, 2017. **61**: p. 183-192.

52. Bian, K. and H. Mao, *Mechanisms and variances of rotation-induced brain injury: a parametric investigation between head kinematics and brain strain.* Biomechanics and modeling in mechanobiology, 2020: p. 1-19.

53. Elkin, B.S., et al., *Brain tissue strains vary with head impact location: A possible explanation for increased concussion risk in struck versus striking football players.* Clinical biomechanics, 2019. **64**: p. 49-57.

54. Zhang, L., K.H. Yang, and A.I. King, *Comparison of brain responses between frontal and lateral impacts by finite element modeling.* Journal of neurotrauma, 2001. **18**(1): p. 21-30.

55. Wright, R.M. and K. Ramesh, *An axonal strain injury criterion for traumatic brain injury.* Biomechanics and modeling in mechanobiology, 2012. **11**(1-2): p. 245-260.

56. Wright, R.M., et al., *A Multiscale Computational Approach to Estimating Axonal Damage under Inertial Loading of the Head.* 2013. **30**(2): p. 102-118.

57. Cloots, R.J., et al., *Multi-scale mechanics of traumatic brain injury: predicting axonal strains from head loads.* Biomechanics and modeling in mechanobiology, 2013. **12**(1): p. 137-150.

58. Sahoo, D., C. Deck, and R. Willinger, *Development and validation of an advanced anisotropic visco-hyperelastic human brain FE model.* journal of the mechanical behavior of biomedical materials, 2014. **33**: p. 24-42.

59. Mao, H., et al., *Development of a finite element human head model partially validated with thirty five experimental cases.* Journal of biomechanical engineering, 2013. **135**(11).

60. Giordano, C. and S. Kleiven, *Evaluation of axonal strain as a predictor for mild traumatic brain injuries using finite element modeling*. 2014, SAE Technical Paper.

61. Fagerholm, E.D., et al., *Disconnection of network hubs and cognitive impairment after traumatic brain injury.* Brain, 2015. **138**(6): p. 1696-1709.

62. Pellman, E.J., et al., *Concussion in professional football: helmet testing to assess impact performance--part 11.* Neurosurgery, 2006. **58**(1): p. 78-96; discussion 78-96.

63. Guskiewicz, K.M. and J.P. Mihalik, *Biomechanics of Sport Concussion: Quest for the Elusive Injury Threshold.* Exercise and Sport Sciences Reviews, 2011. **39**(1).

64. Rowson, S. and S.M. Duma, *Development of the STAR evaluation system for football helmets: integrating player head impact exposure and risk of concussion.* Ann Biomed Eng, 2011. **39**(8): p. 2130-40.

65. Rowson, S., et al., *Rotational Head Kinematics in Football Impacts: An Injury Risk Function for Concussion.* Annals of Biomedical Engineering, 2012. **40**(1): p. 1-13.

66. Rowson, B., S. Rowson, and S.M. Duma, *Hockey STAR: A Methodology for Assessing the Biomechanical Performance of Hockey Helmets.* Ann Biomed Eng, 2015. **43**(10): p. 2429-43.

67. Kraus, J.F., B.D. Anderson, and C.E. Mueller, *The effectiveness of a special ice hockey helmet to reduce head injuries in college intramural hockey.* Medicine and science in sports, 1970. **2**(3): p. 162-164.

68. Robertson, L.S., *Estimates of motor vehicle seat belt effectiveness and use: implications for occupant crash protection.* American Journal of Public Health, 1976. **66**(9): p. 859-864.

69. Lissner, H.R., M. Lebow, and F.G. Evans, *Experimental studies on the relation between acceleration and intracranial pressure changes in man.* Surgery, gynecology & obstetrics, 1960. **111**: p. 329-338.

70. Gurdjian, E.S., et al., *Results of operative treatment of protruded and ruptured lumbar discs based on 1176 operative cases with 82 per cent follow-up of 3 to 13 years.* Journal of neurosurgery, 1961. **18**: p. 783-791.

71. Gurdjian, E., et al., *Mechanisms of head injury.* Clin. Neurosurg., 1966. **12**: p. 112-128.

72. Gadd, C.W., *Use of a Weighted-Impulse Criterion for Estimating Injury Hazard*. 1966, SAE International.

73. Lewis, E., *Head injury and protection.* Ernsting's aviation medicine. Boca Ratoa, FL: CRC Press, Taylor & Francis Groupo, 2006: p. 179-88.

74. Bartsch, A., et al., *Impact test comparisons of 20th and 21st century American football helmets.* Journal of neurosurgery, 2012. **116**(1): p. 222-233.

75. McLean, A. and R.W. Anderson, *Biomechanics of closed head injury.* Head Injury. London: Chapman & Hall, 1997: p. 25-37.

76. Versace, J., *A Review of the Severity Index*. 1971, SAE International.

77. Kleinberger, M., et al., *Development of improved injury criteria for the assessment of advanced automotive restraint systems.* NHTSA Docket, 1998. **4405**(9).

78. Newman, J.A. *A generalized acceleration model for brain injury threshold (GAMBIT)*. in *Proceedings of International IRCOBI Conference, 1986*. 1986.

79. Takhounts, E.G., et al., *Development of brain injury criteria (BrIC)*. 2013, SAE Technical Paper.

80. Lee, E., A. Shrivatri, and S. Ohara, *NHTSA Oblique Test Data Analysis Method by LS-DYNA Modeling.* 2020.

81. Yang, B., et al., *Development of a finite element head model for the study of impact head injury.* BioMed research international, 2014. **2014**.

82. Kleiven, S. and H. von Holst, *Consequences of head size following trauma to the human head.* Journal of biomechanics, 2002. **35**(2): p. 153-160.

83. Takhounts, E.G., et al., *On the development of the SIMon finite element head model*. 2003, SAE Technical Paper.

84. Sanchez, E.J., et al., *Evaluation of head and brain injury risk functions using sub-injurious human volunteer data.* Journal of neurotrauma, 2017. **34**(16): p. 2410-2424.

85. Takhounts, E.G., et al., *Investigation of traumatic brain injuries using the next generation of simulated injury monitor (SIMon) finite element head model.* Stapp car crash journal, 2008. **52**: p. 1-31.

86. Gabler, L.F., J.R. Crandall, and M.B. Panzer, *Development of a metric for predicting brain strain responses using head kinematics.* Annals of biomedical engineering, 2018. **46**(7): p. 972-985.

87. Gabler, L.F., J.R. Crandall, and M.B. Panzer, *Development of a Second-Order System for Rapid Estimation of Maximum Brain Strain.* Annals of biomedical engineering, 2019. **47**(9): p. 1971-1981.

88. Yang, J., *Review of injury biomechanics in car-pedestrian collisions.* International journal of vehicle safety, 2005. **1**(1-3): p. 100-117.

89. Yao, J., J. Yang, and D. Otte, *Investigation of head injuries by reconstructions of real-world vehicle-versus-adult-pedestrian accidents.* Safety science, 2008. **46**(7): p. 1103-1114.

90. John, D. *States: The Abbreviated and the Comprehensive Research Injury Scales*. in *Proceedings of the Thirteenth Stapp Car Crash Conference, New York, SAE Inc*. 1969.

91. Medicine, A.f.t.A.o.A. *The Abbreviated Injury Scale 2005–Update 2008*. 2008. Association for the Advancement of Automotive Medicine Barrington, IL.

92. Loftis, K.L., J. Price, and P.J. Gillich, *Evolution of the Abbreviated Injury Scale: 1990–2015.* Traffic injury prevention, 2018. **19**(sup2): p. S109-S113.

93. Gennarelli, T.A. and E. Wodzin, *Abbreviated injury scale 2005: update 2008*. 2008: Russ Reeder.

94. Zhang, L., et al., *Recent advances in brain injury research: a new human head model development and validation*. 2001, SAE Technical Paper.

95. Kang, H.-S., et al., *Validation of a 3D anatomic human head model and replication of head impact in motorcycle accident by finite element modeling.* SAE transactions, 1997: p. 3849-3858.

96. Raul, J.-S., et al., *Finite-element models of the human head and their applications in forensic practice.* International journal of legal medicine, 2008. **122**(5): p. 359-366.

97. Miller, L.E., J.E. Urban, and J.D. Stitzel, *Validation performance comparison for finite element models of the human brain.* Computer Methods in Biomechanics and Biomedical Engineering, 2017. **20**(12): p. 1273-1288.

98. Kleiven, S., *Evaluation of head injury criteria using a finite element model validated against experiments on localized brain motion, intracerebral acceleration, and intracranial pressure.* International Journal of Crashworthiness, 2006. **11**(1): p. 65-79.

99. Miller, L.E., J.E. Urban, and J.D. Stitzel, *Development and validation of an atlas-based finite element brain model.* Biomechanics and modeling in mechanobiology, 2016. **15**(5): p. 1201-1214.

100. Kimpara, H., et al., *Investigation of anteroposterior head-neck responses during severe frontal impacts using a brain-spinal cord complex FE model*. 2006, SAE Technical Paper.

101. Horgan, T.J. and M.D. Gilchrist, *The creation of three-dimensional finite element models for simulating head impact biomechanics.* International Journal of Crashworthiness, 2003. **8**(4): p. 353-366.

102. Deck, C. and R. Willinger. *Head injury prediction tool for predictive systems optimization*. in *Proceedings of the 7th European LS-DYNA Conference*. 2008.

103. Garimella, H.T. and R.H. Kraft, *Modeling the mechanics of axonal fiber tracts using the embedded finite element method.* International journal for numerical methods in biomedical engineering, 2017. **33**(5): p. e2823.

104. Chatelin, S., et al., *Computation of axonal elongation in head trauma finite element simulation.* Journal of the mechanical behavior of biomedical materials, 2011. **4**(8): p. 1905-1919.

105. Zhao, W. and S. Ji, *White Matter Anisotropy for Impact Simulation and Response Sampling in Traumatic Brain Injury*. Journal of Neurotrauma, 2018. **36**(2): p. 250-263.

106. Goriely, A., et al., *Mechanics of the brain: perspectives, challenges, and opportunities.* Biomechanics and modeling in mechanobiology, 2015. **14**(5): p. 931-965.

107. Bayly, P.V., E.H. Clayton, and G.M. Genin, *Quantitative imaging methods for the development and validation of brain biomechanics models.* Annual review of biomedical engineering, 2012. **14**: p. 369-396.

108. Catani, M. and M.T. de Schotten, *Atlas of human brain connections*. 2012: Oxford University Press.

109. Clay, M.B., K.L. Glover, and D.T. Lowe, *Epidemiology of concussion in sport: a literature review.* Journal of Chiropractic Medicine, 2013. **12**(4): p. 230-251.

110. McKee, A.C., et al., *The spectrum of disease in chronic traumatic encephalopathy.* Brain, 2013. **136**(1): p. 43-64.

111. Gavett, B.E., R.A. Stern, and A.C. McKee, *Chronic Traumatic Encephalopathy: A Potential Late Effect of Sport-Related Concussive and Subconcussive Head Trauma.* Clinics in Sports Medicine, 2011. **30**(1): p. 179-188.

112. Smith, D.H. and D.F. Meaney, *Axonal Damage in Traumatic Brain Injury.* 2000. **6**(6): p. 483-495.

113. Madhukar, A. and M. Ostoja-Starzewski, *Finite Element Methods in Human Head Impact Simulations: A Review.* Annals of Biomedical Engineering, 2019.

114. Takhounts, E.G., et al. *On the Development of the SIMon Finite Element Head Model*. SAE International.

115. Zhao, W., S. Ruan, and S. Ji, *Brain pressure responses in translational head impact: a dimensional analysis and a further computational study.* Biomechanics and Modeling in Mechanobiology, 2015. **14**(4): p. 753-766.

116. Kleiven, S., *Finite element modeling of the human head*. 2002, KTH.

117. Horgan, T.J. and M.D. Gilchrist, *The creation of three-dimensional finite element models for simulating head impact biomechanics.* 2003. **8**(4): p. 353-366.

118. Hardy, W.N., et al., *Investigation of head injury mechanisms using neutral density technology and high-speed biplanar X-ray.* 2001, SAE Technical Paper.

119. Hardy, W.N., et al., *A study of the response of the human cadaver head to impact.* Stapp car crash journal, 2007. **51**: p. 17.

120. Mao, H., et al., *Computational neurotrauma—design, simulation, and analysis of controlled cortical impact model.* 2010. **9**(6): p. 763-772.

121. Cobb, B.R., et al., *Head Impact Exposure in Youth Football: Elementary School Ages 9–12 Years and the Effect of Practice Structure.* Annals of Biomedical Engineering, 2013. **41**(12): p. 2463-2473.

122. Camarillo, D.B., et al., *An Instrumented Mouthguard for Measuring Linear and Angular Head Impact Kinematics in American Football.* 2013. **41**(9): p. 1939-1949.

123. Miller, L.E., et al., *Characterizing head impact exposure in youth female soccer with a custom-instrumented mouthpiece.* Research in Sports Medicine, 2020. **28**(1): p. 55-71.

124. Knowles, B.M. and C.R. Dennison, *Predicting cumulative and maximum brain strain measures from HybridIII head kinematics: A combined laboratory study and post-hoc regression analysis.* Annals of biomedical engineering, 2017. **45**(9): p. 2146-2158.

125. Kleiven, S. *Influence of direction and duration of impacts to the human head evaluated using the finite element method*. in *International IRCOBI Conference*. 2005.

126. Zhou, Z., et al. *A reanalysis of experimental brain strain data: implication for finite element head model validation*. in *SAE 62nd Stapp Car Crash Conference, STAPP 2018; Catamaran Resort Hotel San Diego; United States; 12 November 2018 through 14 November 2018*. 2019. SAE International.

127. Giordano, C. and S. Kleiven, *Development of an unbiased validation protocol to assess the biofidelity of finite element head models used in prediction of traumatic brain injury*. 2016, SAE Technical Paper.

128. Morehouse, C.A., *The Certification of Protective Equipment for Ice Hockey in the United States*, A.B. Ashare, Editor. 2000, ASTM International: West Conshohocken, PA. p. 72-77.

129. Rousseau, P., A. Post, and T. Hoshizaki, *A comparison of peak linear and angular headform accelerations using ice hockey helmets.* Journal of ASTM International, 2008. **6**(1): p. 1-11.

130. Dixon, J.L. and I.K. Brodie, *The New ISO Standards for Ice Hockey Helmets and Face Protectors: Moving Toward International Standards Harmonization and Conformity Assessment*, in *Safety in Ice Hockey: Second Volume*. 1993, ASTM International.

131. Lissner, H., M. Lebow, and F. Evans, *Experimental studies on the relation between acceleration and intracranial pressure changes in man.* Surgery, gynecology & obstetrics, 1960. **111**: p. 329.

132. Gurdjian, E.S., H. Lissner, and L. Patrick. *Concussion: mechanism and pathology*. in *Proceedings: American Association for Automotive Medicine Annual Conference*. 1963. Association for the Advancement of Automotive Medicine.

133. Chou, C.C. and G.W. Nyquist, *Analytical studies of the head injury criterion (HIC).* SAE Transactions, 1974: p. 398-410.

134. Greenwald, R.M., et al., *Head impact severity measures for evaluating mild traumatic brain injury risk exposure.* Neurosurgery, 2008. **62**(4): p. 789-798.

135. Taylor, C.A., et al., *Traumatic brain injury–related emergency department visits, hospitalizations, and deaths—United States, 2007 and 2013.* MMWR Surveillance Summaries, 2017. **66**(9): p. 1.

136. Ryan, L.M. and D.L. Warden, *Post concussion syndrome.* International review of psychiatry, 2003. **15**(4): p. 310-316.

137. Barlow, K.M., *Postconcussion syndrome: a review.* Journal of child neurology, 2016. **31**(1): p. 57-67.

138. Zhang, J., et al. *Brain strains in vehicle impact tests*. in *Annual Proceedings/Association for the Advancement of Automotive Medicine*. 2006. Association for the Advancement of Automotive Medicine.

139. Sahoo, D., C. Deck, and R. Willinger, *Brain injury tolerance limit based on computation of axonal strain.* Accident Analysis & Prevention, 2016. **92**: p. 53-70.

140. Chatelin, S., C. Deck, and R. Willinger, *An anisotropic viscous hyperelastic constitutive law for brain material finite-element modeling.* Journal of Biorheology, 2013. **27**(1): p. 26-37.

141. Wu, T., et al., *Explicit Modeling of White Matter Axonal Fiber Tracts in a Finite Element Brain Model.* Annals of Biomedical Engineering, 2019. **47**(9): p. 1908-1922.

142. Gerber, J.I., H.T. Garimella, and R.H. Kraft, *Computation of history-dependent mechanical damage of axonal fiber tracts in the brain: towards tracking sub-concussive and occupational damage to the brain*. 2018, Cold Spring Harbor Laboratory.

143. Carlsen, R.W. and N.P. Daphalapurkar, *The importance of structural anisotropy in computational models of traumatic brain injury.* Frontiers in neurology, 2015. **6**: p. 28.

144. Li, X., Z. Zhou, and S. Kleiven, *A detailed and personalizable head model with axons for brain injury prediction: Sensitivity of brain strain to inter-subject variability of the brain and white matter tract morphology*. 2020, Cold Spring Harbor Laboratory.

145. Guy, J., et al., *Spectra of G ratio, myelin sheath thickness, and axon and fiber diameter in the guinea pig optic nerve.* Journal of comparative neurology, 1989. **287**(4): p. 446-454.

146. Yeh, F.-C., et al., *Population-averaged atlas of the macroscale human structural connectome and its network topology.* NeuroImage, 2018. **178**: p. 57-68.

147. Arbogast, K.B. and S.S. Margulies, *A fiber-reinforced composite model of the viscoelastic behavior of the brainstem in shear.* Journal of biomechanics, 1999. **32**(8): p. 865-870.

148. Gasser, T.C., R.W. Ogden, and G.A. Holzapfel, *Hyperelastic modelling of arterial layers with distributed collagen fibre orientations.* Journal of the royal society interface, 2006. **3**(6): p. 15-35.

149. Zhang, F., et al. *Deep white matter analysis: Fast, consistent tractography segmentation across populations and dMRI acquisitions*. in *International Conference on Medical Image Computing and Computer-Assisted Intervention*. 2019. Springer.

150. O'Donnell, L.J., et al. *Unbiased groupwise registration of white matter tractography*. in *International Conference on Medical Image Computing and Computer-Assisted Intervention*. 2012. Springer.

151. O'Donnell, L.J. and C.-F. Westin, *Automatic tractography segmentation using a high-dimensional white matter atlas.* IEEE transactions on medical imaging, 2007. **26**(11): p. 1562-1575.

152. Maier-Hein, K.H., et al., *The challenge of mapping the human connectome based on diffusion tractography.* Nature communications, 2017. **8**(1): p. 1-13.

153. Schilling, K.G., et al., *Challenges in diffusion MRI tractography–Lessons learned from international benchmark competitions.* Magnetic resonance imaging, 2019. **57**: p. 194-209.

154. Yeh, F.-C., et al., *Deterministic diffusion fiber tracking improved by quantitative anisotropy.* PloS one, 2013. **8**(11): p. e80713.

155. Jiang, S., et al., *Tri-linear interpolation-based cerebral white matter fiber imaging.* Neural regeneration research, 2013. **8**(23): p. 2155-2164.

156. Liewald, D., et al., *Distribution of axon diameters in cortical white matter: an electron-microscopic study on three human brains and a macaque.* Biological Cybernetics, 2014. **108**(5): p. 541-557.

157. Hajiaghamemar, M., et al., *Embedded axonal fiber tracts improve finite element model predictions of traumatic brain injury.* Biomechanics and Modeling in Mechanobiology, 2020. **19**(3): p. 1109-1130.

158. *White Matter Injury Susceptibility via Fiber Strain Evaluation Using Whole-Brain Tractography*. Journal of Neurotrauma, 2016. **33**(20): p. 1834-1847.

159. Daley, M., et al., *Metabolomics profiling of concussion in adolescent male hockey players: a novel diagnostic method.* Metabolomics, 2016. **12**(12): p. 185.

160. Brazinova, A., et al., *Epidemiology of Traumatic Brain Injury in Europe: A Living Systematic Review.* Journal of Neurotrauma, 2018.

161. Teasdale, G. and B. Jennett, *Assessment and prognosis of coma after head injury.* Acta Neurochirurgica, 1976. **34**(1): p. 45-55.

162. Polinder, S., et al., *A Multidimensional Approach to Post-concussion Symptoms in Mild Traumatic Brain Injury.* Frontiers in neurology, 2018. **9**: p. 1113-1113.

163. Association, A.P., *Diagnostic and statistical manual of mental disorders (DSM-5®)*. 2013: American Psychiatric Pub.

164. Babcock, L., et al., *Predicting Postconcussion Syndrome After Mild Traumatic Brain Injury in Children and Adolescents Who Present to the Emergency Department.* JAMA Pediatrics, 2013. **167**(2): p. 156-161.

165. Wilcox, B.J., et al., *Head impact exposure in male and female collegiate ice hockey players.* Journal of biomechanics, 2014. **47**(1): p. 109-114.

166. Guskiewicz, K.M., et al., *Evidence-based approach to revising the SCAT2: introducing the SCAT3.* British Journal of Sports Medicine, 2013. **47**(5): p. 289.

167. DiFabio, M., K. Breedlove, and T. Buckley, *Head Impact Kinematics do not Predict In-Season Concussion or Lower Extremity Injury in Ice Hockey.* Neurology, 2019. **93**(14 Supplement 1): p. S30-S31.

168. Mihalik, J.P., et al., *Head Impact Biomechanics in Youth Hockey: Comparisons Across Playing Position, Event Types, and Impact Locations.* Annals of Biomedical Engineering, 2012. **40**(1): p. 141-149.

169. Schirner, M., et al., *An automated pipeline for constructing personalized virtual brains from multimodal neuroimaging data.* NeuroImage, 2015. **117**: p. 343-357.

Curriculum Vitae

Name: Yanir Levy

Post-secondary Education and Degrees:
Western University
London, Ontario, Canada
2014-2018 B.E.Sc.

Western University
London, Ontario, Canada
2018-2020 M.E.Sc.

Related Work Experience
Teaching Assistant
Western University
2018-2020

Research Assistant
Western university
2018-2020

Publications:

Prediction of Post-Concussion Symptoms using a Novel Computational Parcellated Axon Fiber Model. Yanir Levy, Mark Daley, Ravi Menon, Haojie Mao. BMES (2020), (Virtual on-demand presentation)

A Novel Computational Analysis of Brain Response Metrics for Mild Traumatic Brain Injury in Ice Hockey. Yanir Levy, Ryan Ouckama, Haojie Mao. BMES (2020), (Virtual poster)

Using a Strain-Based Computational Approach for Ice Hockey Helmet Performance Evaluation. Yanir Levy, Marco B. Gallone, Kewei Bian, Kierra McDougall, Ryan Ouckama, Haojie Mao. IRCOBI (2020), Munich, Germany (International conference, paper & podium presentation)

Predicting Cognitive Impairment Following Traumatic Brain Injury: A Mathematical Approach. Yanir Levy, Kewei Bian, Haojie Mao. IBIA (2019), Toronto, Canada (International conference, poster)

Exploring deep brain response to traumatic brain injury: A mathematical approach. Levy Yanir, Bian K., and Mao H. OBC (2019) Alliston, Canada (Provincial conference, poster)

A novel approach of predicting deep brain response following traumatic brain injury. Levy Yanir, and Mao H. CSME (2019) London, Canada (International conference, podium)